https://doi.org/10.1070/RCR4938

# Huprines — an insight into the synthesis and biological properties

**Eva Mezeiova,[a, b] Ondrej Soukup,[a, b] Jan Korabecny [a, b]**

*[a] Biomedical Research Centre, University Hospital Hradec Kralove, Sokolska 581, 500 05 Hradec Kralove, Czech Republic*
*[b] Department of Toxicology and Military Pharmacy, Faculty of Military Health Sciences, University of Defence in Brno, Trebesska 1575, 500 01 Hradec Kralove, Czech Republic*

The overlapping of tacrine and (−)-huperzine A templates yielded a family of highly potent cholinesterase inhibitors, so-called huprines. A relatively easy access to these compounds led to the development of dozens of huprine derivatives allowing to draw structure – activity relationship mainly for acetylcholinesterase and butyrylcholinesterase enzymes, but also with application to other biological targets of interest. An extension of their pharmacological profile is commonly associated with huprine scaffold binding to some other pharmacophores that yield high-molecular-weight heterodimers. The main purpose in developing the huprine family is related to Alzheimer's disease therapy. However, these compounds are also interesting lead structures in the treatment of other disorders, such as Myasthenia gravis, African trypanosomiasis, malaria, and prion diseases. The present review provides a rationale behind the development of huprines, detailed synthetic routes leading to different classes of huprines, and a thorough discussion of their potential pharmacological applications.
The bibliography includes 174 references.

## Contents

1. Introduction 1000
1.1. Huprine family 1000
1.2. Acetylcholinesterase and butyrylcholinesterase 1001
1.2.1. Structure of cholinesterases 1002
1.2.2. Function of cholinesterases 1002
1.3. Huprines in drug development 1003
1.3.1. Alzheimer's disease 1003
1.3.2. Myasthenia gravis 1004
1.3.3. African trypanosomiasis and malaria 1004
1.3.4. Prion diseases 1005
2. Design and development of huprines 1005
2.1. First generation huprines 1005
2.2. Second generation huprines 1006
2.3. Huprines as homo- and heterodimers 1006
3. Synthesis and biological evaluation of monomeric huprines 1008
3.1. Synthesis of structurally diverse huprines 1009
3.1.1. Synthesis of first generation huprines 1009
3.1.2. Synthesis of huprines with structural modifications at the carbobicyclic substructure 1009
3.1.2.1. Structural modifications at the methylene bridge between positions 7 and 11 1009
3.1.2.2. Structural modifications at the three-carbon bridge between positions 7 and 11 1014
3.1.3. Synthesis and biological evaluation of huprines with structural modifications at the 4-aminoquinoline moiety 1020
3.2. Enantioselective synthesis of huprines, preparation of *syn*-huprines and their biological evaluation 1024
4. Synthesis and biology of huprine homo- and heterodimers 1028
5. Conclusion 1036

The following designations and abbrevations are used:

ABAD — amyloid beta protein,
ABN — 2-aminobenzonitrile,
ABTS — 2,2′-azinobis(3-ethylbenzothiazoline-6-sulfonic acid),
Ac — acetyl,
ACh — acetylcholine,
AChE — acetylcholinesterase,
AChEI(s) — acetylcholinesterase inhibitor(s),
AD — Alzheimer's disease,
Ala — alanine,
All — allyl,
AMNT — aminomalonitrile tosylate,
APP — amyloid precursor protein,
Asp — aspartic acid,
Aβ — amyloid beta,

**E.Mezeiova**. RNDr, PhD (Organic chemistry), Postdoctoral fellow at the Biomedical Research Centre, University Hospital Hradec Kralove, Postdoctoral fellow at the Department of Toxicology and Military Pharmacy at the University of Defence in Brno.
Telephone: +420(973)255 – 167, e-mail: eva.mezeiova@gmail.com
**O.Soukup**. PharmDr, PhD (Toxicology), Associate professor, Head of the Biomedicinal Research Centre, University Hospital Hradec Kralove, Deputy Head of the Biochemical Laboratory at the Department of Toxicology and Military Pharmacy at the University of Defence in Brno.
Telephone: +420(495)833 – 447, e-mail: ondrej.soukup@fnhk.cz
**J.Korabecny**. PharmDr, PhD (Pharmacy), Junior researcher at the Biomedical Research Centre, University Hospital Hradec Kralove, Head of the Organic Chemistry Laboratory at the Department of Toxicology and Military Pharmacy at the University of Defence in Brno.
Telephone: +420(973)255 – 167, e-mail: jan.korabecny@fnhk.cz
**Current research interests of the authors**: drug development including medicinal chemistry, *in vitro* and *in vivo* evaluation, toxicokinetics, analytical chemistry methods applied in the research of neurodegenerative disorders with particular focus on Alzheimer's disease, organophosphate poisoning.

**Received 31 December 2019**

© 2020 Uspekhi Khimii, ZIOC RAS, Russian Academy of Sciences and IOP Publishing Limited

BACE-1 — beta-secretase 1,
BBB — blood-brain barrier,
9-BBN-9-borabicyclo[3.3.1]nonane,
BChE — butyrylcholinesterase,
*be*AChE — bovine AChE,
BINAP — 2,2′-bis(diphenylphosphino)-1,1′-binaphthyl,
Boc — *tert*-butoxycarbonyl protecting group,
BOP — benzotriazol-1-yloxytris(dimethylamino)phosphonium hexafluorophosphate,
CAS — catalytic active site,
ChE — cholinesterase,
ChEI(s) — cholinesterase inhibitor(s),
CNS — central nervous system,
COSY — correlation spectroscopy,
Cy 5.0 — cyanine 5.0 dye,
DAST — diethylaminosulfur trifluoride,
DBU — 1,8-diazabicyclo[5.4.0]undec-7-ene,
DCC — *N*,*N*′-dicyclohexylcarbodiimide,
DCE — 1,2-dichloroethane,
DEG — diethylene glycol,
DIBAl-H — diisobutylaluminium hydride,
DIEA — *N*,*N*-diisopropylethylamine,
DIMCARB — dimethylammonium dimethyl carbamate,
DMAP — 4-dimethylaminopyridine,
DMF — *N*,*N*-dimethylformamide,
DMSO — dimethyl sulfoxide,
DPPH — 2,2-diphenyl-1-picrylhydrazyl,
EDC — 1-ethyl-3-(3-dimethylaminopropyl)carbodiimide,
*ee* — enantiomeric excess,
Glu — glutamic acid,
Gly — glycine,
GSK-3β — glycogen synthase kinase 3 beta,
HAT — Human African trypanosomiasis,
His — histidine,
HMDS — hexamethyldisilazide,
HOBt — hydroxybenzotriazole,
HPLC — high performance liquid chromatography,
5-HT — 5-hydroxytryptamine,
HupA — huperzine A,
HupX — huprine X,
HupY — huprine Y,
$IC_{50}$ — half maximal inhibitory concentration,
KA — kainic acid,
LDA — lithium diisopropylamide,
$M_1$ — muscarinic acetylcholine receptor 1,
$M_2$ — muscarinic acetylcholine receptor 2,
MAO — monoamine oxidase,
MAPK — mitogen-activated protein kinase,
*m*CPBA — *meta*-chloroperoxybenzoic acid,
MPLC — medium performance liquid chromatography,
MG — Myasthenia gravis,
Ms — mesyl,
MS — molecular sieves,
MTDL — multi-target directed ligand,
*n*AChR — nicotinic acetylcholine receptor,
NMDA — *N*-methyl-D-aspartate,
NMP — *N*-methyl-2-pyrrolidone,
NOS — nitric oxide synthase,
NSAID(s) — nonsteroidal anti-inflammatory drug(s),
OS — oxidative stress,
PAMPA — parallel artificial membrane permeability assay,
PAS — peripheral anionic site,
PET — positron emission tomography,
PKC — protein kinase C,
PP2A — protein phosphatase 2,
PPA — polyphosphoric acid,
PrD — prion diseases,
PrP — prion protein,
*p*-TsOH — *para*-toluenesulfonic acid,
Py — pyridine,
ROS — reactive oxygen species,
SAR — structure-activity relationship,
Ser — serine,
SI — selectivity index,
Tau protein — microtubule-associated protein tau,
TBAI — tetra-n-butylammonium iodide,
TFA — trifluoroacetic acid,
TGS — target-guided synthesis,
THA — 1,2,3,4-tetrahydro-9-acridinamine (tacrine),
TMG — 1,1,3,3-tetramethylguanidine,
Ts — tosyl,
Tyr — tyrosine.

# 1. Introduction

## 1.1. Huprine family

Huprines are a family of compounds designed and developed as inhibitors of acetylcholinesterase (AChE, EC 3.1.1.7), an enzyme that terminates neurotransmission at cholinergic synapses.[1,2] Most of huprines have been tested for their anti-AChE activity. Indeed, these small molecules are highly potent inhibitors and, in many cases, even better inhibitors than their parent molecules, *i.e.* 1,2,3,4-tetrahydro-9-acridinamine (tacrine, THA) and (−)-huperzine A [(−)-HupA] (Fig. 1).[1,3] The first reports about huprines date back to the early 1990s.[4–6] They were generated by a framework combination approach merging two substructures into a novel core scaffold. Huprines contain the carbobicyclic bridged moiety of (−)-HupA and the 4-aminoquinoline system of THA (see Fig. 1).

The derivatives used in the design of huprines are well-known inhibitors of cholinesterases (ChEs). Tacrine (see Fig. 1) was identified as the first reversible AChE inhibitor (AChEI) that received approval for the symptomatic treatment of Alzheimer's disease (AD).[7] It is a non-selective, reversible non-competitive AChE inhibitor endowed with high affinity for butyrylcholinesterase (BChE, EC 3.1.1.8).[8] It effectively crosses the blood-brain barrier (BBB) and inhibits central AChE in the sub-micromolar range. In the late 1990s, THA was withdrawn from the market due to its hepatotoxicity.[9–11] However, THA is still used as a leading molecule in the design and development of new derivatives, especially in so-called multi-target directed ligands (MTDLs) that serve as potential drug candidates with improved toxicological profiles and(or) additional pharmacological properties.[12,13]

Huperzine A is a nootropic alkaloid isolated from the Chinese folk medicinal plant *Huperzia serrata*. The structures of HupA and other alkaloids isolated from the same source (such as huperzine B or huperzine U) are characterized by a bicyclo[3.3.1]nonane scaffold with one or two piperidine rings at different oxidation levels.[14] Huperzine A is a potent reversible inhibitor of AChE[15] that may affect other neurotransmitter systems to improve memory, confer neuroprotection against amyloid beta (Aβ) proteins, oxygen-free radicals and glutamate.[16–19] HupA is clinically used in China for AD treatment and has been marketed

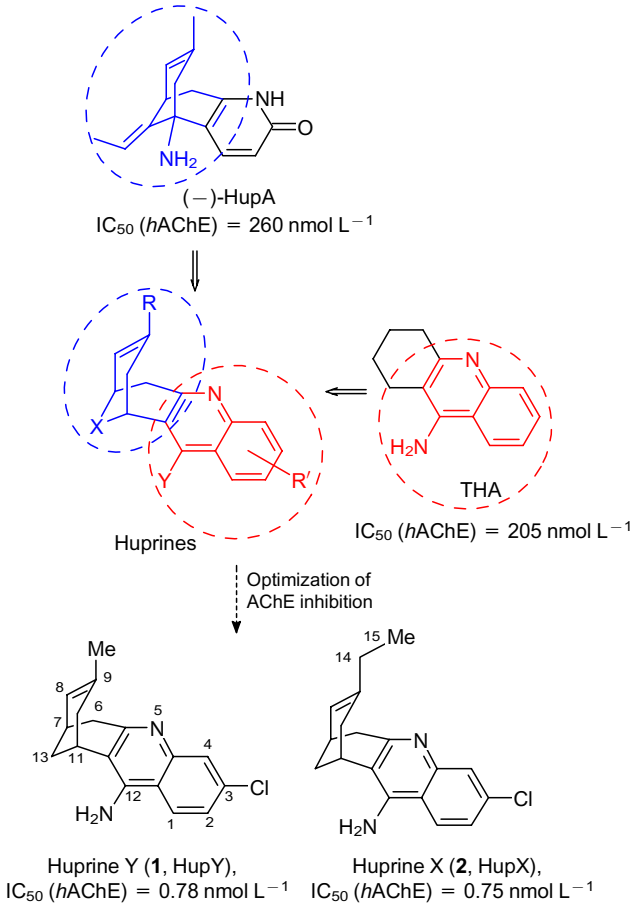



**Figure 1.** Design of huprines from (−)-huperzine A (HupA) and tacrine (THA) and the structures of the two most active AChE inhibitors from first generation huprines — huprine Y (**1**, HupY) and huprine X (**2**, HupX) with corresponding atom numbering.

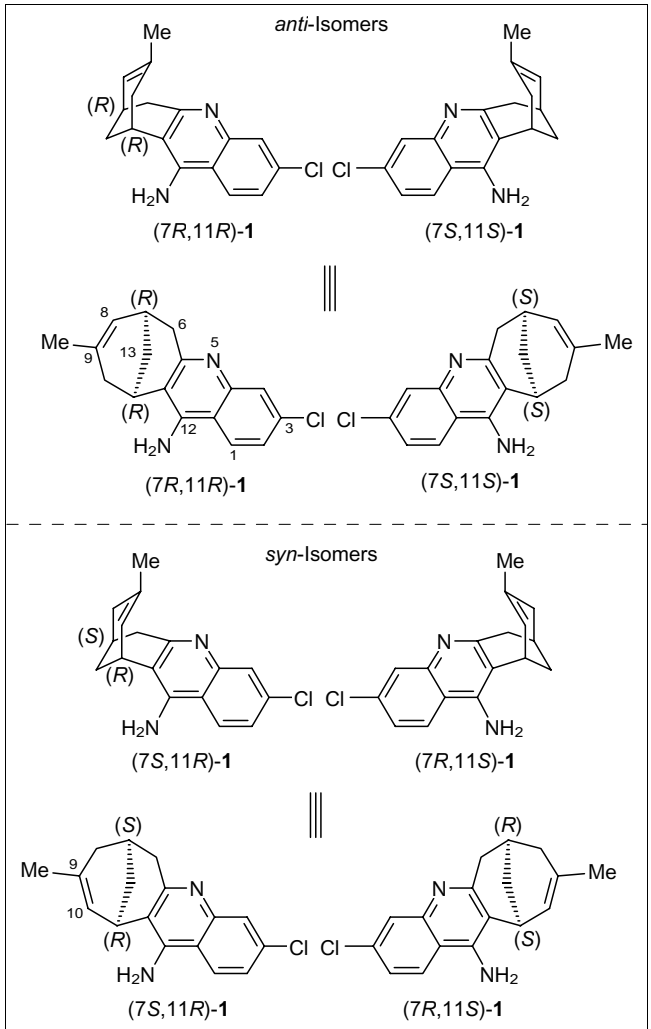



**Figure 2.** Structures of *anti*- and *syn*-isomers of hurpine Y (**1**).

elsewhere as a dietary supplement with claims made for its ability to improve memory and mental function.[16]

Although huprines combine the fragments of two known molecules, they still represent a unique class of compounds. Further, various huprine modifications have been made in order to determine the structure–activity relationship (SAR) in AChE inhibition. Accordingly, these biological assays highlighted two lead compounds designated as first generation — huprine Y (**1**, HupY) and huprine X (**2**, HupX, see Fig. 1).[20] Most of the prepared huprines were racemic mixtures. In order to obtain enantioenriched samples, chiral high performance liquid chromatography (HPLC) or medium performance liquid chromatography (MPLC) methods have been applied. The majority of the synthesized huprines were *anti*-isomers. This *syn-anti* notation refers to the relative position of the double bond at the three-carbon bridge between C(7) and C(11) atoms and the heterocyclic ring. If the endocyclic C=C bond is between positions 8 and 9 it forms an *anti*-arrangement. *syn*-Isomers contain this double bond between positions 9 and 10.[1] The structures of both enantiomers of **1** are depicted in Fig. 2.

The purpose of this review is to provide an in-depth and comprehensive summary of the structurally diverse huprine family, thoroughly describe their syntheses, and pharmacological profile. This review is a complete compilation of the chemistry of huprines starting from the very first compounds containing the huprine scaffold that were developed in 1994, continuing with the development of the first and second huprine generations, finally leading to their use as core pharmacophores in MTDLs. For better understanding of their pharmacological profile, the introduction contains short chapters regarding the primary target of huprines, *i.e.* acetylcholinesterase and butyrylcholinesterase. Since huprines are interesting lead structures not only for the treatment of Alzheimer's disease but also for Myasthenia gravis, African trypanosomiasis, malaria and prion diseases, we include brief information about each of them.

### 1.2. Acetylcholinesterase and butyrylcholinesterase

Acetylcholinesterase (EC 3.1.1.7) and butyrylcholinesterase (EC 3.1.1.8) are members of the hydrolase family catalyzing the hydrolysis of different types of substrates. AChE and BChE are responsible for the cleavage of choline-based esters and are thus called ChEs. AChE is also known as erythrocyte ChE, ChE I or 'specific' ChE, whereas that BChE is termed as plasmatic ChE, ChE II, 'nonspecific' ChE or 'pseudocholinesterase'. Both of these enzymes are also classified as serine hydrolases characterized by the presence of a serine residue as a part of a catalytic triad machinery [serine (Ser), histidine (His) and glutamic (Glu) amino acids] in the active site, which is responsible for substrate hydrolysis.[2]

Acetylcholine (ACh, Fig. 3) is one such substrate, neurotransmitter or messenger that help transmit signals across a chemical synapse. On the other hand, butyrylcholine is a synthetic molecule used to differentiate between the two types of ChEs. Acetylcholinesterase has a narrow specificity for ACh and very low or none activity on longer-chain choline esters.[21] Butyrylcholinesterase can hydrolyze ACh in addition to other (bulkier) choline esters (*e.g.*, butyrylcholine and succinylcholine), noncholine conjugates (*e.g.*, cocaine, acetylsalicylic acid and heroin) and arylamides (*e.g.*, the synthetic compound *o*-nitroacetanilide).[2] Some of the known substrates for BChE are displayed in Fig. 3. BChE is less specific for ACh and can be inhibited by a broader spectrum of ligands while retaining almost the same catalytic activity as AChE. These substrate specificity and activity differences in ChEs go hand in hand with their structural characteristics. Whereas AChE is a catalytic enzyme with several well-conserved aromatic residues lining the cavity gorge, BChE possesses more aliphatic amino residues (especially in the peripheral anionic site) responsible for broader substrate specificity, thus being able to accommodate bulkier substrates.[22, 23]

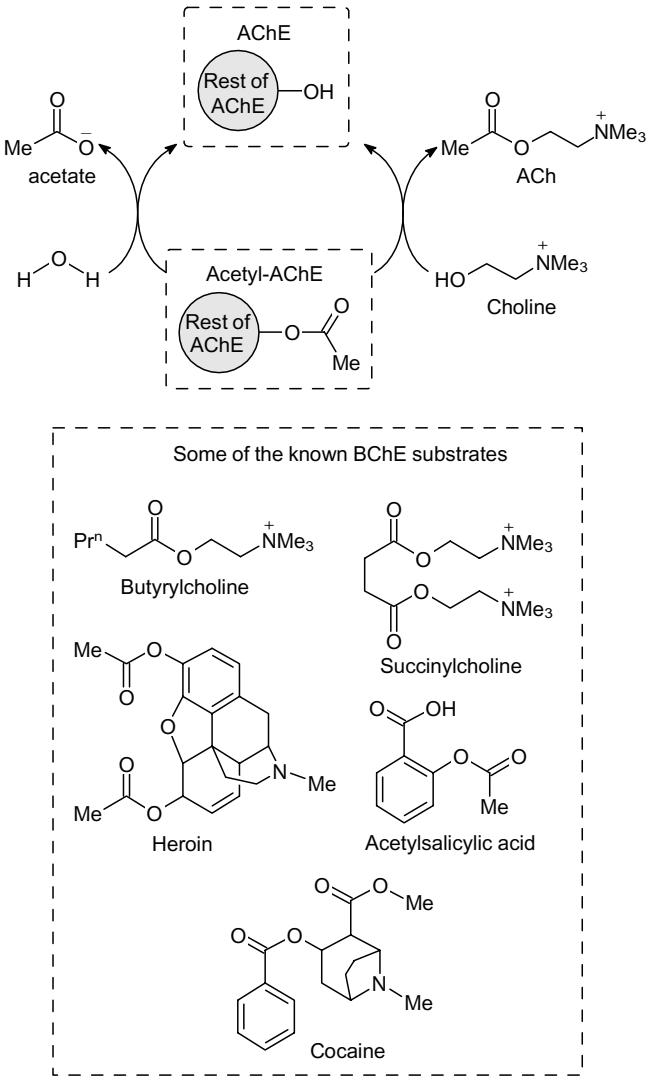



**Figure 3.** The catalytic mechanism of ACh hydrolysis and chemical structures of different BChE substrates.

### 1.2.1. Structure of cholinesterases

The first crystal structure of AChE from *Torpedo californica* (*Tc*AChE; Protein Data Bank entry 1EA5) was determined by Sussman *et al.*[24] in 1991. From this point, a large number of crystal structures of human AChE (1B41, 1F8U) and homologous AChEs from different organisms (*Mus musculus*, 1N5M, 1N5R, 1JO6, 1JO7; *Electrophorus electricus*, 1C2O; *Drosophila melanogaster*, 1QO9, *etc.*) have been solved, as well as the crystal structures of human BChE (1P0I) and its complexes with several substrates (with *choline*, 1P0M; *tacrine*, 4BDS; *tabun*, 3DJY. 3DKK, *etc.*).[22, 25] For the purpose of this review, we consider the crystal structures of tacrine (1ACJ, Fig. 4*a*),[26] HupA (1VOT, Fig. 4*b*),[27] **1** (1E66, Fig. 4*c*)[28] and their spatial overlap (Fig. 4*d*) in the active site of *Tc*AChE. Cholinesterases belong to the α/β-fold hydrolase family. This means that they contain a β-sheet platform surrounded by α-helices. The central β-sheet bears the catalytic machinery, and the α-helices and loops are responsible for specificity. The hydrolysis of any substrate takes place in the active site of the enzyme. ChEs have their active sites located at the bottom of a 20 Å deep gorge and the hydrolytic process is mediated by the so-called catalytic triad formed by His, Glu and Ser residues. Amino acid residues of the so-called anionic site, also located in the active site of the enzyme, can bind the cationic quaternary nitrogen of choline-based esters (or other substrates) providing proper orientation for the molecule in the gorge. The acyl pocket is another part of the active site ensuring substrate orientation during substrate catalysis.[22, 23]

The catalytic mechanism is a two-step procedure. It starts with the formation of an acyl-enzyme intermediate at Ser of the catalytic triad, followed by water-induced cleavage of the formed ester leading to the regeneration of the unbound Ser residue, which can then re-enter the next reaction cycle (see Fig. 3).[2] The transition state established during the enzymatic reaction is stabilized by the amino acid residues of the oxyanion hole [two glycine (Gly) amino acids and alanine (Ala) residue] through hydrogen bonds.[22, 23]

One of the important architectural differences in the active sites between AChE and BChE is their size. The gorge (especially the acyl binding pocket) of BChE is bulkier than that of AChE due to the presence of different amino acid residues. In more detail, a number of aromatic residues ubiquitous in AChE are replaced by aliphatic ones in BChE, including those of polar nature. Another significant structural discrepancy between the ChEs is the peripheral anionic site (PAS) located at the entrance of the enzyme's active site; it serves as an attraction center for outer-space substrates. The PAS of AChE consists of five tyrosine (Tyr) residues (human AChE (*h*AChE) numbering: Tyr72, Asp74, Tyr124, Tyr 286, Tyr 341), whereas in BChE some of them are missing; human BChE (*h*BChE), in particular, does not own the AChE counterparts for three aromatic amino acids (Tyr72, Tyr124, Tyr286).[23, 29]

### 1.2.2. Function of cholinesterases

The primary function of AChE is to terminate ACh neurotransmission at nicotinic and muscarinic ACh receptors. These receptors are ubiquitous in the central nervous system (CNS) and at neuromuscular junctions.[2] In addition to its primary role, AChE has 'non-classical' activities that do not require its catalytic function. Having said that, it is involved in protein adhesion during synaptic development and main-

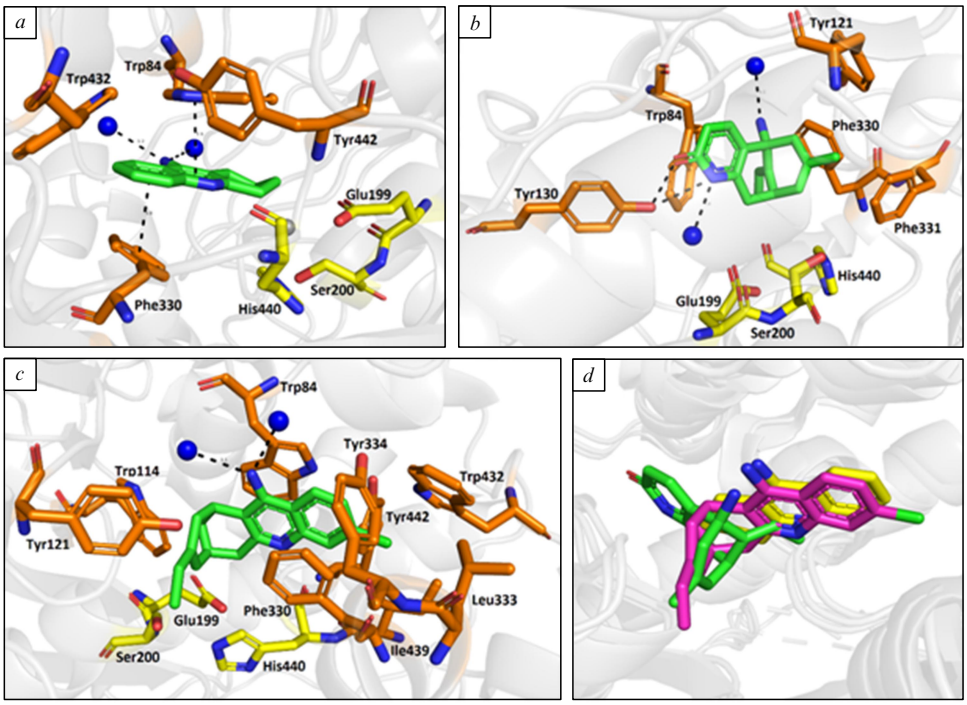



**Figure 4.** Complexes of *Tc*AChE with tacrine (*a*),[26] huperzine A (*b*)[27] and (−)-hurpine Y (**1**) (*c*).[28] Generally, ligands (*a*, *b*, *c*) are depicted in green, important amino acid residues in orange and the catalytic triad in yellow. Water molecules enabling ligand anchoring are shown as blue spheres. Only important interactions like hydrogen bonds and hydrophobic interactions are displayed as dashed lines. Figure *d* represents the spatial overlap of (−)-**1** (purple), tacrine (yellow) and HupA (green) in the *Tc*AChE active site. The rest of the enzyme is rendered as a light-grey ribbon. The figures were created with the PyMOL Molecular Graphics System, Version 2.0 Schrödinger, LLC.

tenance, in dopaminergic neuron functioning, neurite growth and promotes the assembly of Aβ peptide into amyloid fibrils.[30, 31] The physiological function of BChE is still unknown. Since BChE is widely distributed in the CNS, it is possibly involved in neural function. In a healthy brain, AChE is responsible for the majority of ChE activity (about 80%) while BChE contributes to the remaining 20%. However, the activity of AChE decreases to only 10% – 15% of normal activity with the progression of AD, whereas that of BChE stays at the same level or it is even increased, compensating for the loss of AChE activity.[32 – 34] In plasma, BChE is involved in the inactivation of some drugs or activation of prodrugs.[35] It also detoxifies organophosphate and carbamate inhibitors, preventing toxic AChE inhibition.[36]

## 1.3. Huprines in drug development

### 1.3.1. Alzheimer's disease

Alzheimer's disease (AD) has been described as a complex neurodegenerative disorder associated with the malfunction in cholinergic neurotransmission. Basically, AD is characterized by progressive memory impairment with subsequent appearance of other cognitive, behavioural and neuropsychiatric changes that impair social function and daily living activities.[37] The first therapies for AD were developed pursuing the correction of neurochemical alterations found in autoptic samples of post-mortem brain tissue from AD patients.[38] In line with the cholinergic hypothesis, the activity of choline acetyltransferase, an enzyme responsible for the synthesis of ACh, is decreased during AD onset (progression); further, ACh release and choline uptake in nerve terminals to renew the synthesis of ACh were reduced in the same tissues.[39 – 42] These and several other observations were the keystones in the formulation of the cholinergic hypothesis stating that the degeneration of cholinergic neurons and associated loss of cholinergic neurotransmission in the cerebral cortex and other areas contributed significantly to the impairment of cognitive functions in AD patients.[43] Seeking to improve cholinergic neurotransmission, viable therapeutic approaches concentrated on ChEs inhibitors able to compensate for the decreased synthesis and synaptic availability of ACh. In contrast, current AD therapies (donepezil, rivastigmine and galantamine, Fig. 5) provide symptomatic relief delaying the disease progression, as measured by cognitive and functional indicators.[44] However, there is no evidence that these compounds have any disease-modifying effect by interfering with other pathophysiological mechanisms of AD, such as Aβ or tau proteins.[45]

Alzheimer's disease is a chronic and complex disorder with multifactorial etiology (Fig. 6).[46, 47] Two primary pathological hallmarks of AD have been identified in the form of Aβ and hyperphosphorylated tau protein aggregates.[48, 49] Their respective hypotheses (*i.e.* amyloid cascade and tau hypotheses) suggest that amyloid plaques and neurofibrillary tangles are the causative features of AD.[50, 51] Other theories take other factors into consideration, such as oxidative stress (OS),[52, 53] biometal dyshomeostasis,[54] neuroinflammation,[55] mitochondrial disfunction,[56] *etc.* Because of the multifactorial character of AD, the search for novel therapeutics has shifted from targeting each pathological aspect of the disease to single chemical molecules able to act in a synergistic way on multiple targets. There is a considerable amount of research describing MTDLs, to which the readers are kindly referred.[13, 57 – 61]

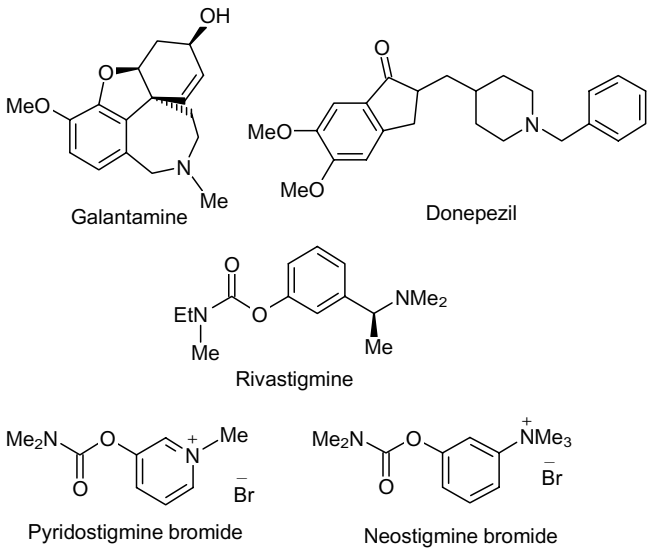



**Figure 5.** Chemical structures of currently available AChEIs for the treatment of AD (galantamine, donepezil, rivastigmine) and MG (pyridostigmine bromide, neostigmine bromide).

### 1.3.2. Myasthenia gravis

Myasthenia gravis (MG) is an autoimmune disorder affecting the endplate of the postsynaptic neuromuscular junctions. It is a rare disease characterized by muscular weakness and fatigue.[62] This disorder is caused by autoantibodies directed towards nicotinic ACh receptors (nAChRs) at the junction between the nerves and muscles. Blocking, downregulating or destroying the nAChRs reduces the number of available receptors interacting with the ACh released from the presynaptic nerve terminal. A complementary loss of sodium channels results in reduced neuromuscular transmission.[63] Acetylcholinesterase inhibitors (AChEIs) provide temporary, symptomatic treatment for all forms of MG. AChEIs such as pyridostigmine bromide or neostigmine bromide (see Fig. 5), inhibit ACh hydrolysis at the neuromuscular junction improving the probability of successful neuromuscular transmission. These inhibitors are usually effective in patients with ocular or early MG; therefore, they are convenient for patients who cannot receive immunosuppressive or adjunctive treatment after immunotherapy with residual myasthenic weakness.[64, 65]

### 1.3.3. African trypanosomiasis and malaria

Human African trypanosomiasis (HAT) (also known as sleeping sickness) and malaria are caused by protozoan parasites.[79] The first disease is caused by infection of *Trypanosoma brucei* (*T. brucei*) which is transmitted by infected tsetse flies. Malaria is a mosquito-borne protozoal infection caused by parasites of the genus *Plasmodium*, of which five species are currently known to cause this disease in humans. In general, both HAT and malaria affect the same populations (219 million cases in 2017).[79 – 82] The discovery of novel therapeutic drugs for HAT and malaria stems mainly from the increased drug resistance, limited range of available drugs, as well as their high cost and significant toxicity. An interesting approach was presented by introducing derivatives with dual anti-plasmodial – trypanocidal profile, such as 4-amino-7-chloroquinolines [83, 84] or their close analogues, *e.g.*, 9-amino-6-chloroacridines.[85 – 89] These compounds could circumvent the issues with resistant *Plasmodium* strains and result in better cost-effective treatments.[88] Since huprines are 4-aminoquinoline-

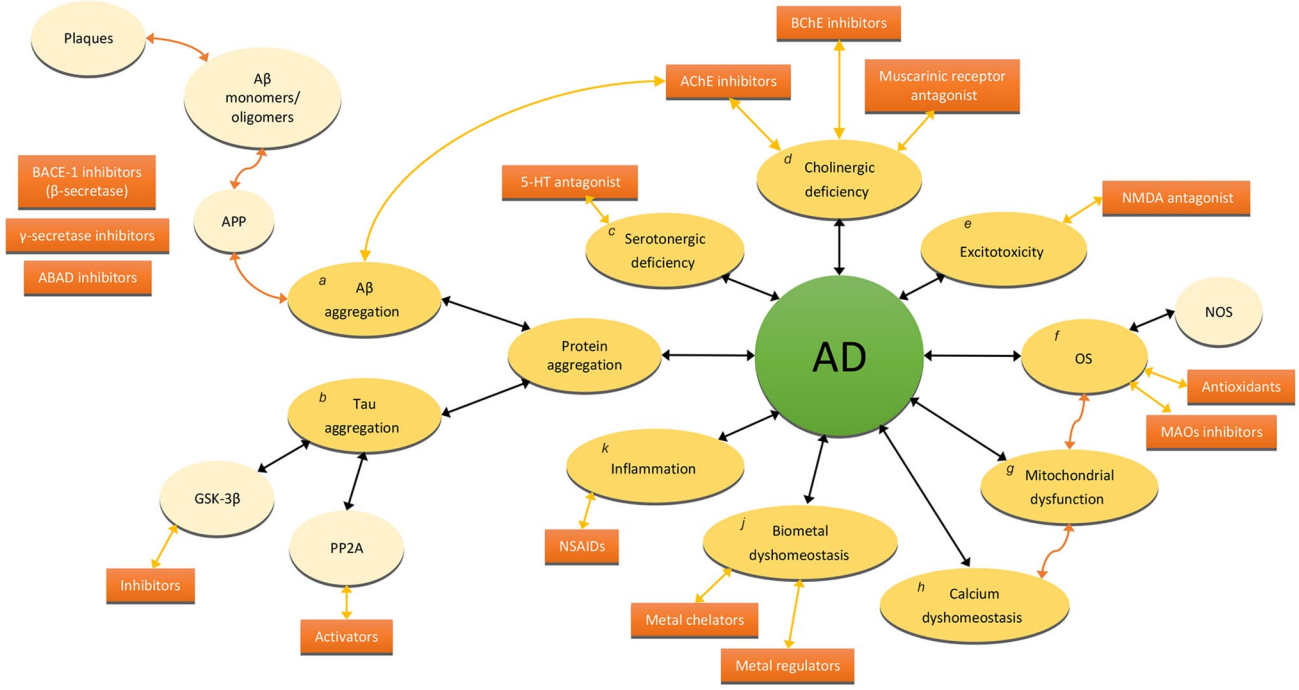



**Figure 6.** Some of the pathogenic hallmarks, drug targets and potential drug strategies for the treatment of AD. For more details, readers are kindly referred to the particular references: (*a*) Aβ protein,[50, 66] (*b*) tau protein,[51, 67] (*c*) serotonergic deficiency,[68] (*d*) cholinergic deficiency,[38, 69] (*e*) excitotoxicity,[70 – 72] (*f*) OS,[52, 53, 73] (*g*) mitochondrial dysfunction,[56, 74, 75] (*h*) calcium dyshomeostasis,[76, 77] (*j*) biometal dyshomeostasis,[54] and (*k*) inflammation.[55, 78]

based compounds, able to cross the BBB, some of the monomeric derivatives and heterodimers were tested for their trypanocidal and anti-plasmodial activities.

#### 1.3.4. Prion diseases

Prion diseases (PrD), also referred to as transmissible spongiform encephalopathies, are a group of neurodegenerative disorders caused by the conversion of the normal prion protein ($PrP^{C}$) into its abnormal amyloidogenic isoform, $PrP^{Sc}$, which stands for *proteinaceous infectious particle*.[90] The 'prion only hypothesis' postulates that the multiplication of prion infectivity occurs in an exponential manner, with the post-translational conversion of PrPC or a precursor into PrPSc appearing to be mandatory. A PrPSc molecule might interact with a PrPC molecule to form a heterodimer, which is further transformed into two PrPSc molecules. In the next cycle, two PrPSc molecules combine with two PrPC molecules resulting in the formation of four PrPSc molecules, which further combine with four PrPC molecules, giving rise to an exponential process.[90] Sporadic Jakob-Creutzfeldt disease is the most common form of human prion diseases. Fortunately, this fatal degenerative brain disorder is relatively rare, affecting approximately one individual in one million people per year.[91]

Despite the significant differences in pathophysiology and clinical symptomatology, AD and PrD share common hallmarks. Some of the common features of both diseases are pathogenic factors such as reactive oxidative species (ROS), transition metal ions and, the most evident, misfolded and aggregated proteins.[92–94] The Aβ peptide and PrP are key molecules in the pathogenesis of these disorders, both of them undergo structural transitions that have been associated with a gain of toxic function leading to neurodegeneration.[95] Thanks to these similarities, therapeutic approaches involving antioxidants, metal chelators and protein aggregation inhibitors could be beneficial for both types of disorders.[94,96]

Obviously, AD and MG are diseases sharing ChEs as a specific target of interest. Designing and developing novel chemical entities for the respective disorders reflect mostly their physicochemical properties. In other words, the drugs for AD must be active in the brain and thus crossing BBB in order to target ChEs in the CNS. On the other hand, drugs for MG are supposed to target ChEs in the periphery. To ensure the peripheral effect, small charged molecules are widely used. Currently available AChEIs for the treatment of AD (galantamine, donepezil, rivastigmine, see Fig. 5) are uncharged compounds with ability to penetrate BBB. AChEIs used for the symptomatic treatment of MG (pyridostigmine and neostigmine bromides, see Fig. 5) are quaternary ammonium salts.[64,97] The high inhibition profile of huprines for ChEs is rather unfavourable for their use in the treatment of HAT, malaria and PrD. 4-Aminoquinoline moiety is a widely accepted template to be further modified to cope with these disorders. Indeed, the potential use of huprines against protozoan infections (HAT, malaria) is based on their structural similarity to currently used chloroquine and its derivatives.[83–85] For the further development of huprine-based drugs for these disorders, it is necessary mostly to decrease their ChE inhibitory potency and simultaneously enhance affinities for the known targets (for instance, specific targets of interests for HAT might be methionyl-tRNA synthetase, *N*-myristoyl transferase or GSK-3 enzyme and others). Huprine derivatives are also considered as lead structures for treatment of PrD based on their ability to disrupt the architecture of misfolded proteins, similarly to β-sheets of Aβ in AD.[94–96]

## 2. Design and development of huprines

### 2.1. First generation huprines

The design and development of the first generation of huprines and the follow-up work are described in two previous reports by Camps and Muñoz-Torrero in 2001 and 2008, respectively.[1,3] Huprines were constructed in an attempt to find a molecule with high affinity for the active site of AChE. However, at the time of design only the structure of *Tc*AChE had been solved by X-ray crystallography, whereas the crystal structures of AChE with THA and (−)-HupA were still unknown. Therefore, these THA – HupA hybrids had to be designed on the assumption that the heterocyclic 4-aminoquinoline and the carbocyclic moiety can both span the different regions of AChE, thus providing more plausible interactions with the enzyme.

The first reported huprine was derivative **3**, which was classified as the lead for further structural modifications (Fig. 7).[5] Despite the lack of the ethylidene appendage characteristic of (−)-HupA, it still was a more potent AChE inhibitor [bovine AChE (*be*AChE): $IC_{50}$ = 65 nmol $L^{-1}$] than the parent molecules [*be*AChE: $IC_{50}$(THA) = 130 nmol $L^{-1}$, $IC_{50}$[(−)-HupA = 74 nmol $L^{-1}$]. A newer generation of huprines was composed with different substructure variations in both HupA-like and THA-like subunits (see Fig. 7).[5,98] The carbobicyclic unit was modified at the methylene bridge or the three carbon bridges between C(7) and C(11) atoms. The introduction of any group at C(13), the replacement of methylene at this position by *o*-phenylene group, saturation or isomerization of the C(8)=C(9) double bond or the replacement of the methyl group at position 9 resulted in an activity drop. Further, the SAR study disclosed that 9-ethyl substituted huprine had a slightly superior inhibitory capacity than compound **3**. The replacement of the benzene ring of the 4-aminoquinoline moiety by a cyclopentene ring led to a complete activity loss. Moreover, the second modification took place at an aromatic tacrine-like moiety by mono-substituting positions 1, 2 or 3, or disubstituting 1 and 3 concomitantly (equivalents to positions 8, 7 and 6 of THA) with halogen atoms (F, Cl) or methyl groups. Among these analogues (and among all first generation huprines), the monosubstituted compounds (±)-**1** and (±)-**2** were highlighted and selected as the most potent compounds. Their racemic mixtures were 330- and 260-fold more potent human AChE inhibitors than THA and HupA, respectively. In enantiopure form, (−)-**2** and (−)-**1** reached an outstanding inhibitory capacity >800- and 640-fold more potent than the parent compounds, *i.e.* THA and HupA, respectively.

Derivatives with either *E*- or *Z*-configuration of the ethylidene appendage at position 13 were, surprisingly, less potent *be*AChE inhibitors when compared to **1** [$IC_{50}$(*E*-isomer) = 320 nmol $L^{-1}$, $IC_{50}$(*Z*-isomer) = 1.150 nmol $L^{-1}$].[5] The 3D structures of the THA and (−)-HupA complexes with *Tc*AChE were solved in 1993[26] and 1997,[27] respectively (see Fig. 4). According to these crystallographic data, the cyclohexene ring of THA and the carbobicyclic system of (−)-HupA occupied a similar binding site of AChE. In contrast to the design of huprines, the 4-aminoquinoline system of THA and the pyridine ring of HupA point to opposite directions. The crystallographic

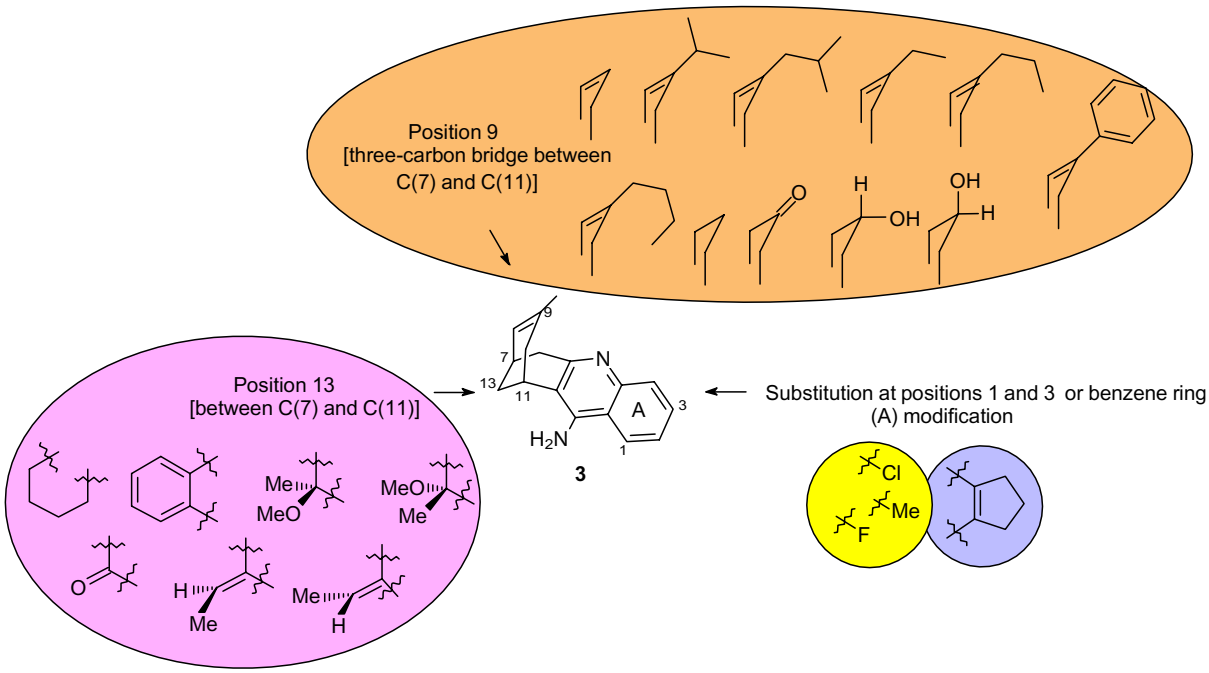



**Figure 7.** Structure – activity relationschip study of huprine **3** with selected structural modifications yielding the first generation huprines.

structure of the complex *Tc*AChE-(−)-**2** was elucidated in 2002.[28] Despite this fact, the binding mode of huprines to AChE is still consistent with the used hybridization strategy that closely mimics the THA binding pattern of the 4-aminoquinoline moiety. Regarding the carbobicyclic system, only the unsaturated bridge between C(7) and C(11) atoms from both (−)-**2** and (−)-HupA compounds occupy the same binding site. All these observations provide sufficient rational background for giving rise to huprines as highly potent AChEIs. In general, this can be attributed to the extensive binding within the enzyme active site compared to the parent ligands.

## 2.2. Second generation huprines

Further huprine development was driven by molecular modeling studies exploiting the X-ray crystallographic structures of the *Tc*AChE complexed with either THA, HupA or (−)-**2** and also with other AChE enzymes reported in the Protein Data Bank. Some of these huprines are depicted in Fig. 8.

The idea for 13-amidohuprines by Camps *et al.*[99–101] arose from the presumption that neither HupA nor any huprines fully expand the catalytic active site (CAS) of AChE. Accordingly, the introduction of a small amido group attached to position 13 could have enabled some additional interaction with the AChE cavity gorge. However, these expectations were fruitless, giving rise to huprines with a detrimental AChE inhibitory capacity below that of **1**.

Other modifications of the huprine scaffold were inspected by Ronco *et al.*[102–105] With the intention of improving the activity of huprines against AChE and in order to obtain deeper insight into their binding ability, three parts of the basic core were altered: a) the benzene ring of the 4-aminoquinoline subunit was substituted by heteroaromatic rings with different electron densities, or it was substituted at position 2 and 3 with electron donating groups like methoxy, b) reactive linkers were introduced to the huprine scaffold at position 12, and c) various functional groups were built into position 9. All of the huprine analogues modified at the benzene ring, likewise at position 12, were less active in AChE inhibition compared to **2**.

The functionalization at position 9 resulted in a number of novel derivatives. The parent molecule in this case, ester **4** (see Fig. 8), was synthetized in three steps from the starting diketone and was then modified into new analogues with carboxyl, hydroxyl, amino, amido groups, *etc.*[104] Among them, several new compounds exerted an *h*AChE inhibitory potency with $IC_{50}$ in the low nanomolar range; however, none exceeded the activity of compound **2**. The introduction of a triazole, attached *via* two-carbon tether at position 9, led to significantly decreased anti-AChE activity. On the other hand, the elongation of a two-carbon chain between the huprine scaffold and the triazole into a four-carbon linker generated two analogues with higher inhibitory activity than **2**.[105]

## 2.3. Huprines as homo- and heterodimers

Huprine homo- and heterodimers were developed in accordance with the concept of MTDLs seeking to broaden their biological profile to simultaneously confront the disease at multiple levels (Fig. 9). The concept of MTDLs was mostly postulated in regard to selective ligands lacking clinical efficacy. Several manners to develop these MTDLs have been proposed, including linking, fusing and merging approaches to deliver the desired activity into a molecule.[106] The development strategy has been described in a plethora of studies.[12, 53, 105] Huprine homo- and heterodimers were designed on the basis to a linking approach in which molecular pharmacophores are separated by a distinct linker group that is not found in either of the selective ligands.[107]

The first huprine-based MTDLs were reported in 2005.[108] A series of huprine – tacrine heterodimers have been developed by the connection of **1** to THA through a linker of appropriate length allowing the simultaneous

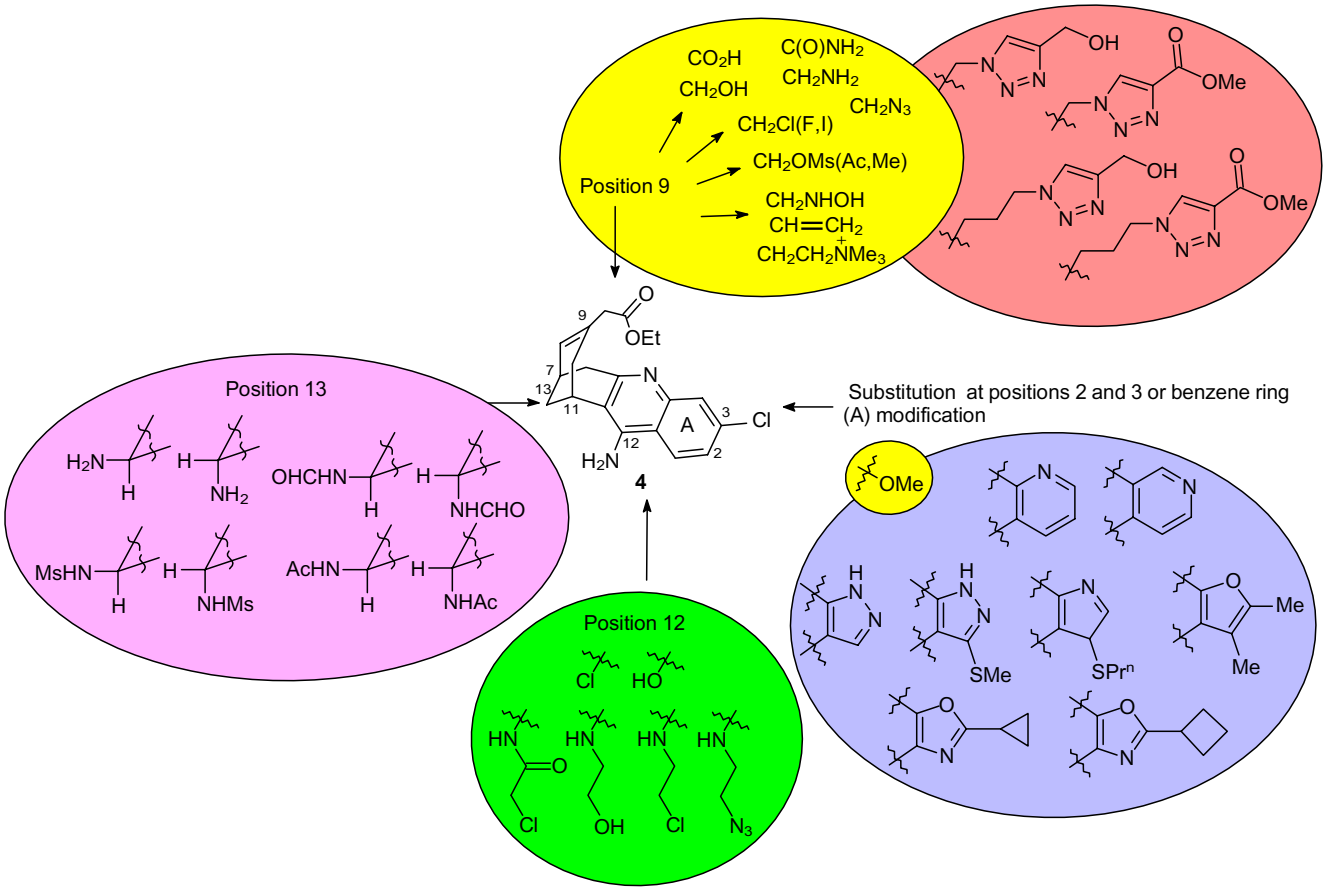



**Figure 8.** Structural modification of second generation huprines.

interaction with both binding sites of AChE. Applying a dual binding site strategy, a huprine moiety binds to the active site and the tacrine-related unit binds to the peripheral site, providing an increased affinity for AChE. The ligand accommodation is in line with the compounds' affinities, *i.e.* a more potent moiety is oriented within CAS enzyme. Almost all of the dimers were more active human ChE inhibitors (ChEIs) than the parent molecules. This set of huprine – tacrine heterodimers was broadened for another series of several racemic and enantiopure dimers composed of **1** and THA or 6-chlorotacrine.[96] *In vitro* data demonstrated a highly potent *h*AChE inhibition, and, more importantly, an additional effect mitigating the chaperone effect of AChE against Aβ, and PrP aggregation. Heterodimers of the latter series were also tested for trypanocidal and anti-plasmodial activity.[109] The molecular dimerization had been successfully applied to a number of 4-aminoquinoline derivatives to overcome drug resistance in malaria patients.[110, 111] All the tested dimers were found to be potent trypanocidal and anti-plasmodial agents with $IC_{50}$ values in the sub-micromolar range.

Other combinations for huprine-based MTDLs contain pharmacophores such as (*S*)-levetiracetam,[112] [6]-shogaol,[113] rhein [114, 115] or a *N*-benzylpiperidine moiety from donepezil (see Fig. 9).[116] Beyond the ChEs inhibitory activity, these heterodimers exhibited a broader pharmacological profile. Collectively, these heterodimers displayed one of the most pronounced pathological features in AD – Aβ and tau protein aggregation. It is well known that the dual binding site inhibitors of AChE are able to block the AChE-induced Aβ aggregation through their interaction with the PAS region.[117, 118] Some compounds were even able to inhibit spontaneous Aβ aggregation by directly interacting with it, likely due to the presence of aromatic planar moieties in their structure.[119 – 121] The ability of dimers to affect Aβ aggregation was tested *in vitro* and *in vivo*. The biological evaluation included the inhibition of beta-secretase 1 (BACE-1), AChE-induced and self-induced Aβ aggregation and efficacy studies in an AD mouse model. $Aβ_{42}$ and tau anti-aggregating activity was determined in intact *Escherichia coli* cells overexpressing these proteins. Besides the overproduction and aggregation of Aβ and tau proteins, oxidative stress (OS) was reported as one of the earliest causative factors of AD.[122, 123] In this regard, rhein – huprine and Shogaol – huprine hybrids exhibited potent antioxidant properties.[113, 115]

Huprine pharmacophores were also coupled with two structures of general formula **5** (see Fig. 9) to produce dual-site inhibitors, which were higher-affinity (about 10 000-fold) towards AChE in comparison with BChE.[102] The 'click chemistry' approach exploiting Huisgen 1.3-dipolar cycloaddition was used for the preparation of compounds with general formula **6** (see Fig. 9) following target-guided synthesis (TGS) strategy.[124] In this concept, the target enzyme was directly involved in the choice of its suitable ligands.

Homodimers based on compound (+)-**1** were prepared in 2014.[125] This molecular dimerization was performed to develop better antiprotozoal agents. Indeed, the strategy was successful for many dimers of the 4-aminoquinoline

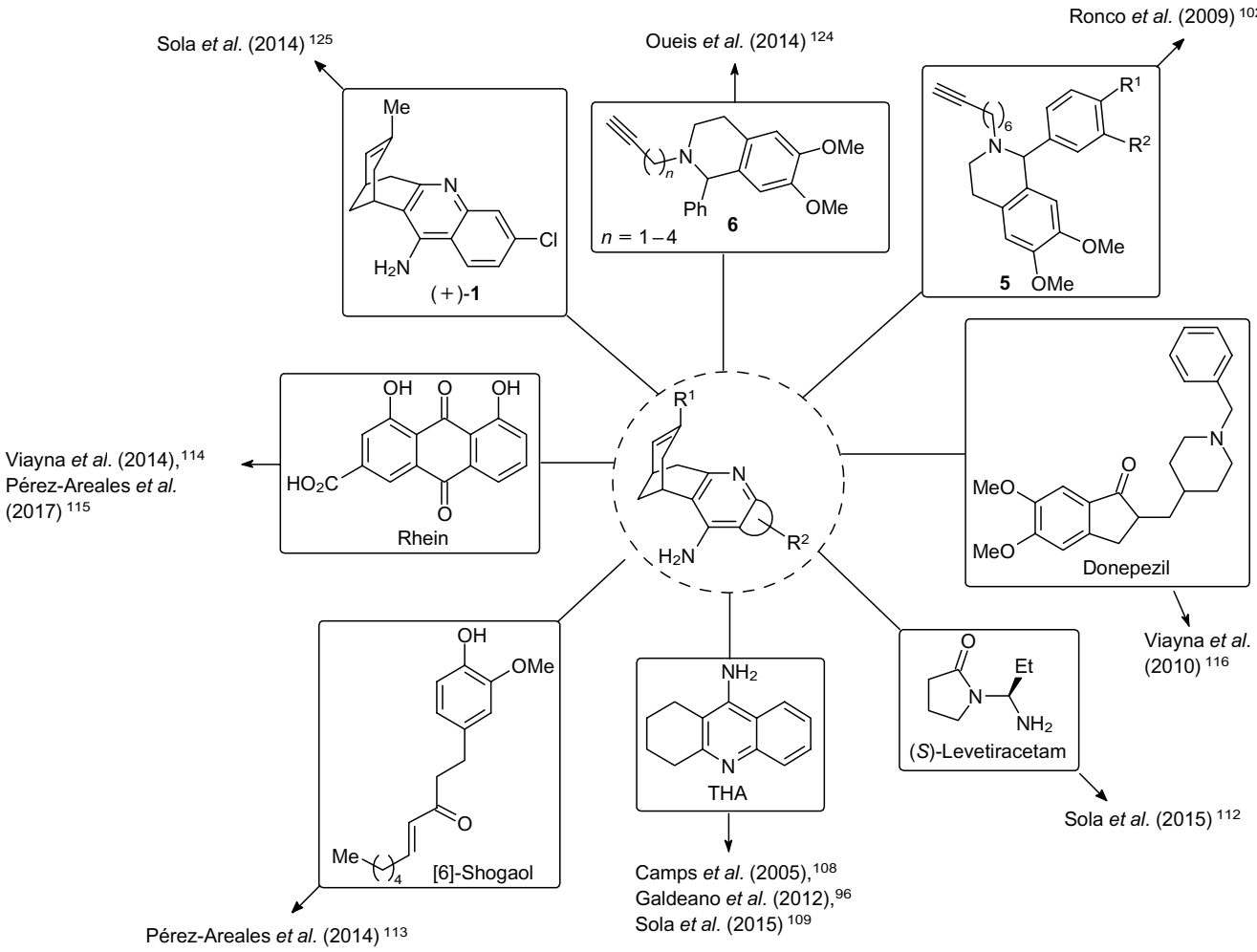



**Figure 9.** Concept map showing some of the model molecules and fragments used in the design of huprine homo- and heterodimers.

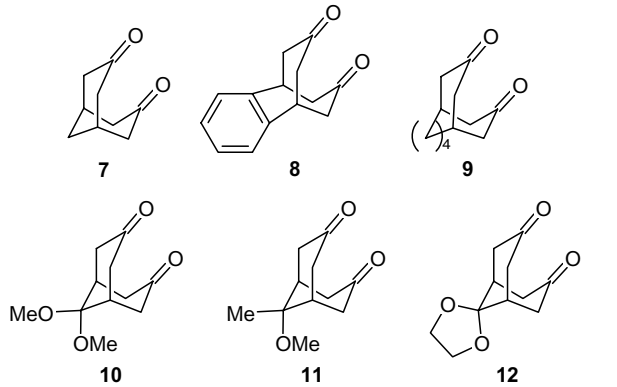
family. Most of these dimers have more potent and selective trypanocidal activity than the parent (+)-**1**, although they were devoid of antimalarial activity. Nevertheless, all of them were potent AChEIs, which is, however, a significant drawback for antiprotozoal agents.[125]

## 3. Synthesis and biological evaluation of monomeric huprines

The carbobicyclic huprine substructure employs diketone as a starting material for the most part, as it is commercially available or can easily be prepared. Compound **7** was extensively used as a starting building block in the synthesis of huprines with structural modifications at position 9. Diketones **8**–**12** were applied in the case of huprines modified at the bridge between positions 7 and 11 (or position 13).

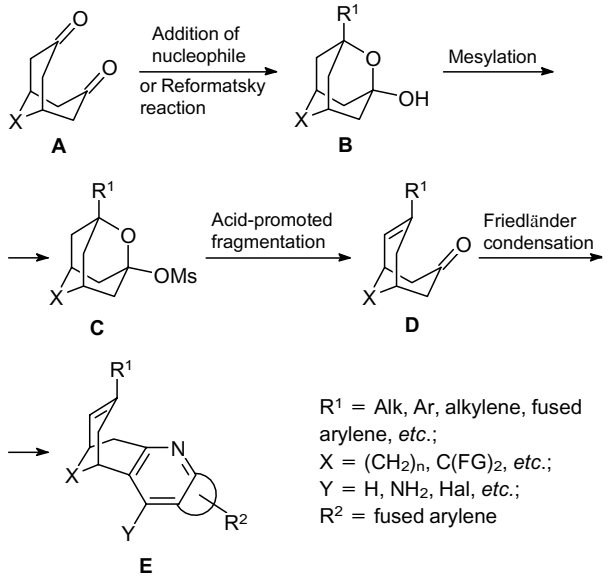
The general synthesis of huprines is depicted in Scheme 1. The nucleophilic addition of various organolithium or organomagnesium reagents to a starting diketone **A** furnished the attachment of different alkyl, alkenyl or aryl groups giving various oxaadamantanols **B**. This approach is limited by the use of organometallic reagents that do not allow a substitution into position 9. Therefore, the incorporation of ester functionality at position 9 was achieved through the Reformatsky reaction, which is

**Structures 7 – 12**




defined as the metal-induced reaction of an α-carbonyl halide with an electrophile.[126] The coupling reaction of diketone **A** with α-halo ester in the presence of zinc enabled the preparation of desired product **B**. This synthetic route led to huprines with an ethyl ester moiety at position 9 that easily be easily functionalized. The activation of the alcohol group of compound **B** with methanesulfonyl was followed by acid-induced fragmentation of the generated mesylate **C** to produce ketone **D** (mostly as a racemic mixture). Enone **D** was submitted to a Friedländer-type condensation[127] with

**Scheme 1**



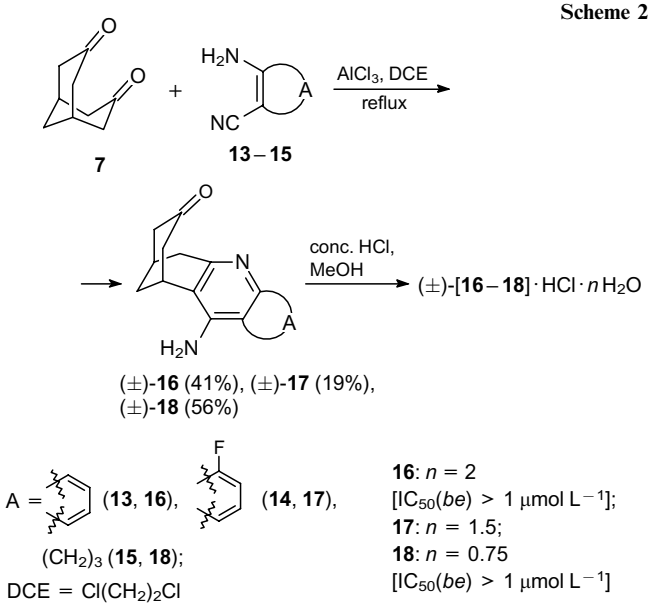

corresponding 2-aminoarylnitrile or 2-aminocycloalkenylnitrile to produce huprine **E** (as a racemic mixture) (Scheme 1).

## 3.1. Synthesis of structurally diverse huprines

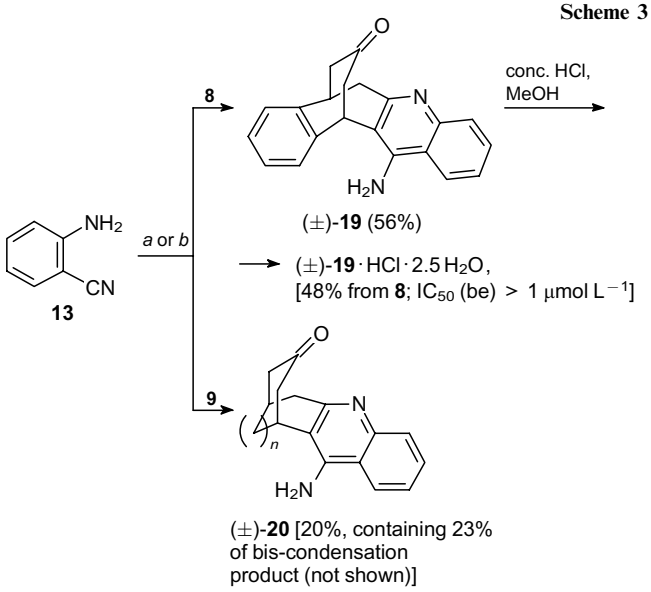
### 3.1.1. Synthesis of first generation huprines

The first huprine reports date back to 1994 when Aguado *et al.*[4] developed a series of compounds (±)-**16**–**20** through the Friedländer condensation of corresponding diketones **7**–**9** with 2-aminobenzonitrile (**13**, ABN), 2-amino-6-fluorobenzonitrile (**14**) or 2-aminocyclopentenecarbonitrile (**15**) in the presence of aluminium trichloride as a catalyst in 1,2-dichloroethane (DCE) under reflux (or zinc chloride in nitrobenzene at 120–130 °C). These reactions resulted in mixtures of a mono-condensed product, *i.e.* huprine (Schemes 2 and 3) and bis-condensed adducts (not shown) that were separated by column chromatography. Huprines (±)-**16**–**20** were then converted into hydrochloride salts by treating them with concentrated HCl upon heating in

**Scheme 2**




**Scheme 3**




(*a*) $AlCl_3$, DCE, reflux; (*b*) $ZnCl_2$, $PhNO_2$, 120 °C

methanol.[4] Some of these huprines were moisture sensitive and retained some water molecules. The elemental analysis of the products pointed to the presence of water in different amounts that could not be removed, even after drying. This phenomenon was more noticeable in the case of hydrochloride salts. Some of the developed derivatives were tested for inhibitory activity against *be*AChE, suggesting that all huprine analogues were inactive in the studied concentration range, *i.e.* $IC_{50}$ was higher than 1 μmol $L^{-1}$.

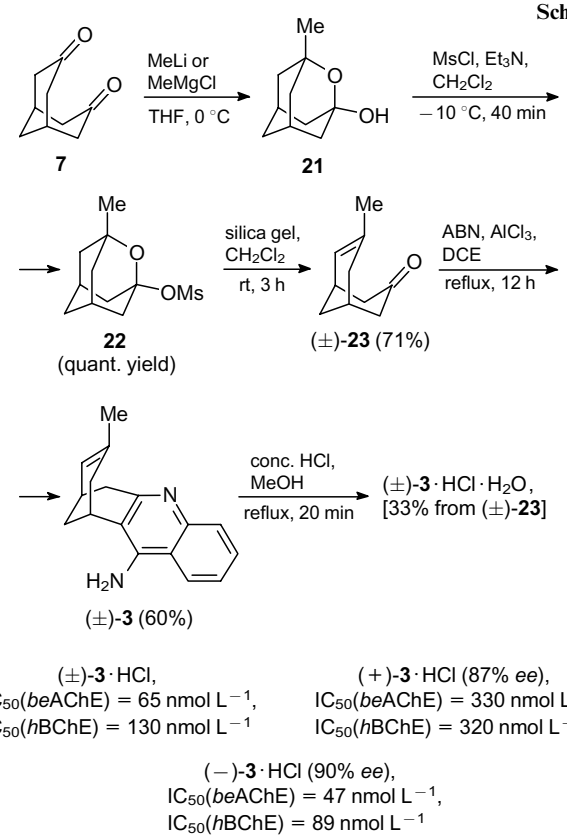
### 3.1.2. Synthesis of huprines with structural modifications at the carbobicyclic substructure

#### 3.1.2.1. Structural modifications at the methylene bridge between positions 7 and 11

The carbobicyclic bridged moiety was modified at two different regions. The first one is located between C(7) and C(11) atoms, and in position 13. The first synthetized huprine (±)-**3** beared a methylene bridge. During the hit-to-lead optimization process, huprines with a *o*-phenylene bridge, methoxy, methyl, keto, ethylidene or different amino groups at this position were developed.

Intermediate (±)-**23** (7-methylbicyclo[3.3.1]non-6-en-3-one) had been previously prepared by distinct procedures starting from adamantine derivatives. Camps *et al.*[128] reported the synthesis of (±)-**23** in four steps from diketone **7** (Scheme 4) and this pathway has been generally used in the preparation of several huprines (see Scheme 1). The initial step in the synthesis of compound (±)-**3** was the nucleophilic addition of a methyllithium or methylmagnesium reagent to bicyclo [3.3.1]nonane-3,7-dione (**7**). This resulted in the formation of hemiacetal **21**. Its transformation(dehydration) into a racemic mixture of enone (±)-**23** was attempted with *p*-toluenesulfonic acid (*p*-TsOH) or 4 Å molecular sieves in refluxing toluene; however, it did not yield the desired product. Instead, the mesylation of **21** was achieved using methanesulfonyl chloride in the presence of $Et_3N$ to produce mesylate **22**. The reaction of **22** with lithium diisopropylamide (LDA) did not result in a base-induced fragmentation to produce (±)-**23**. However, the treatment of **22** with silica gel (acid-promoted fragmenta-

**Scheme 4**

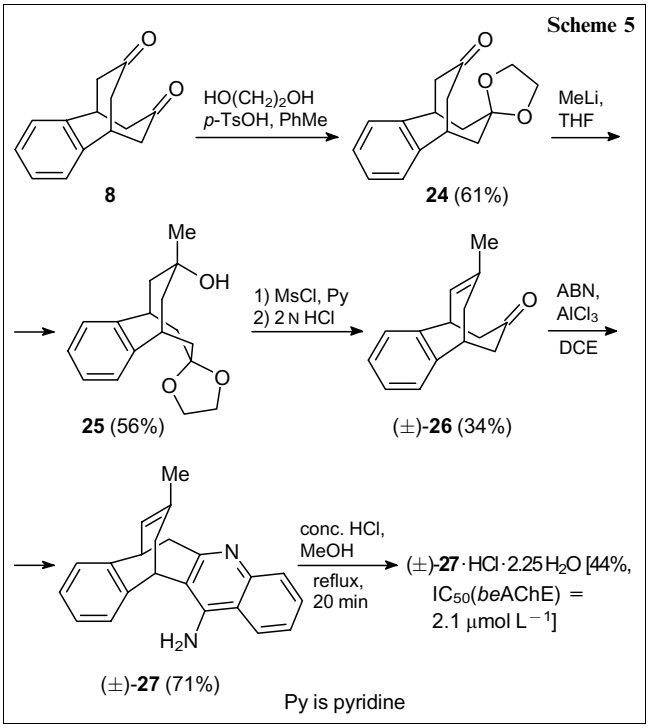



ABN is 2-aminobenzonitrile; Ms is mesyl

tion) enabled the isolation of intermediate (±)-**23** with small traces of oxaadamantanol **21** as a side product.[128] Huprine (±)-**3** was obtained by the Friedländer condensation of ketone (±)-**23** with 2-aminobenzonitrile and was then converted into the corresponding hydrochloride using concentrated HCl.[5] The resolution of the racemic mixture (±)-**3** was achieved by chiral MPLC, through this method samples of (−)-**3** [>90% enantiomeric excess (*ee*)] and (+)-**3** (>80% *ee*) were obtained. Both enantiomers were modified into hydrochlorides (−)-**3**·HCl·0.5 $H_2O$ and (+)-**3**·HCl·2/3 $H_2O$.[6] The racemic mixture (±)-**3** ($IC_{50}$ = 65 nmol $L^{-1}$) displayed two-times higher inhibitory potency against *be*AChE than THA. Its eutomer (−)-**3** showed an even better activity, with $IC_{50}$ = 47 nmol $L^{-1}$, being roughly seven-times more potent than its enantiomer (+)-**3**.

Huprine (±)-**27** possesses a *o*-phenylene bridge between positions 7 and 11. Accordingly, diketone **8** (6,7,8,9-tetrahydro-5,9-propane-5*H*-benzocycloheptene-7,11-dione) was applied for its synthesis (Scheme 5). Synthesis of (±)-**26** was firstly attempted following the synthetic route illustrated in Scheme 1.[128] Acid-promoted fragmentation of the corresponding mesylate failed possibly due to relative stability of the carbocation formed during this reaction. Huprine (±)-**27** was furnished by selecting an altered synthetic procedure described below (see Scheme 5). Treatment of diketone **8** with ethylene glycol in the presence of *p*-TsOH resulted in the protection of one C=O group to produce dioxolane **24**.[129] Its transformation into alcohol **25** was achieved *via* nucleophilic addition of methyllithium. The reaction of **25** with MsCl, followed by elimination of the OMs group and removal of acetal resulted in enone

**Scheme 5**




(±)-**26** which was subjected to the Friedländer condensation to produce a final product, (±)-**27**, exerting moderate potency against *be*AChE ($IC_{50}$ = 2.1 μmol $L^{-1}$).[5,129]

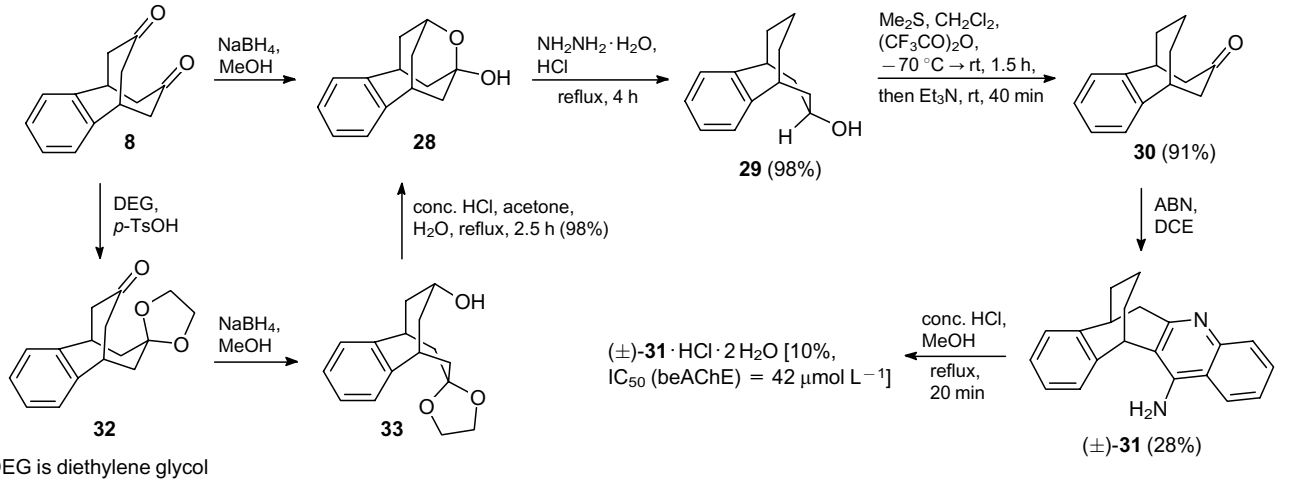
Another huprine bearing a *o*-phenylene bridge is compound (±)-**31**. Its synthesis was initiated similarly, *i.e.* with diketone **8**, which was converted into hemiacetal **28** using sodium borohydride in methanol (Scheme 6).[129] The exposure of oxaadamantanol **28** to Wolff–Kishner reduction conditions furnished alcohol **29**. Ketone **30** was generated upon treatment of **29** with $Me_2S$ and $(CF_3CO)_2O$ and then with $Et_3N$ (Swern oxidation) with ongoing 2-aminobenzonitrile condensation to provide huprine (±)-**31**.[5,129] The alternative synthetic route for intermediate **28** started with protecting one of the carbonyl functionalities of diketone **8** that led to derivative **32**. Its reduction with $NaBH_4$ produced alcohol **33**. Removal of the ketal group using HCl was followed by intramolecular cyclization to give hemiacetal **28**.[129]

Compounds (±)-**19** (see Scheme 3) and (±)-**34** contain an *o*-phenylene bridge between positions 7 and 11 but differ in a substituent at position 9. Huprine (±)-**19** was prepared directly by the Friedländler condensation of **8** with 2-aminobenzonitrile and retained the keto functional group at position 9. Derivative (±)-**34** was derived from ketone (±)-**19** by reduction with $NaBH_4$ producing *endo*-hydroxyl at position 9 (Scheme 7).[5]

All analogues carrying the benzobicyclo[3.3.2]decane scaffold, (±)-**27** (see Scheme 5), (±)-**31** (see Scheme 6) and (±)-**34** (see Scheme 7) replacing the bicyclo[3.3.1]nonane moiety characteristic of (−)-HupA, were much less active inhibitors of *be*AChE than THA. On the other hand, the derivative with a methyl group at position 9 was the most active [(±)-**27**: $IC_{50}$(*be*AChE) = 2.1 μmol $L^{-1}$].[5,129]

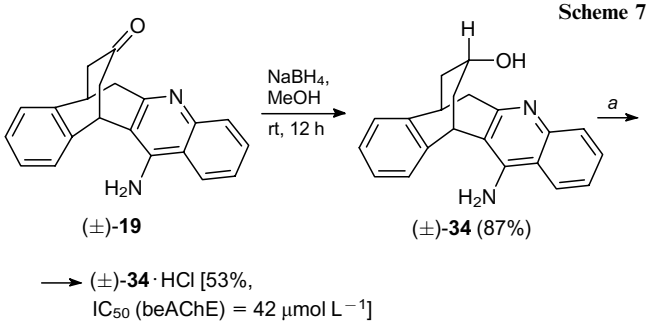
The reaction of 9,9-dimethoxybicyclo[3.3.1]nonane-3,7-dione (**10**) with methyllithium or methylmagnesium chloride gave oxaadamantanol **35** (Scheme 8).[128] Mesylate **36**, obtained from **35** by a standard procedure (MsCl, $Et_3N$), did not react with silica gel at room temperature to produce the corresponding enone. Using more forceful

**Scheme 6**




DEG is diethylene glycol

**Scheme 7**



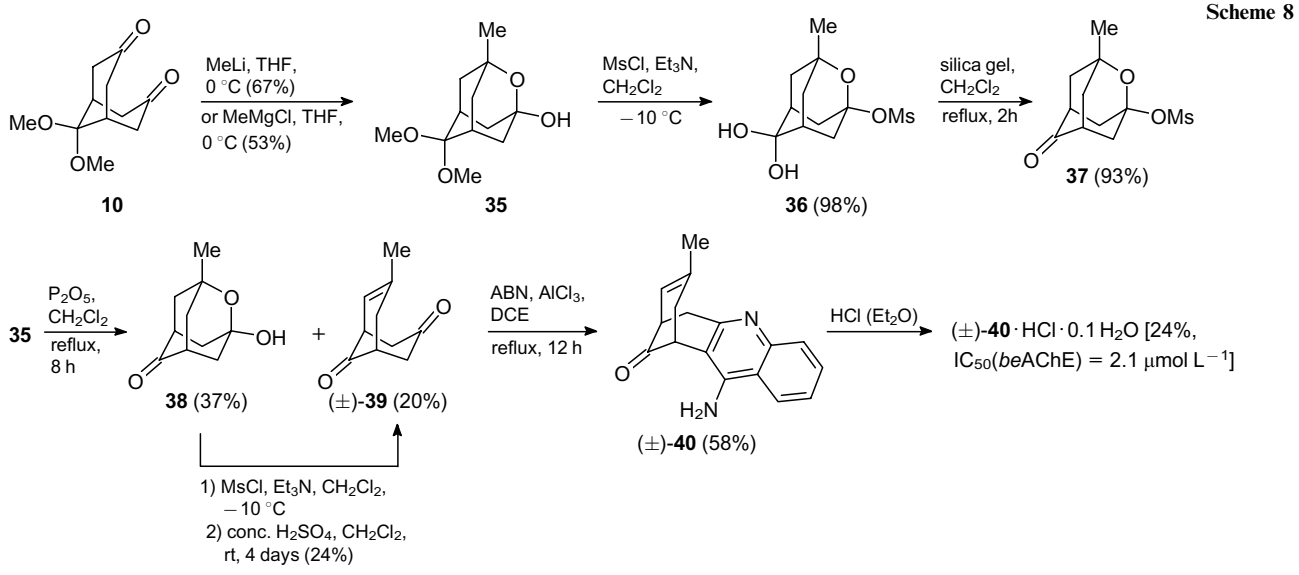

(*a*) conc. HCl, MeOH, reflux, 20 min

conditions (heating to reflux), the acetal functional group of compound **36** was hydrolyzed and compound **37** was obtained instead of the desired fragmentation product. The reaction of oxaadamantanol **35** with $P_2O_5$ afforded a mixture of **38** and enone (±)-**39**. The mesylation of compound **38** and ongoing fragmentation of the prepared corresponding intermediate with concentrated $H_2SO_4$ resulted in enone (±)-**39**.[128] The Friedländer condensation of (±)-**39** with 2-aminobenzonitrile produced a racemic mixture of huprine (±)-**40** that was converted into its hydrochloride using HCl.[5]

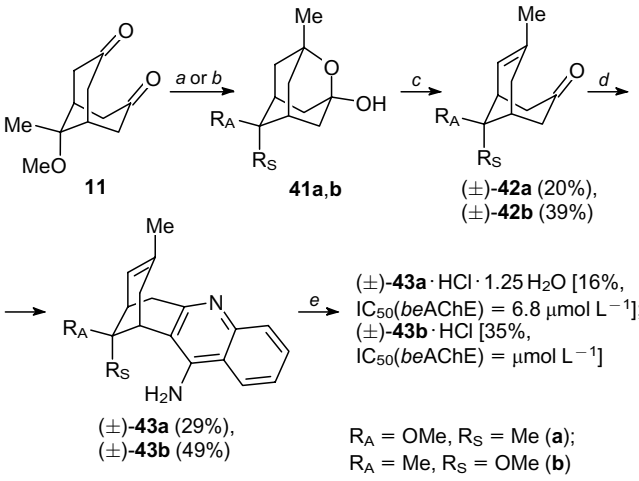
9-Methoxy-9-methylbicyclo[3.3.1]nonane-3,7-dione (**11**) was used as a starting molecule for huprines (±)-**43a**,**b** with methyl and methoxy groups, respectively, at position 13 (Scheme 9).[128] The addition of a nucleophile (methyl group) to diketone **11** was carried out with MeMgCl (conditions *a*) or MeLi (conditions *b*) resulting in a mixture of products **41a**,**b**. They were partially separated by column chromatography (18% and 36% yields for **41a** and **41b**, respectively) thus allowing the isolation of separate isomers. The configuration of oxaadamantanol **41b** was established by X-ray diffraction analysis. The reactions of **41a**,**b** with methanesulfonyl chloride (conditions *c*) provided mesylates that underwent silica gel-promoted fragmentation to enones (±)-**42a**,**b**. Their condensation with 2-aminobenzonitrile in the presence of $AlCl_3$ (conditions *d*) afforded huprines (±)-**43a**,**b** further obtained as hydrochloride salts (conditions *e*).[5]

Derivatives with polar substituents at position 13, namely, (±)-**40** (see Scheme 8) and (±)-**43a**,**b** (see Scheme 9), displayed inhibitory capacity against *be*AChE in the low micromolar range. The best potency was exerted by huprine (±)-**43b** with $IC_{50}$ = 1.3 μmol $L^{-1}$, which was roughly 21-fold less potent than the unsubstituted analogue

**Scheme 8**



**Scheme 9**



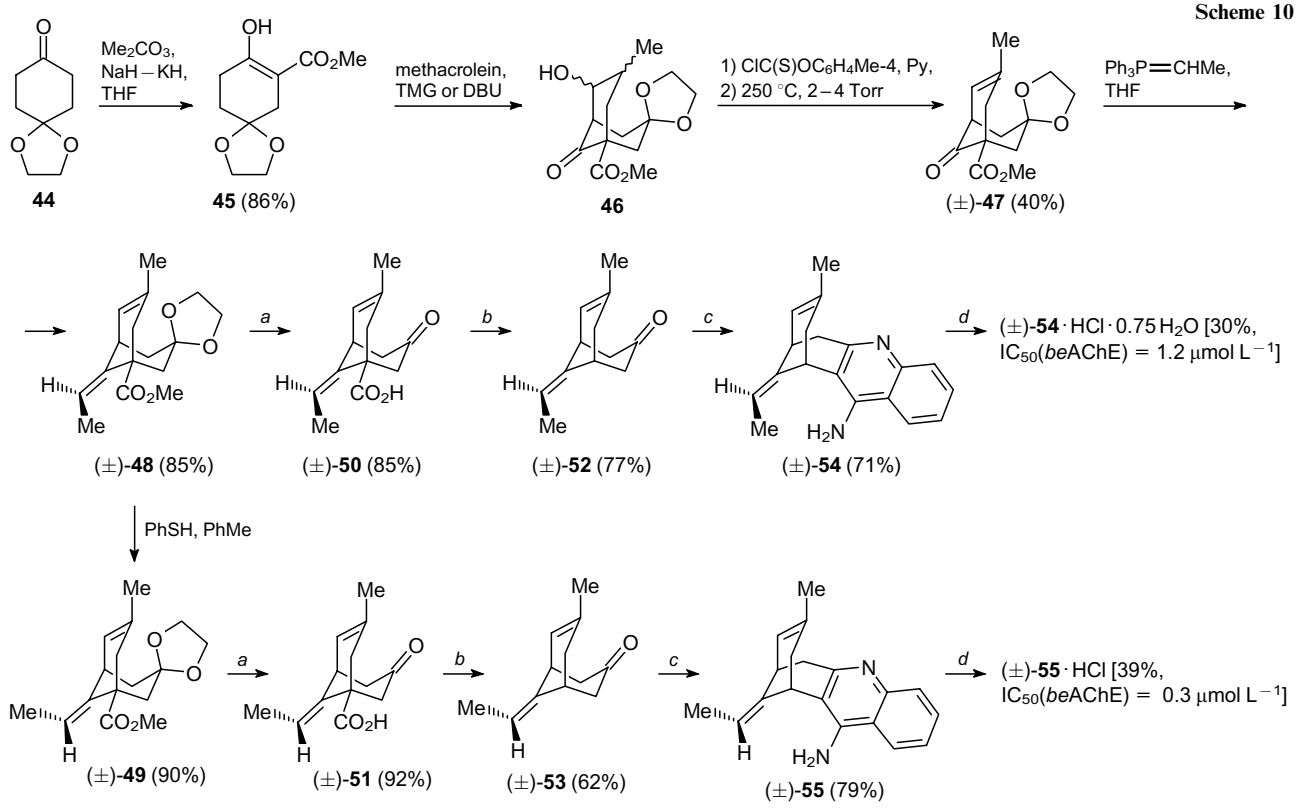

(*a*) MeMgCl, THF, 0 °C (88% combined yield **41a** : **41b** = 3 : 4);
(*b*) MeLi, THF, 0 °C (97% combined yield);
(*c*) MsCl, $Et_3N$, $CH_2Cl_2$, −10 °C; silica gel, $CH_2Cl_2$, rt;
(*d*) ABN, $AlCl_3$, DCE; reflux, 12 h;
(*e*) solution of HCl in $Et_2O$

(±)-**3** [$IC_{50}$(*be*AChE) = 65 nmol $L^{-1}$] and 10-fold less potent than THA [$IC_{50}$(*be*AChE) = 0.1 μmol $L^{-1}$].

Huprines (±)-**54** and (±)-**55** with an ethylidene group at position 13 were synthesized from ketone **44** converted into ester **45** by treatment with $Me_2CO_3$ (Scheme 10).[5] Its exposure to methacrolein together with catalytic amounts of 1,1,3,3-tetramethylguanidine (TMG) or 1,8-diazabicyclo[5.4.0]undec-7-ene (DBU) furnished a mixture of alcohols **46**. Treatment of **46** with *O*-(*p*-tolyl)thiocarbonate with follow-up heating at 250 °C enabled their dehydration and keto ester (±)-**47** was isolated in 40% yield.[130] The Wittig reaction of intermediate (±)-**47** with triphenylethylidenephosphorane led to a mixture of corresponding alkenes.[5] This mixture contained (*Z*)-isomer (±)-**48** as a major component and about 5% of (*E*)-isomer (±)-**49**. The hydrolysis of (±)-**48** afforded acid (±)-**50** which did not contain ester or acetal functional groups. Its decarboxylation through Barton procedure[131] produced enone (±)-**52**, which was submitted to condensation with 2-aminobenzonitrile to produce the final (±)-**54**. Thiophenol-induced isomerization of (±)-**48** resulted in a mixture of esters with (*E*)-isomer (±)-**49** (95%) prevailing over (*Z*)-isomer (5%). Huprine (±)-**55** was synthesized from (±)-**49** following the same sequence of reactions as huprine (±)-**54** which, in turn, was derived from ester (±)-**48** [through a three-step procedure: a) hydrolysis, b) decarboxylation and c) Friedländer condensation]. Both isomers were converted into corresponding hydrochlorides.[5] Derivatives (±)-**54** and (±)-**55** slightly resemble (−)-HupA by possessing a carbobicyclic substructure; based on this fact, it was assumed that these compounds would have better anti-AChE properties than the reference compounds. However, huprines (±)-**54** and (±)-**55** were less potent *be*AChEI than THA [$IC_{50}$(*be*AChE) = 0.1 μmol $L^{-1}$] with $IC_{50}$ values of 0.3 μmol $L^{-1}$ and 1.2 μmol $L^{-1}$, respectively.

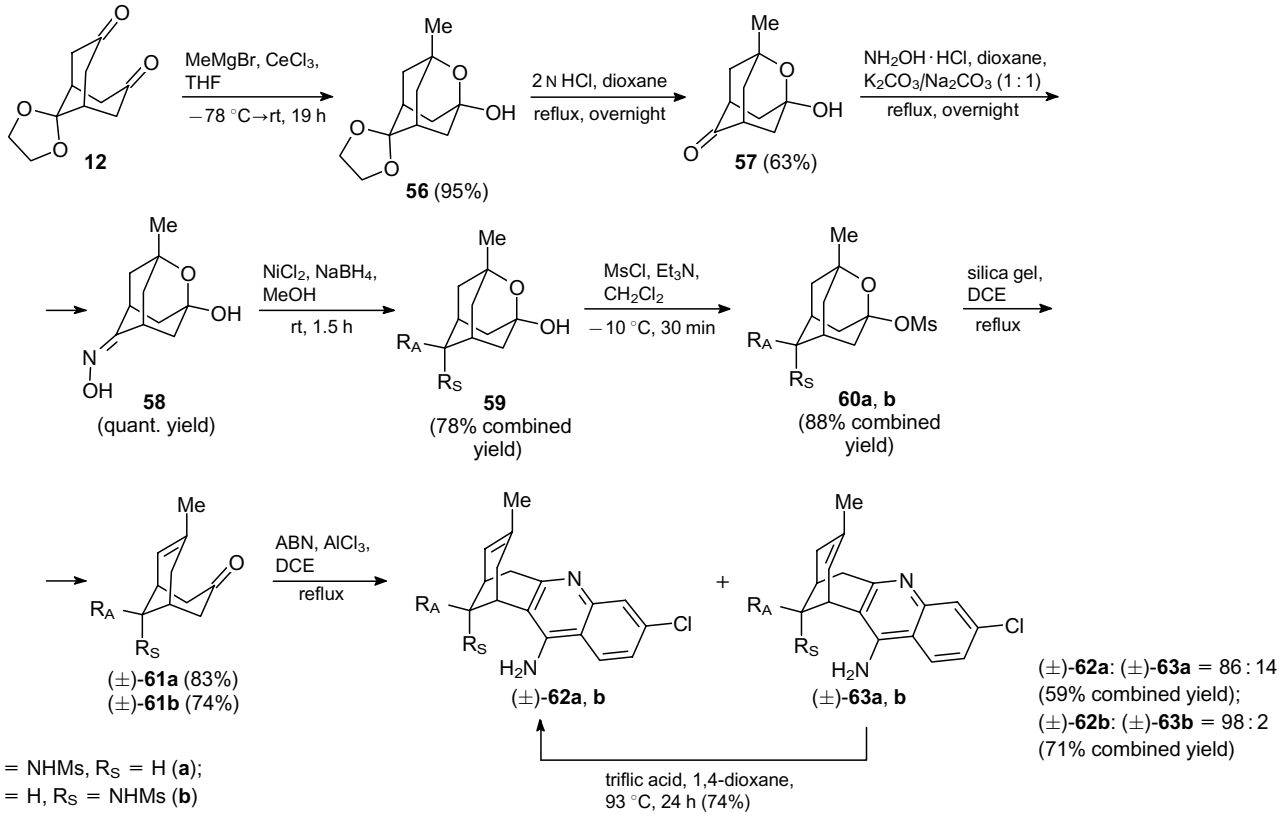
The synthesis of 13-amino and 13-amido derivatives of **1** was reported by Camps *et al.*[99,100] The treatment of diketone **12** with $MeCeCl_2$ resulted in a methyl group addition into one of the keto functionalities from the starting

**Scheme 10**




(*a*) 1) 20% NaOH, $H_2O$, MeOH, THF, Δ, 48 h; 2) 2 N HCl, dioxane, rt, 4 h; (*b*) 1) $SOCl_2$, PhMe, 80 °C, 4 h, 2) Bu$^t$SH, DMAP, PhMe, 2-mercaptopyridine *N*-oxide sodium salt, reflux, 14 h; (*c*) ABN, $AlCl_3$, 1DCE; (*d*) solution of HCl in $Et_2O$; TMG = $Me_2NC(=NH)NMe_2$, DBU is 1,8-diazabicyclo[5.4.0]undec-7-ene

**Scheme 11**




(±)-**62a**: $IC_{50}$(*be*AChE) = 39 nmol $L^{-1}$, $IC_{50}$(*h*AChE) = 41 nmol $L^{-1}$; $IC_{50}$(*h*BChE) ⩾ $10^5$ nmol $L^{-1}$; (±)-**62b**: $IC_{50}$(*be*AChE) = 2500 nmol $L^{-1}$

material to produce oxaadamantanol **56** (Scheme 11).[99] Ketone transformation into **57** was achieved by hydrolyzing acetal with HCl in dioxane. The amino group was inserted in two steps. An initial reaction of **57** with $NH_2OH$ yielded oxime **58** which was transformed into an inseparable mixture of amine **59** by combining nickel chloride and $NaBH_4$. Mesylation of **59** was accomplished with MsCl in the presence of $Et_3N$ to obtain a mixture of mesylates **60a**,**b**, which were then separated by column chromatography. Their recrystallization from EtOAc resulted in diastereopure **60a**,**b**. The *anti*–*syn* arrangement of methanesulfonamido and methanesulfonyloxy groups of **60a**,**b** was concluded through the observation of cross-peaks in the COSY $^1H-^1H$ spectrum and later confirmed by X-ray analysis. Compounds **60a**,**b** were subjected to the reaction with silica gel in 1,2-dichloroethane under reflux to produce enones (±)-**61a** (83%) and (±)-**61b** (74%). When the fragmentation of **60a** took longer than 45 min, the formation of enone (±)-**61b** was observed instead of (±)-**61a** (see Scheme 11). The condensation of (±)-**61a** and (±)-**61b** with 2-amino-4-chlorobenzonitrile was achieved in the presence of $AlCl_3$ to produce an inseparable mixture of huprine (±)-**62a** and its *syn*-isomer (±)-**63a** [(±)-**62a** : (±)-**63a** = 86 : 14, $^1H$ NMR] and a mixture of huprine (±)-**62b** and its *syn*-isomer (±)-**63b**, which were separated by column chromatography. An inseparable mixture of (±)-**62a** and (±)-**63a** with triflic acid allowed the isomerization of (±)-**63a**, from which only (±)-**62a** was isolated.[99]

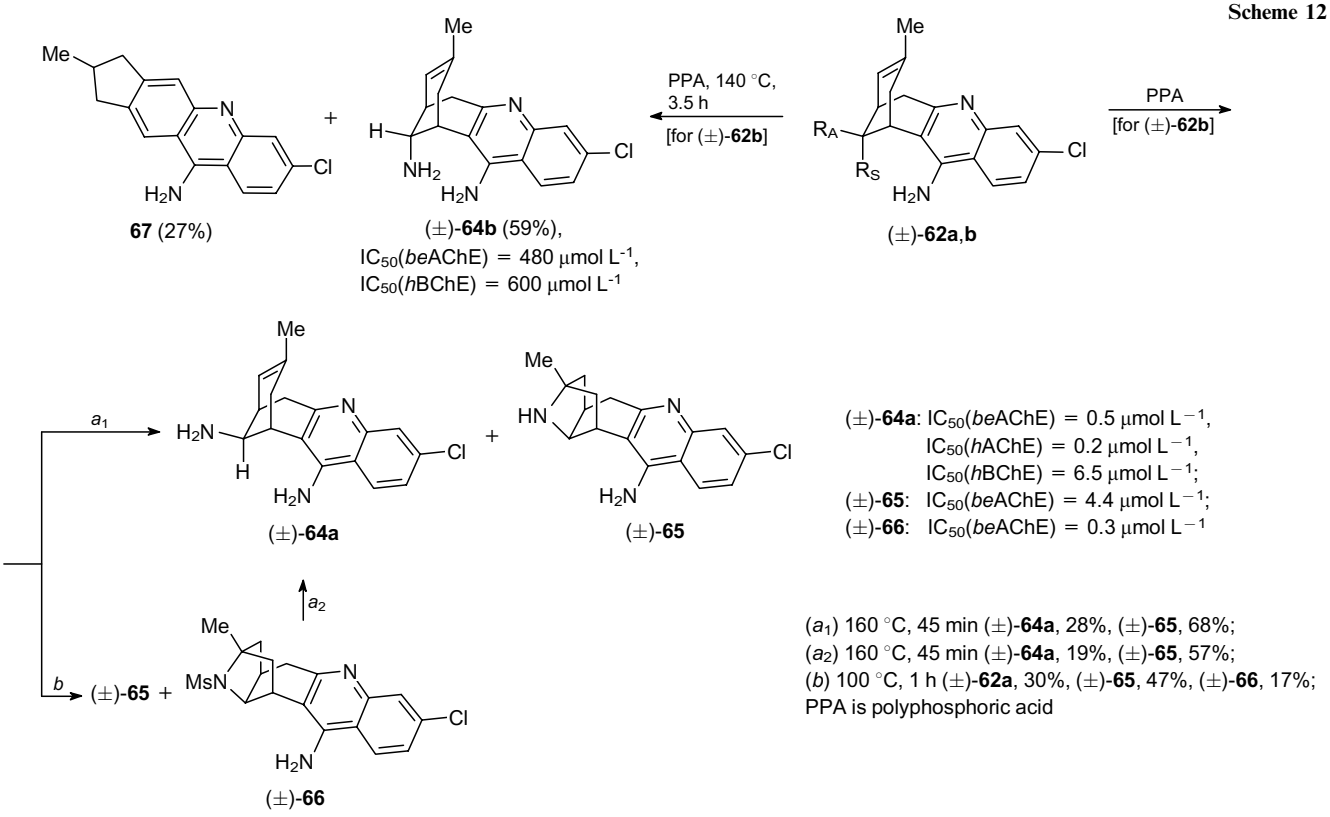
The methanesulfonyl group of huprine (±)-**62a** was deprotected by hydrolysis with polyphosphoric acid (PPA).[100] The conditions of choice for this reaction included 160 °C for 45 min (conditions *a*) allowing the formation of the desired amine (±)-**64a** (though in low yield) and by-product (±)-**65** which were separated *via* column chromatography (Scheme 12). At 100°C for 1 h (conditions *b*) two products were generated; however, neither of them was the expected compound (±)-**64a**. Also, unreacted (±)**62a** (30%) remained. The treatment of (±)-**66** with PPA at 160 °C for 45 min yielded amines (±)-**64a** and (±)-**65**. The methanesulfonamide (±)-**62b** was converted into (±)-**66** only in a reversible manner by applying successive treatment with PPA followed by heating, probably by protonation of the C=C bond at the less substituted carbon atom to produce a tertiary carbocation, followed by the intramolecular addition of the sulfonamide nitrogen atom and deprotonation.[100]

Similarly, the Ms protecting the amide group of (±)-**62b** was removed with PPA (see Scheme 12). The best conditions for this reaction were found to be 140 °C for 3.5 h allowing the formation of amine (±)-**64b** and a by-product **67**. In this case, the generation of aminocyclopentaacridine **67** was probably due to 1,2-migration of C(10) from C(11) to C(13) (resulting in an electron deficiency when leaving the protonated sulfonamide group, together with deprotonation of the resulting carbocation and isomerization of the C=C bond).[100]

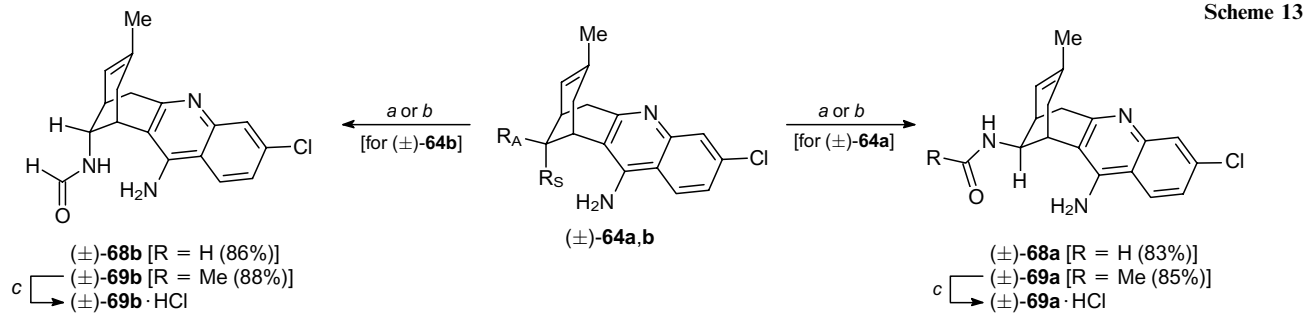
Amines (±)-**64a**,**b** were subjected to a reaction with mixtures of $HCO_2H-Ac_2O$ or $AcOH-Ac_2O$ to produce formamides (±)-**68a**,**b** and acetamides (±)-**69a**,**b**, which were transformed into hydrochlorides (±)-**69a**,**b**·HCl (Scheme 13).[100]

The discovered 13-amidohuprines (±)-**62a**,**b**, (±)-**68a**,**b**, (±)-**69a**,**b**, as well as 13-aminohuprines (±)-**64a**,**b** and by-products **65** and **66** were tested for their inhibitory capacity

**Scheme 12**




**Scheme 13**




(*a*) $HCO_2C$, $Ac_2O$, reflux [for (±)-**68a**]; (*b*) AcOH, $Ac_2O$, reflux [for (±)-**69a**]; (c) HCl, MeOH, rt;
(±)-**68a**: $IC_{50}$(*be*AChE) = 84 nmol $L^{-1}$, $IC_{50}$(*h*AChE) = 98 nmol $L^{-1}$, $IC_{50}$(*h*BChE) $\geqslant 10^5$ nmol $L^{-1}$; (±)-**69a**: $IC_{50}$(*be*AChE) = 1400 nmol $L^{-1}$;
(±)-**68b**: $IC_{50}$(*be*AChE) = 720 nmol $L^{-1}$; (±)-**69b**: $IC_{50}$(*be*AChE) = 1300 nmol $L^{-1}$

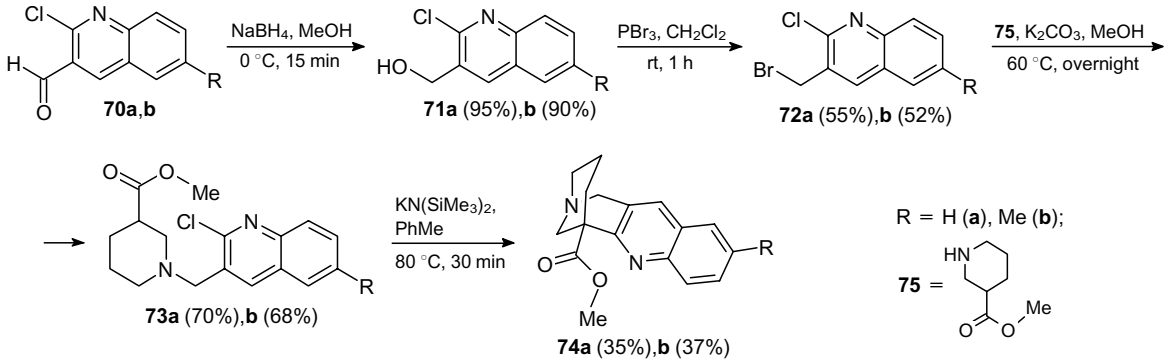
against *be*AChE, *h*AChE and *h*BChE. The derivatives of the **a** series were more potent *be*AChEIs than their counterparts from the series **b**. The most active inhibitors were (±)-**62a** [$IC_{50}$(*be*AChE) = 39 nmol $L^{-1}$] and (±)-**68a** [$IC_{50}$(*be*AChE) = 84 nmol $L^{-1}$]. Their inhibition efficacy was also increased regarding *h*AChE [for (±)-**62a**: $IC_{50}$(*h*AChE) = 41 nmol $L^{-1}$, for (±)-**68a**: $IC_{50}$(*h*AChE) = 98 nmol $L^{-1}$]. Moreover, these compounds were found to be more potent *h*AChEIs than THA and (−)-HupA, but less potent than the parent **1**. Derivatives (±)-**62a** and (±)-**64a** were highly selective for *h*AChE over *h*BChE.

The structures of **74a**,**b** apparently mimic the huprine scaffold by containing a quinoline moiety and a bicyclic bridge subunit. The preparation of the analogues **74a** and **74b** started with the reduction of carbonyl functionality of **70a** and **70b**, respectively, by using sodium borohydride (Scheme 14).[132] The substitution of the OH group was mediated by $PBr_3$ to produce quinolines **71a** and **71b**. The treatment of bromides **72a**,**b** with methyl 3-piperidinecarboxylate (**75**) in the presence of $K_2CO_3$ resulted in their amination to produce intermediates **73a**,**b**, respectively. Base-promoted deprotonation of ester α-carbon and the subsequent nucleophilic aromatic substitution resulted in the final products **74a**,**b**. However, these two derivatives were inactive against electric eel AChE (*Ee*AChE).

#### 3.1.2.2. Structural modifications at the three-carbon bridge between positions 7 and 11

As a second part, the three-carbon bridge between C(7) and C(11) atoms or position 9 of huperzine A-like carbobicyclic compound was modified. The 'simplest' huprine contained a hydrogen atom at position 9. Camps *et al.*[5] reported huprines containing different alkyl, alkenyl or aryl groups using the nucleophilic addition of the appropriate organometallic reagent to diketone **7**. Huprines with functional

**Scheme 14**



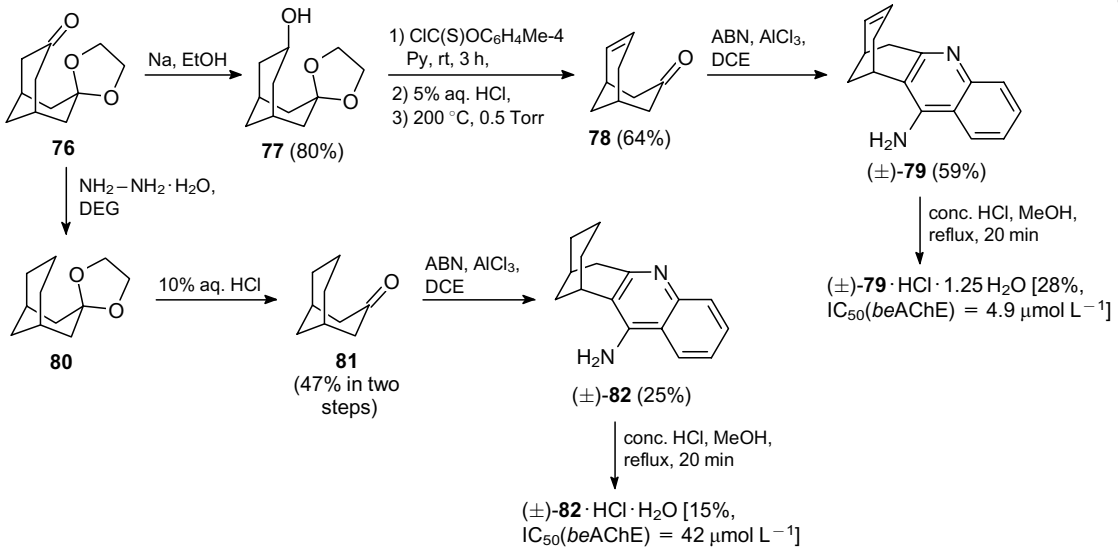

groups at this position were also synthesized. The preparation of derivatives with *endo* – *exo* alcohol functionality at position 9 were prepared as well as huprines with carbon chains terminated with other groups, including ester, carboxy, hydroxy, amido, amino, azido, methoxy, mesyl, nitro, *etc*., was reported.

The synthesis of huprines (±)-**79** and (±)-**82** with a hydrogen atom at position 9 but different in the character of the bond between C(8) and C(9) (unsaturated for compound **79**, saturated for **82**) started from the known protected ketone **76** (Scheme 15).[5] Reduction of the keto group of **76** using sodium afforded *exo*-alcohol **77**. Its treatment with $ClC(S)OC_6H_4Me$-4 and then with HCl resulted in dehydrated adduct **78** which was subjected to the Friedländer condensation resulting in huprine (±)-**79**. The Wolff – Kishner reduction of carbonyl functionality of compound **76** yielded acetal **80**. Acidic hydrolysis of **80** upon treatment with HCl produced ketone **81** and the final product (±)-**82** was prepared through the reaction of **81** with 2-aminobenzonitrile. Both huprines were converted into hydrochlorides. Biological evaluation revealed that unsaturated compound (±)-**79** was, by one-digit, a better inhibitor than its saturated analogue (±)-**82**, being 38-times less active than THA.

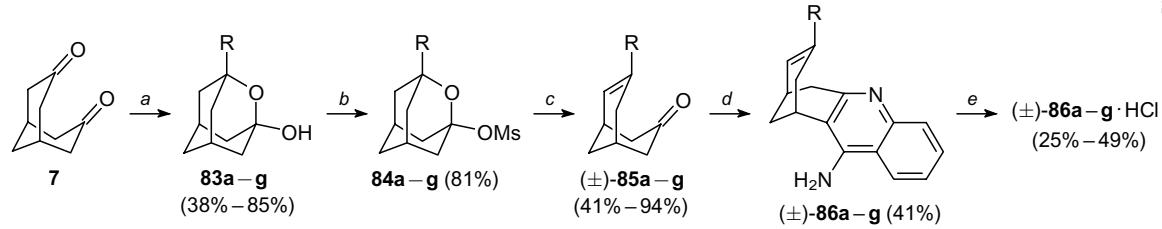
Huprines (±)-**86a** – **g**, differing in substitution at position 9, were obtained in four steps from diketone **7** (Scheme 16).[5,133] Initially, organometallic reagents were employed in the attachment to oxaadamantanols **83a** – **g**. Each final huprine was obtained as the corresponding hydrochloride salt. The separation of (±)-**86a** was achieved by MPLC and this method offered (−)-**86a** (> 90% *ee*) and (+)-**86a** (> 85% *ee*) which were converted into hydrochlorides (−)-**86a** · HCl (99% *ee*) and (+)-**86a** · HCl (99% *ee*), respectively.[6] All these huprines were tested for their inhibitory capacity against *be*AChE; in the case of ethyl derivatives [(−)-**86a** · HCl and (+)-**86a** · HCl] also against *h*BChE. The best *be*AChEI was huprine (±)-**86a** bearing an ethyl substituent at position 9, the introduction of bulkier substituents in this position decreased their inhibitory potency. Analogues with $Pr^i$ [(±)-**86c**], allyl [(±)-**86f**] and phenyl [(±)-**86g**] substituents exhibited almost equal AChE affinity comparable to THA [$IC_{50}$(*be*AChE) = 0.1 μmol $L^{-1}$], while the analogues with $Pr^n$ [(±)-**86b**], $Bu^n$ [(±)-**86d**] and $Bu^t$ [(±)-**86f**] substituents were two – three-fold less active. The ethyl derivative [(±)-**86a**] was more active than its methyl analogue (±)-**3** [$IC_{50}$(*be*AChE) = 65 nmol $L^{-1}$, Scheme 4]. The levorotatory isomer of **86a** was nearly 32-times more active than its enantiomer [for (−)-**86a**: $IC_{50}$(*be*AchE) = 27 nmol $L^{-1}$; for (+)-**86a**: $IC_{50}$(*be*AChE) = 890 nmol $L^{-1}$].

Huprines (±)-**88** and (±)-**89** bearing an alcohol moiety at position 9 are *exo*- and *endo*-isomers, respectively. Derivative (±)-**88** was prepared from *exo*-alcohol **87** in two steps (Scheme 17).[5] The first step involved the acid hydrolysis using AcOH giving ketone **87** that, in turn, condensed with 2-aminobenzonitrile affording *exo*-derivative (±)-**88**. Analogue (±)-**89** was synthetized from diketone **7** in two steps. The Friedländer reaction of **7** with 2-amino-

**Scheme 15**

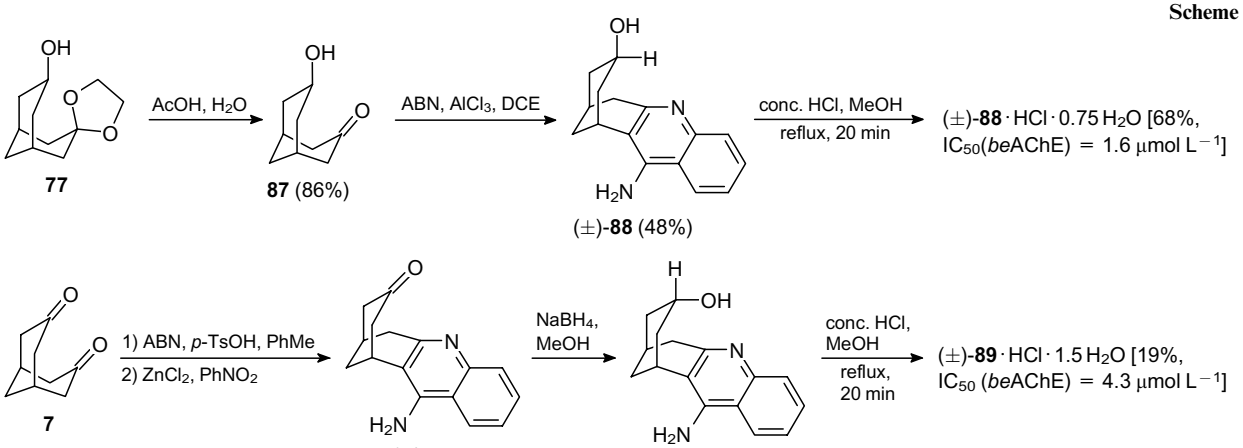


**Scheme 16**




(*a*) RLi or RMgHal, THF, $CeCl_3 \cdot 7H_2O$ (for **83b – c**, **83e**); (*b*) MsCl, $Et_3N$, $CH_2Cl_2$; (*c*) silica gel, $CH_2Cl_2$; (*d*) $AlCl_3$, ABN, DCE, reflux;
(e) MeOH, solution of HCl in $Et_2O$; R = Et (**a**), $Pr^n$ (*b*), $Pr^i$ (**c**), $Bu^n$ (**d**), $Bu^t$ (**e**), All (**f**), Ph (**g**);
(±)-**86a** · HCl: $IC_{50}$(*be*AChE) = 0.04 mmol $L^{-1}$, $IC_{50}$(*h*AChE) = 0.04 mmol $L^{-1}$, $IC_{50}$(*h*BChE) = 0.08 mmol $L^{-1}$;
(±)-**86b** · HCl: $IC_{50}$(*be*AChE) = 0.4 mmol $L^{-1}$; (±)-**86c** · HCl: $IC_{50}$(*be*AChE) = 0.1 mmol $L^{-1}$; (±)-**86d** · HCl: $IC_{50}$(*be*AChE) = 0.3 mmol $L^{-1}$;
(±)-**86e** · HCl: $IC_{50}$(*be*AChE) = 0.3 mmol $L^{-1}$; (±)-**86f** · HCl: $IC_{50}$(*be*AChE) = 0.2 mmol $L^{-1}$; (±)-**86g** · HCl: $IC_{50}$(*be*AChE) = 0.1 mmol $L^{-1}$

**Scheme 17**



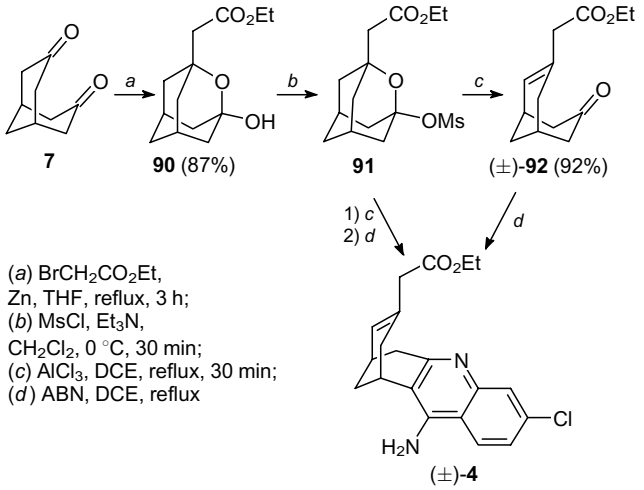

Ts is tosyl

benzonitrile produced ketone (±)-**16**,[4] which underwent carbonyl reduction upon treatment with $NaBH_4$ yielding *endo*-derivative (±)-**89**.[5] Both alcohols were converted into corresponding hydrochlorides. The $IC_{50}$ values for *be*AChE inhibition laid in the low micromolar range, slightly favouring *exo*-analogue (±)-**88**; however, it did not reach the inhibition efficacy of THA [$IC_{50}$(*be*AChE) = 0.1 μmol $L^{-1}$].

Ronco *et al.*[103] discovered ester (±)-**4**, which represents a precursor for a family of novel huprines with functionalized position 9. The ester group at position 9 was introduced *via* the Reformatsky reaction of diketone **7** with ethyl bromoacetate in the presence of activated zinc dust, affording oxaadamantanol **90** (Scheme 18).[103] Its mesylation was performed under standard conditions resulting in intermediate **91**. The next step, acid-promoted fragmentation, was attempted as described previously using silica gel with dichloromethane but it was fruitless. The optimized conditions for the fragmentation of mesylate **91** included aluminium trichloride as Lewis acid in 1,2-dichloroethane under reflux to produce enone (±)-**92**. Huprine (±)-**4** was prepared from ketone (±)-**92** by the Friedländer condensation using the standard protocol. The one-pot procedure for the fragmentation and Friedländer condensation were applied and compound (±)-**4** was obtained from **91**.[103] Oxaadamantanols **22** and **84a** were also subjected to this procedure to obtain huprines (±)-**1** and (±)-**2** (Scheme 19).

In an effort to expand the huprine family, (±)-**93b – d** with a chlorine atom at position 12 were discovered also in a one-pot procedure using $AlCl_3$ for the fragmentation of

**Scheme 18**

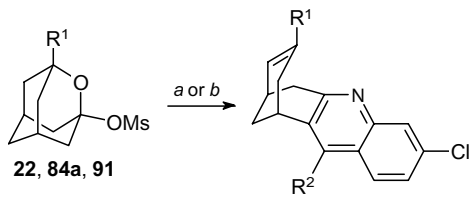



(*a*) $BrCH_2CO_2Et$, Zn, THF, reflux, 3 h;
(*b*) MsCl, $Et_3N$, $CH_2Cl_2$, 0 °C, 30 min;
(*c*) $AlCl_3$, DCE, reflux, 30 min;
(*d*) ABN, DCE, reflux

mesylates **22**, **84a** and **91**. This resulted in the formation of the corresponding enones that were directly submitted to the reaction with 2-amino-4-chlorobenzoic acid and then $POCl_3$ to produce the final products **93b – d**.[103]

After the successful development of the synthetic pathway for (±)-**4**, twenty three new huprine analogues (±)-**94 – 116** were prepared in one to five steps by trans-

**Scheme 19**




**22**, **84a**, **91**

(±)-**1** (89%), (±)-**2** (85%),
(±)-**93b** (40%), (±)-**93c** (37%),
(±)-**93d** (44%)

(*a*) 1) $AlCl_3$, DCE, reflux, 30 min; 2) ABN, DCE, reflux, overnight;
(*b*) 1) $AlCl_3$, 4 Å MS, DCE, reflux, 30 min; 2) ABN, 1-4-dioxane, rt, 10 min then $POCl_3$, 0 °C → reflux, overnight;
(±)-**1**, (±)-**2**: $R^2$ = Cl; **93**: $R^2$ = Cl: $R^1$ = Me (**b**), Et (**c**), $CO_2Et$ (**d**);
$R^1$ = Me (**22**), Et (**84a**), $CH_2CO_2Et$ (**91**)

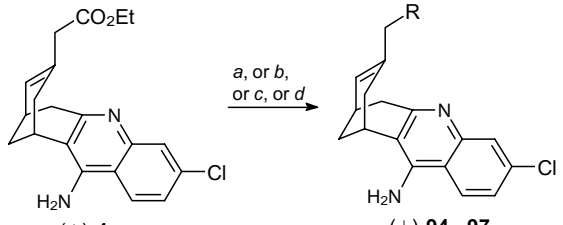
forming its ethyl ester functionality at position 9 of (±)-**4** into various functional moieties representing polar, protic and hydrogen-bond donating groups using the conditions described below (Schemes 20 – 24).[104]

Reduction of the ester from (±)-**4** into alcohol (±)-**94** was accomplished with $LiAlH_4$ (Scheme 20). Amide (±)-**95** was generated upon treatment of (±)-**4** with $NH_3$ in the presence of a catalytic amount of NaCN. Alkaline hydrolysis was undertaken with a 2 M NaOH solution producing acid (±)-**96**, which was submitted to the reaction with $SOCl_2$ and then DMF to afford (±)-**97**.[104]

Exposure of alcohol (±)-**94** to different electrophilic reagents ($Ac_2O$, $(CF_3CO)_2O$, MsCl) yielded esters (±)-**98**, (±)-**99** and sulfonic ester (±)-**102** (Scheme 21).[104] Modification of (±)-**94** giving halogenated derivatives (±)-**100** and (±)-**101** was accomplished with thionyl chloride and diethylaminosulfur trifluoride (DAST). The treatment of (±)-**94** with triphosgene and subsequently with ammonia allowed the formation of amide (±)-**103** and ester (±)-**104** using acrylic acid chloride.[104]

Several huprine analogues were developed by mesylate (±)-**102** conversion (Scheme 22). Accordingly, treatment of (±)-**102** with different nucleophilic reagents (MeONa, KCN, NaI, $NaN_3$) enabled the substitution of the OMs group in methyl ether (±)-**105**, nitrile (±)-**106**, iodide (±)-**107** and azide (±)-**110**. Compound (±)-**102** was subjected to the reaction with (Boc)NHO(Boc) to obtain

**Scheme 20**

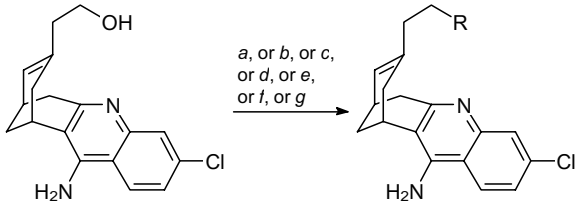



(±)-**4** (±)-**94** – **97**

(*a*) $LiAlH_4$, THF, 0 °C → rt, 1 h [(±)-**94**, 99%];
(*b*) NaCN, $NH_3$, EtOH, reflux, 6 days [(±)-**95**, 7% after prep. HPLC];
(*c*) aq. 2 M NaOH, reflux, 6.5 h [(±)-**96**, 99%];
(*d*) $SOCl_2$, DMF, 75 °C, 1.5 h [(±)-**97**, 65% after prep. HPLC];
(±)-**94**: R = $CH_2OH$, $IC_{50}$(*h*AChE) = 1.1 nmol $L^{-1}$,
$IC_{50}$(*h*BChE) = 1.2 μmol $L^{-1}$;
(±)-**95**: R = $C(O)NH_2$, $IC_{50}$(*h*AChE) = 29 nmol $L^{-1}$;
(±)-**96**: R = $CO_2H$, $IC_{50}$(*h*AChE) = 5.3 nmol $L^{-1}$;
(±)-**97**: R = $C(O)N(Me)_2$, $IC_{50}$(*h*AChE) = 26 nmol $L^{-1}$

(±)-**108**. Subsequent removal of its *tert*-butyloxycarbonyl (Boc) protecting group by acid hydrolysis yielded hydroxylamine (±)-**109**. Amine (±)-**111** was generated from azide (±)-**110** by following Staudinger procedure ($Ph_3P$, $H_2O$).[104, 134]

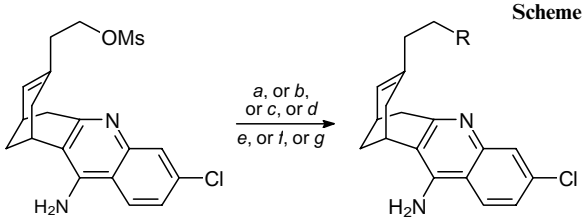
**Scheme 21**




(±)-**94** (±)-**98** – **104**

(*a*) $Ac_2O$, $Et_3N$, THF, reflux, 21 h [(±)-**98**, 18%];
(*b*) $(CF_3CO)_2O$, $Et_3N$, THF, rt, 40 min [(±)-**99**, 83%];
(*c*) $SOCl_2$, EtOAc, 60 °C, 14 h [(±)-**100**, 25% after prep. HPLC];
(*d*) DAST, THF, −78 °C, 1.5 h [(±)-**101**, 58%]; DAST = $Et_2NSF_3$;
(*e*) MsCl, $Et_3N$, THF, 0 °C → rt, 30 min [(±)-**102**, 94%];
(*f*) 1) triphosgene, MeCN, 65 °C, 20 min, then rt, 1.5 h,
2) $NH_3$ [(±)-**104**, 58% after prep HPLC];
(*g*) $CH_2{=}CHC(O)Cl$, $Et_3N$, THF, rt, 1 h [(±)-**103**, 34%];
(±)-**98**: R = OAc, $IC_{50}$(*h*AChE) = 1.4 nmol $L^{-1}$;
(±)-**99**: R = $OC(O)CF_3$, $IC_{50}$(*h*AChE) = 1.7 nmol $L^{-1}$;
(±)-**100**: R = Cl, $IC_{50}$(*h*AChE) = 3.6 nmol $L^{-1}$;
(±)-**101**: R = F, $IC_{50}$(*h*AChE) = 4.2 nmol $L^{-1}$;
(±)-**102**: R = OMs, $IC_{50}$(*h*AChE) = 8.5 nmol $L^{-1}$;
(±)-**103**: R = $OC(O)NH_2$, $IC_{50}$(*h*AChE) = 19 nmol $L^{-1}$;
(±)-**104**: R = $OC(O)CH{=}CH_2$, $IC_{50}$(*h*AChE) = 20 nmol $L^{-1}$

**Scheme 22**

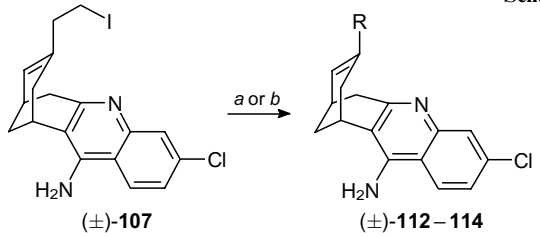



(±)-**102** (±)-**105** – **111**

(*a*) Na, MeOH, 65 °C, 24 h [(±)-**105**, 44%];
(*b*) KCN, TBAI, MeCN : DMF : DMSO (6 : 3 : 2, v/v/v), 70 °C, 5 h [(±)-**106**, 57%]; TBAI = $Bu^n_4NI$;
(*c*) NaI, acetone, reflux, 12 h [(±)-**107**, 54%];
(*d*) BocNH-OBoc, NaH, DMF, rt, 30 min, then 60 °C, 5 h [(±)-**108**, 46%];
(*e*) TFA : $CH_2Cl_2$ (1 : 2, v/v), rt, 48 h [(±)-**109**, 45% after prep. HPLC];
(*f*) $NaN_3$, DMF, 70 °C, 6 h [(±)-**110**, 84%];
(*g*) $Ph_3P$, $H_2O$, 0 °C → rt, 13 h [(±)-**111**, 60%];
(±)-**105**: R = OMe, $IC_{50}$(*h*AChE) = 1.7 nmol $L^{-1}$;
(±)-**106**: R = CN, $IC_{50}$(*h*AChE) = 3.1 nmol $L^{-1}$;
(±)-**107**: R = I, $IC_{50}$(*h*AChE) = 2.7 nmol $L^{-1}$;
(±)-**108**: R = N(Boc)O(Boc), $IC_{50}$(*h*AChE) = 15 nmol $L^{-1}$;
(±)-**109**: R = NHOH, $IC_{50}$(*h*AChE) = 9.7 nmol $L^{-1}$;
(±)-**110**: R = $N_3$, $IC_{50}$(*h*AChE) = 5.6 nmol $L^{-1}$;
(±)-**111**: R = $NH_2$, $IC_{50}$(*h*AChE) = 240 nmol $L^{-1}$;
Boc = $C(O)OBu^t$

Further nucleophilic substitution of iodide of (±)-**107** upon treatment with $HNMe_2$ and $NMe_3$ produced amine (±)-**112** and ammonium salt (±)-**113**, respectively. Compound (±)-**114** was isolated as an elimination by-product (Scheme 23).[104]

**Scheme 23**

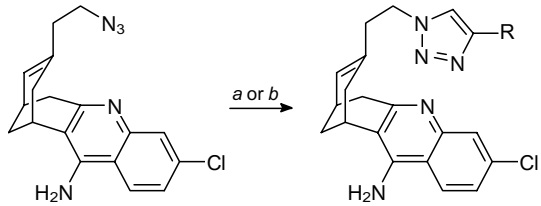


(±)-**107** (±)-**112** – **114**

(*a*) $HNMe_2 \cdot HCl$, $NaHCO_3$, EtOAc : MeCN (5 : 1, v/v), 76 °C, 13 h [(±)-**112**, 14% after prep HPLC];
(*b*) $NMe_3$, MeCN, 55 °C, 13 h [(±)-**113**, 27%, (±)-**114**, 55% after prep. HPLC];
(±)-**112**: R = $CH_2CH_2NMe_2$, $IC_{50}$(*h*AChE) = 100 nmol $L^{-1}$;
(±)-**113**: R = $[CH_2CH_2NMe_3]^+[CF_3COO]^-$, $IC_{50}$(*h*AChE) = 260 nmol $L^{-1}$;
(±)-**114**: R = CH=$CH_2$, $IC_{50}$(*h*AChE) = 260 nmol $L^{-1}$

1,2,3-Triazole derivative (±)-**115** was prepared through the 1,3-dipolar cycloaddition (Huisgen cycloaddition) of azide (±)-**110** and methyl propiolate (Scheme 24). The reduction of the ester group with $LiAlH_4$ resulted in alcohol (±)-**116**.[104]

**Scheme 24**

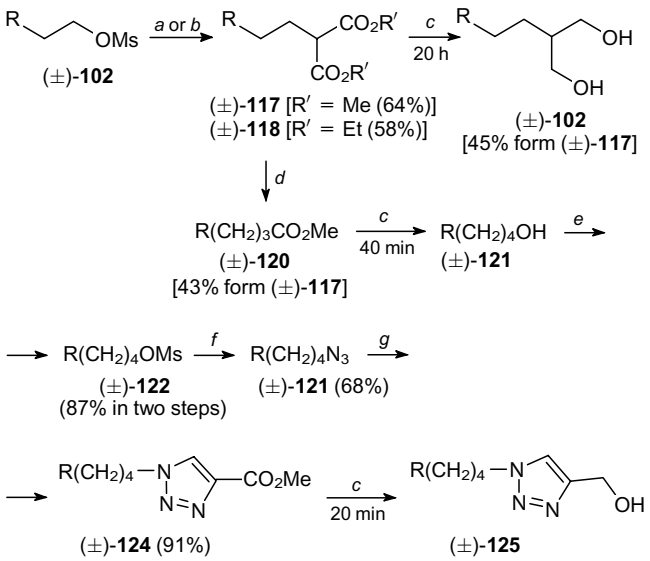


(±)-**110** (±)-**115**, **116**

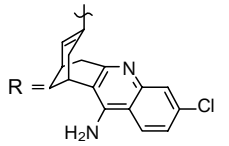
(*a*) HC≡$CCO_2Me$, CuI, MeCN, 25 h, rt [(±)-**115**, 60%];
(*b*) $LiAlH_4$, THF, 0 °C → rt, 30 min [(±)-**116**, 57% after prep. HPLC];
(±)-**115**: R = $CO_2Me$, $IC_{50}$(*h*AChE) = 130 nmol $L^{-1}$;
(±)-**116**: R = $CH_2OH$, $IC_{50}$(*h*AChE) = 210 nmol $L^{-1}$

All of the prepared derivatives were potent inhibitors of *h*AChE with $IC_{50}$ values in the nanomolar range.[104] The top-ranked derivative in the series was compound **94** [$IC_{50}$(*h*AChE) = 1.1 nmol $L^{-1}$, $IC_{50}$(*h*BChE) = 1.2 μmol $L^{-1}$] having almost the same activity as the reference huprine (±)-**2** [$IC_{50}$(*h*AChE) = 0.8 nmol $L^{-1}$, $IC_{50}$(*h*BChE) = 240 nmol $L^{-1}$]. Additionally, **94** also exerted the highest AChE selectivity index (SI for AChE = 1130). Regarding SAR, its inhibitory activity against AChE decreased with increasing bulkiness of the substituents. This finding was further corroborated through a molecular modeling study. Huprine (±)-**125** was developed in order to contact simultaneously both sites of AChE, CAS and PAS. Compounds (±)-**117** – **124** were obtained as intermediates during the synthesis of (±)-**125** (Scheme 25).[105] Compound (±)-**125** differs from (±)-**116** (see Scheme 24) by the length of the carbon chain between carbobicyclic and 1,2,3-triazole moieties. The synthesis of (±)-**125** started from mesylate (±)-**102**, which was converted into diesters (±)-**117** and (±)-**118** using dimethyl or diethyl malonate in the presence of Na. The exposure of ester (±)-**117** to sodium chloride in DMSO at high temperatures (Krapcho decarboxylation)[135] furnished intermediate (±)-**120**. Alcohol (±)-**125** was prepared from (±)-**120** in

**Scheme 25**



(*a*) $CH_2(CO_2Me)_2$, Na, THF, reflux, 5 days;
(*b*) $CH_2(CO_2Et)_2$, Na, EtOH, reflux, 44 h;
(*c*) $LiAlH_4$, THF; 0 °C → rt;
(*d*) NaCl, DMSO, $H_2O$, 170 °C, 7 h;
(*e*) MsCl, $Et_3N$, THF; 0 °C → rt, 30 min;
(*f*) $NaN_3$, DMF; 70 °C, 6 h;
(*g*) HC≡$CCO_2Me$, CuI, MeCN, rt, 23 h;



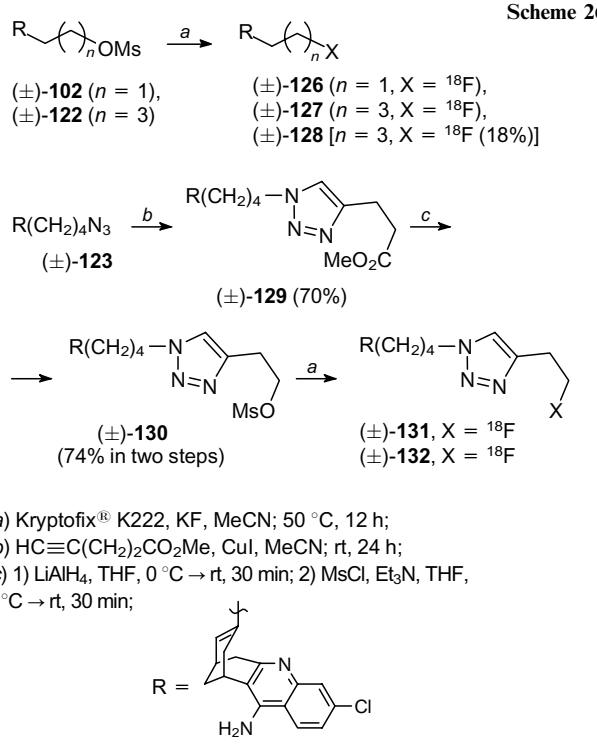
(±)-**117**: $IC_{50}$(*h*AChE) = 9.1 nmol $L^{-1}$, $IC_{50}$(*h*BChE) = 55 nmol $L^{-1}$;
(±)-**118**: $IC_{50}$(*h*AChE) = 4.8 nmol $L^{-1}$, $IC_{50}$(*h*BChE) = 0.2 μmol $L^{-1}$;
(±)-**119**: $IC_{50}$(*h*AChE) = 14 nmol $L^{-1}$, $IC_{50}$(*h*BChE) = 0.5 μmol $L^{-1}$;
(±)-**120**: $IC_{50}$(*h*AChE) = 8.4 nmol $L^{-1}$, $IC_{50}$(*h*BChE) = 33 nmol $L^{-1}$;
(±)-**122**: $IC_{50}$(*h*AChE) = 30 nmol $L^{-1}$, $IC_{50}$(*h*BChE) = 0.1 μmol $L^{-1}$;
(±)-**122**: $IC_{50}$(*h*AChE) = 8.0 nmol $L^{-1}$, $IC_{50}$(*h*BChE) = 80 nmol $L^{-1}$;
(±)-**123**: $IC_{50}$(*h*AChE) = 20 nmol $L^{-1}$, $IC_{50}$(*h*BChE) = 85 nmol $L^{-1}$;
(±)-**124**: $IC_{50}$(*h*AChE) = 0.5 nmol $L^{-1}$, $IC_{50}$(*h*BChE) = 0.3 μmol $L^{-1}$;
(±)-**125**: $IC_{50}$(*h*AChE) = 0.4 nmol $L^{-1}$, $IC_{50}$(*h*BChE) = 0.2 μmol $L^{-1}$

the same way as (±)-**116** from ester (±)-**4** (see Schemes 20 – 24).

All derivatives displayed good inhibitory activity against *h*AChE with $IC_{50}$ in the nanomolar range.[105] The most active were compounds **124** [$IC_{50}$(*h*AChE) = 0.5 nmol $L^{-1}$] and **125** [($IC_{50}$(*h*AChE) = 0.4 nmol $L^{-1}$] being five and six times more potent than the reference (±)-**2** [$IC_{50}$(*h*AChE) = 2.7 nmol $L^{-1}$]. Contrary to previously synthesized analogues **115** and **116** (see Scheme 24), novel huprines exhibited AChE inhibitory potency three orders of magnitude higher. This activity increment can be attributed to additional interactions of the triazole ring in the mid-gorge AChE region which was consequently confirmed by the X-ray diffraction analysis of a complex between **125** and *Mus musculus* AChE. Derivatives **124** and **125** also displayed an intriguing selectivity for AChE over BChE up to 560-fold.

Radiotracers can be used for non-invasive study of the cholinergic system. AChE tracers available for positron emission tomography (PET) are [$^{11}$C]-radiolabeled analogues of acetylcholine (*e.g.*, *N*-$^{11}$C-methylpiperidin-4-yl propionate) or AChE inhibitors such as [$^{11}$C]-physostigmine or [$^{11}$C]-donepezil.[136, 137] Besides [$^{11}$C]-labeled PET radiotracers, compounds labeled with $^{18}$F can be used for PET imaging.[138] In the work of Branquinho *et al.*[139] three huprine analogues (±)-**126**, (±)-**127** and (±)-**131** were syn-

**Scheme 26**

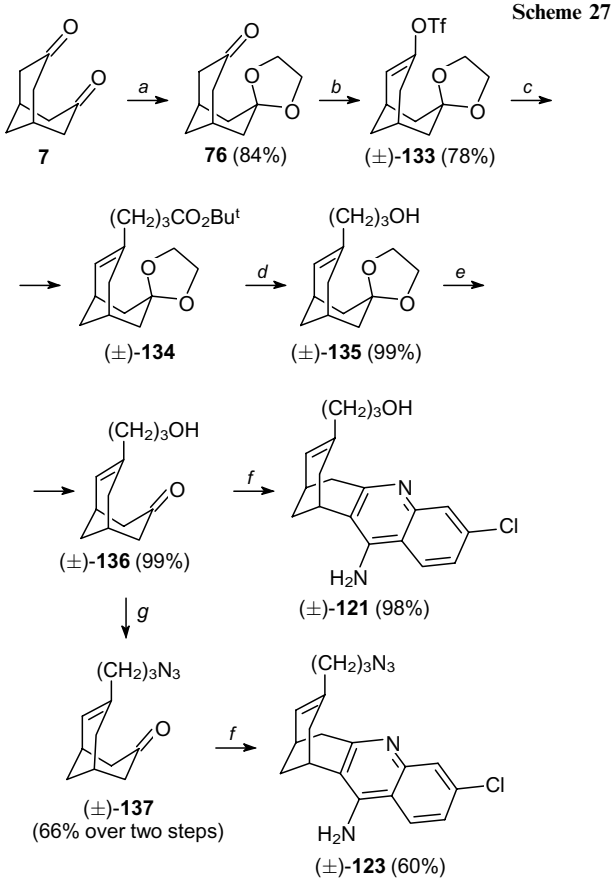



thesized and labeled with fluorine-18. Compounds (±)-**126**–**128** were synthesized from intermediates (±)-**102** and (±)-**122** in one step (Scheme 26). Mesylate (±)-**122** was converted into huprine (±)-**128** by treatment with Kryptofix® K222 and KF. Derivatives (±)-**131** and (±)-**132** were prepared starting from azide (±)-**123** in four steps. Ester (±)-**129** was generated upon treatment of azide (±)-**123** with methyl 4-pentynoate in the presence of copper iodide. The reduction of (±)-**129** with $LiAlH_4$ produced corresponding alcohol, which was subjected to mesylation with methanesulfonyl chloride and $Et_3N$ to give derivative (±)-**130**. Its reaction with Kryptofix® K222 and KF formed huprine (±)-**132**.

[$^{18}$F]-Labeled huprines were then used for *in vitro* and *in vivo* PET studies in two different animal species — laboratory rats and cats. Unfortunately, preliminary biological results demonstrated the inability of these compounds to visualize AChE *in vivo* because of their poor brain penetration.

Oukoloff *et al.*[140] improved the synthesis of huprines functionalized at position 9 by implementing the Suzuki–Miyaura cross-coupling of vinyl triflate (±)-**133** with various borane derivatives and the Friedländer condensation as the last step. The first reaction in this approach was the selective protection of diketone **7** using ethylene glycol in the presence of *p*-TsOH resulting in ketal **76** formation (Scheme 27). Its enolization was carried out by employing a strong base (NaHMDS) and the generated enolate was then trapped with $PhNTf_2$ that resulted in the desired product (±)-**133**. Suzuki-Miyaura cross-coupling with 9-borabicyclo[3.3.1]nonane (9-BBN)-derivative of *tert*-butyl pent-4-enolate under optimized conditions resulted in ester (±)-**134**. Reduction of the ester group of (±)-**134** with $LiAlH_4$ and consequent treatment of the generated alcohol (±)-**135** with PTSA produced ketone (±)-**136**. Its alcohol moiety was converted into azide in two steps (mesylation and substitution with $NaN_3$) and compound (±)-**137** was

**Scheme 27**

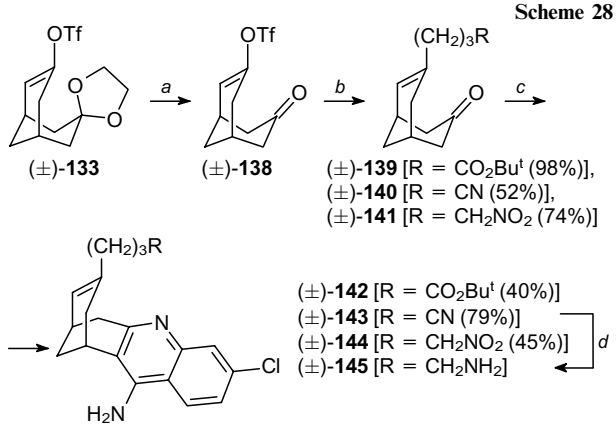



isolated in good yield. The Friedlander condensation of (±)-**136** and (±)-**137** with 2-amino-4-chlorobenzonitrile resulted in huprine (±)-**121** and (±)-**123**, respectively.[140]

Using slightly modified conditions, five other huprine analogues were prepared (Scheme 28).[140] The treatment of ketal (±)-**133** with *p*-TsOH gave ketone (±)-**138**, which was converted into derivatives (±)-**139**–**141** *via* Suzuki–Miyaura cross-coupling with boronate derivatives bearing different functional groups. Final products (±)-**142**–**144** were isolated following reactions of appropriate ketones with 2-amino-4-chlorobenzonitrile. Reduction of (±)-**143** with Raney Ni resulted in huprine (±)-**145**.[140]

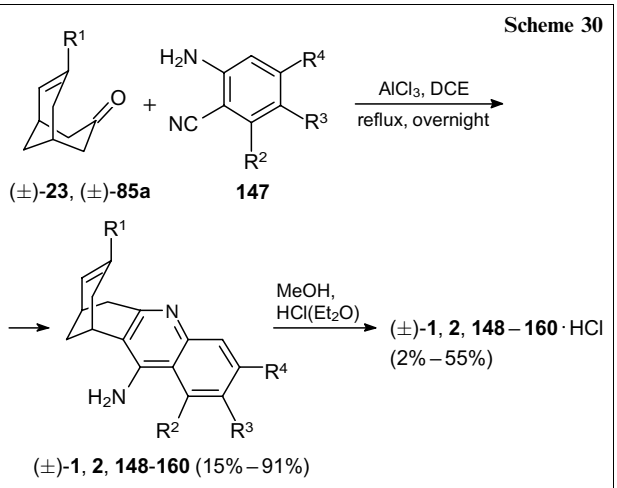
To detect and visualize AChE in different tissues, two near infra-red fluorescent probes were developed utilizing a huprine scaffold that was extended with cyanine 5.0 dye (Cy 5.0).[141] Fluorescent derivatives (±)-**146a** and (±)-**146b** were developed by inserting an amide bond between huprine analogues (±)-**111** and (±)-**145** with Cy 5.0 in the presence of BOP (benzotriazol-1-yloxytris(dimethylamino)phosphonium hexafluorophosphate) as a coupling reagent and *N*,*N*-diisopropylethylamine (DIEA) as a base (Scheme 29). Both novel probes showed inhibitory activity against *h*AChE in the nanomolar range, demonstrating high selectivity for this

**Scheme 28**




(*a*) *p*-TsOH, acetone, rt, 4 h;
(b) 1) *tert*-butyl pent-4-enolate, 9-BBN, THF, 0 → 80 °C, 2.5 h, then $H_2O$, 2) (±)-**133**, $K_3PO_4$, THF, $PdCl_2$(dppf), 80 °C, 16 h;
(*c*) ABN, $AlCl_3$, DCE, reflux;
(*d*) Raney Ni, EtOH, 7 N $NH_3$ (MeOH), rt, overnight (56%)

**Scheme 30**




$R^1$ = Me (±)-**23**, Et (±)-**85a**; $R^2$, $R^3$, $R^4$ = H, Me, F, Cl

enzyme over *h*BChE. The fluorescent derivatives were then used to visualize AChE *in situ*.

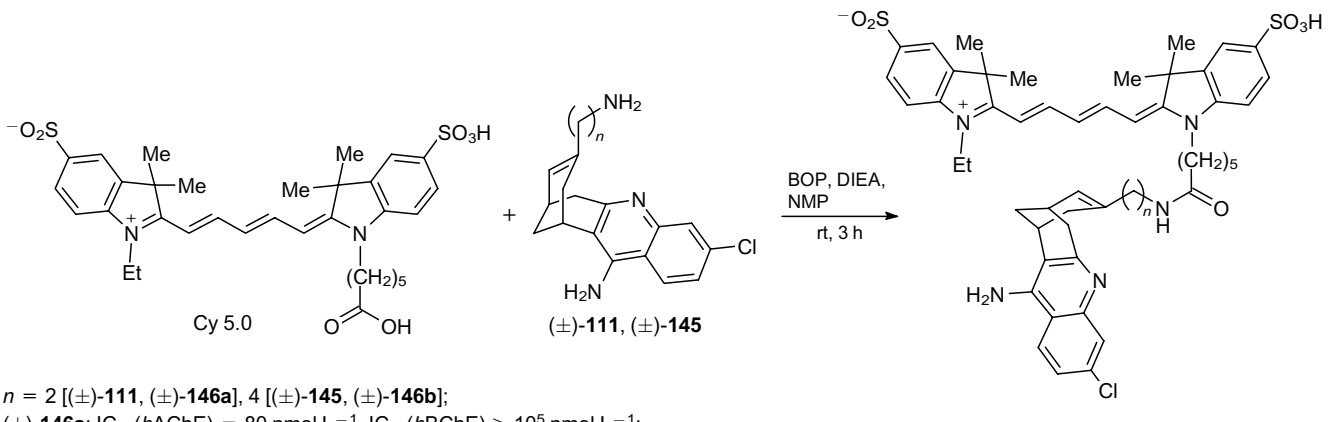
### 3.1.3. Synthesis and biological evaluation of huprines with structural modifications at the 4-aminoquinoline moiety

The modified 4-aminoquinoline moiety of huprines was inspired by previous studies on tacrine structures and the introduction of halogen atoms or methyl groups into different positions of its benzene ring.[142, 143] Derivatives (±)-**1**, (±)-2 and (±)-**148** – **160** possess a methyl or ethyl group at position 9 (Scheme 30).[6, 20, 98, 133] The benzene ring of the 4-aminoquinoline moiety is substituted at one or two positions with methyl, fluorine or chlorine. Huprines (±)-**148** – **160** were synthesized by condensing ketones (±)-**23** or (±)-**85a** with corresponding 2-aminobenzonitriles **147** in the presence of $AlCl_3$ and were then converted into hydrochlorides. Only *anti*-regioisomers were detected. The resolutions of (±)-**1**, (±)-**2**, (±)-**149**, (±)-**152**, (±)-**155** were furnished by MPLC.[6, 20, 98]

All novel huprines were tested for inhibitory capacity against *be*AChE, *h*AChE and *h*BChE. The results are summarized in Table 1. Most derivatives were potent bovine and human AChEIs, showing higher activity when compared to reference compounds (−)-HupA [$IC_{50}$(*be*AChE) = 74 nmol $L^{-1}$, $IC_{50}$(*h*AChE) = 260 nmol $L^{-1}$] and THA [$IC_{50}$(*be*AChE) = 130 nmol $L^{-1}$, $IC_{50}$(*h*AChE) = 210 nmol $L^{-1}$]. When separated using MPLC, the levorotatory enantiomers were much more active than the dextrorotatory counterparts. The best inhibitors of *h*AChE from both methyl and ethyl series were monosubstituted at position 3, analogues **2** and **1**, respectively. All tested derivatives preferentially inhibited AChE over BChE.

Compound **2** was examined for its effect on cholinergic receptors [muscarinic ($M_1$, $M_2$) and nicotinic ones (nAChRs)] isolated from rat brains (male Spargue – Dawley rats) using radioligand binding and functional studies (synaptosomal superfusion method).[144, 145] Racemate (±)-**2** displayed the ability to displace [$^3$H]-pirenzepine and [$^3$H]-quinuclidinyl benzilate binding in hippocampus membranes,[144] showing 14-fold higher affinity for $M_1$ over $M_2$ receptors. In functional studies, (±)-**2** (1 μmol $L^{-1}$) increased the release of [$^3$H]-dopamine in cortical synaptosomes. This effect was partially reverted by atropine and mecamylamine, suggesting an agonistic effect on $M_1$. The inhibitory effect of (±)-**2** (10 μmol $L^{-1}$) on [$^3$H]ACh release and the subsequent reversion by atropine suggest that the drug also has an agonistic effect on $M_2$ receptors. Racemate (±)-**2** showed an agonistic effect on nAChRs in basic

**Scheme 29**




*n* = 2 [(±)-**111**, (±)-**146a**], 4 [(±)-**145**, (±)-**146b**];
(±)-**146a**: $IC_{50}$(*h*AChE) = 80 nmol $L^{-1}$, $IC_{50}$(*h*BChE) ⩾ $10^5$ nmol $L^{-1}$;
(±)-**146b**: $IC_{50}$(*h*AChE) = 31 nmol $L^{-1}$, $IC_{50}$(*h*BChE) ⩾ 12 500 nmol $L^{-1}$

**Table 1**. Inhibitory capacity of huprine derivatives **1**, **2** and **148** – **160** against *be*AChE, *h*AChE and *h*BChE. Grey area in the table highlights the most active huprines.

| Compound No. [*ee* (%)] | $R^1$ | $R^2$ | $R^3$ | $R^4$ | *be*AChE (*h*AChE), $IC_{50}$ /nmol $L^{-1}$ | *h*BChE, $IC_{50}$ /nmol $L^{-1}$ | Ref. |
|---|---|---|---|---|---|---|---|
| (±)-**148** | Me | H | H | Me | 12 | 450 | 98, 133 |
| (±)-**149** | Me | H | H | F | 8.5 (4.6) | 200 | 98, 133 |
| (+)-**149** (99% *ee*) | Me | | | | 1.500 | 2.900 | 98 |
| (−)-**149** (99% *ee*) | Me | | | | 3.5 | 140 | 98 |
| (±)-**150** | Me | F | H | H | 31 (35) | 540 | 98, 133 |
| (±)-**151** | Me | F | H | F | 2.4 (2.2) | 960 | 98 |
| (±)-**1** | Me | H | H | Cl | 4.2 (0.8) | 240 | 98 |
| (+)-**1** (87% *ee*) | Me | | | | 36 (120) | 153 | 98 |
| (−)-**1** (99% *ee*) | Me | | | | 1.2 (0.3) | 247 | 98 |
| (±)-**152** | Et | H | H | Me | 12 | 210 | 133 |
| (+)-**152** (96% *ee*) | Et | | | | 480 | 120 | 133 |
| (−)-**152** (97% *ee*) | Et | | | | 4.5 | 350 | 133 |
| (±)-**153** | Et | Me | H | H | 30 | 510 | 133 |
| (±)-**154** | Et | Me | H | Me | 3.6 (5.0) | 33 | 98 |
| (±)-**155** | Et | H | H | F | 7.4 (3.8) | 57 | 98 |
| (+)-**155** (94% *ee*) | Et | | | | 130 (110) | 190 | 98 |
| (−)-**155** (95% *ee*) | Et | | | | 6.7 (2.1) | 32 | 98 |
| (±)-**156** | Et | F | H | H | 46 (30) | 110 | 98 |
| (±)-**157** | Et | F | H | F | 2.6 (1.8) | 190 | 98 |
| (±)-**2** | Et | H | H | Cl | 2.8 (0.8) | 16 | 98 |
| (+)-**2** (97% *ee*) | Et | | | | 400 (23) | 58 | 98 |
| (−)-**2** (99% *ee*) | Et | | | | 1.3 (0.3) | 160 | 98 |
| (±)-**158** | Et | H | Cl | H | 260 (430) | 760 | 98 |
| (±)-**159** | Et | Cl | H | H | 16 (12) | 330 | 98 |
| (±)-**160** | Et | Cl | H | Cl | 40 (1.4) | 1 200 | 98 |

conditions (3 mM $K^+$) and potentiated [$^3$H]ACh release induced by ACh.[145]

Also, compound **2** exhibited a protective effect against neurotoxicity induced by $H_2O_2$ and kainic acid (KA).[146, 147] The neuroprotective effect of **2** and **1** (0.01 – 1 μmol $L^{-1}$) against oxidative insult (injury induced by 200 μmol $L^{-1}$ $H_2O_2$) has been analyzed under two different conditions *in vitro*: using undifferentiated and nerve growth factor (NGF) differentiated PC12 cells.[146] Both huprines showed a similar protective effect in both cell types; however, the structural differences seem irrelevant for the neuroprotective effect. The involvement of cholinergic receptors in the protection by huprines was investigated with the help of atropine (muscarinic antagonist, 0.1 μmol $L^{-1}$) and mecamylamine (nicotinic antagonist, 100 μmol $L^{-1}$). The neuroprotective activity of huprines was reverted only in differentiated cells, suggesting that the observed effects were mediated by cholinergic receptors. Moreover, huprines increased the activity of superoxide dismutase suggesting the ability of these drugs to decrease ROS accumulation in response to oxidative stress (OS). Compound **2** (0.8 mg $kg^{-1}$, 21 days) also displays neuroprotective activity against neuronal injury caused by acute administration of KA (28 mg $kg^{-1}$).[147] Further, pre-treatment with **2** protected mice against changes in the pro(anti)-apoptotic pathways (pAkt1, Bcl2, pGSK3β and CDK5) and in the neuroinflammatory process (GFAP and Iba-1) induced by KA.

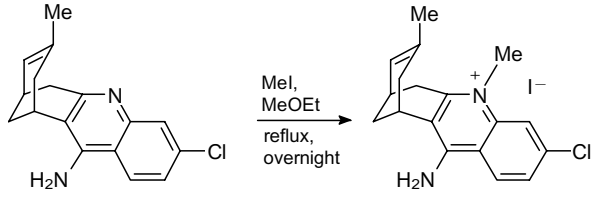
The *in vivo* effects of **2** were investigated in two AD-relevant mouse models, APPswe and 3 × Tg AD mice.[148, 149] In this regard, 6 – 7 month old transgenic mice (APPswe and 3 × Tg) and non-transgenic controls were treated daily with (±)-Hup X (0.12 μmol $kg^{-1}$, i.p.) or saline (0.9% NaCl solution, i.p.) for 21 consecutive days.[148] Chronic treatment with (±)-**2** reduced the levels of insoluble $A\beta_{1\text{-}40}$ in the hippocampus of 3 × Tg-AD mice with no apparent effect in APPswe mice. Moreover, (±)-**2** increased cortical synaptophysin levels and decreased the levels of α7 nAChRs in the caudate nucleus of 3 × Tg-AD mice while increasing hippocampal α7 nAChRs in APPswe mice. The different response observed in each mouse model is probably due to brain neuropathology. The modulation of Aβ and synaptophysin by (±)-**2** in 3 × Tg-AD mice might be due to its interaction with PAS of AChE and(or) *via* cholinergic mechanisms involving the activation of cholinergic receptors.[148]

An aged AD animal model (12 month old 126/Sv × C57b/6 male mice) was used to investigate the

behavioural effects of **2** as well as its effects on the regulation of protein kinase C (PKC), mitogen activated protein kinase (MAPK) and α-secretase (ADAM10 and TACE/ADAM17) in relation to APP processing.[150] The open-field and corner tests showed that compound **2** facilitates learning and memory in the Morris water maze and improves some emotional indicators without inducing adverse effects, affecting motor activity or anxiety-like behaviour, in a dose dependent manner. Huprine X (**2**) decreased full-length APP in the membrane of both cortex and hippocampus of treated mice in comparison to saline-treated animals. Moreover, the animals treated with the highest dose of (±)-**2** (0.12 μmol $kg^{-1}$) showed increased levels of PKC and MAPK isoforms (phospho-PKCα and phospho-42/44 MAPK). The activation of the PKC/MAPK signaling pathway may underlie the observed behavioural effects as well as the stimulation of the non-amyloidogenic processing of APP.

In an attempt to tackle peripheral AChE and its potential implication in MG, an analogue of **1** with a permanently charged quaternary nitrogen, compound (±)-**161**, was developed (Scheme 31).[151] Methylation of the corresponding nitrogen atom was performed using excess iodomethane in refluxing methyl ethyl ketone and the final product was isolated in high yield. Quaternization of (±)-**1** [$IC_{50}$(*h*AChE) = 1.07 nmol $L^{-1}$, $IC_{50}$(*h*BChE) = 180 nm] decreased the AChE inhibitory activity from 1.1 nmol $L^{-1}$ [for (±)-**1**] to 59 nmol $L^{-1}$ [for (±)-**161**]. A parallel artificial membrane permeability assay (PAMPA) was used to predict the ability of derivative (±)-**161** to cross the BBB. Derivative (±)-**161** showed a lower *Pe* value than the uncharged parent **1** [*Pe* 10.9 *vs.* 23.8 ($10^{-6}$ cm $s^{-1}$) for (±)-**161** and (±)-**1**, respectively]; however, it still fell within the range of high probability of BBB permeation by passive diffusion.

**Scheme 31**



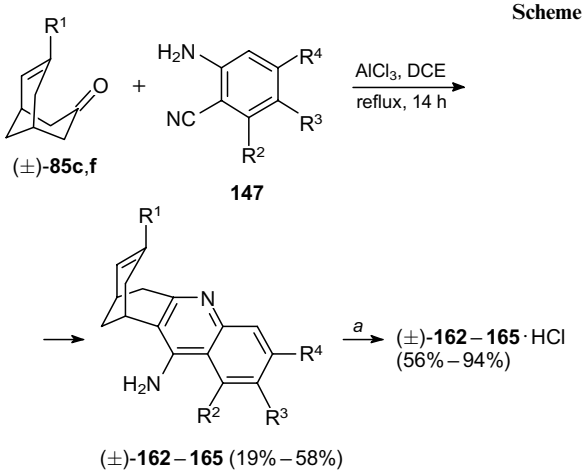

(±)-HupY

(±)-**161** [77%, $IC_{50}$(*h*AChE) = 59 nmol $L^{-1}$, $IC_{50}$(*h*BChE) = 3000 nmol $L^{-1}$, PAMPA: CNS +]

Huprine derivatives (±)-**162** – **165** were designed by fixing halogen atoms at position 3 while varying alkyl appendage at position 9 (isopropyl or allyl group) (see Scheme 16).[152] Novel huprines were prepared by the Friedländer condensation starting from enones (±)-**85c**,**f** (see [133]) with corresponding nitriles **147** in the presence of $AlCl_3$ in refluxing 1,2-dichloroethane (Scheme 32). The final products were then converted into their HCl salts.

Analogues (±)-**162** – **165**, parent huprines **2**, **1**, as well as some previously prepared 9-substituted derivatives [*i.e.* (±)-**86a**,**c** – **g**] (see Scheme 16) as well as (±)-**148**, (±)-**150**, (±)-**153**, (±)-**155** – **156** and (±)-**158** – **159** (see Scheme 30) were tested for their trypanocidal, anti-plasmodial activities and cytotoxicity in mammalian L6 cells.[152] All tested compounds displayed trypanocidal potency, with $IC_{50}$ values in the nano- to micromolar range ($IC_{50}$ values

**Scheme 32**




(±)-**85c**,**f**

**147**

(±)-**162** – **165** (19% – 58%)

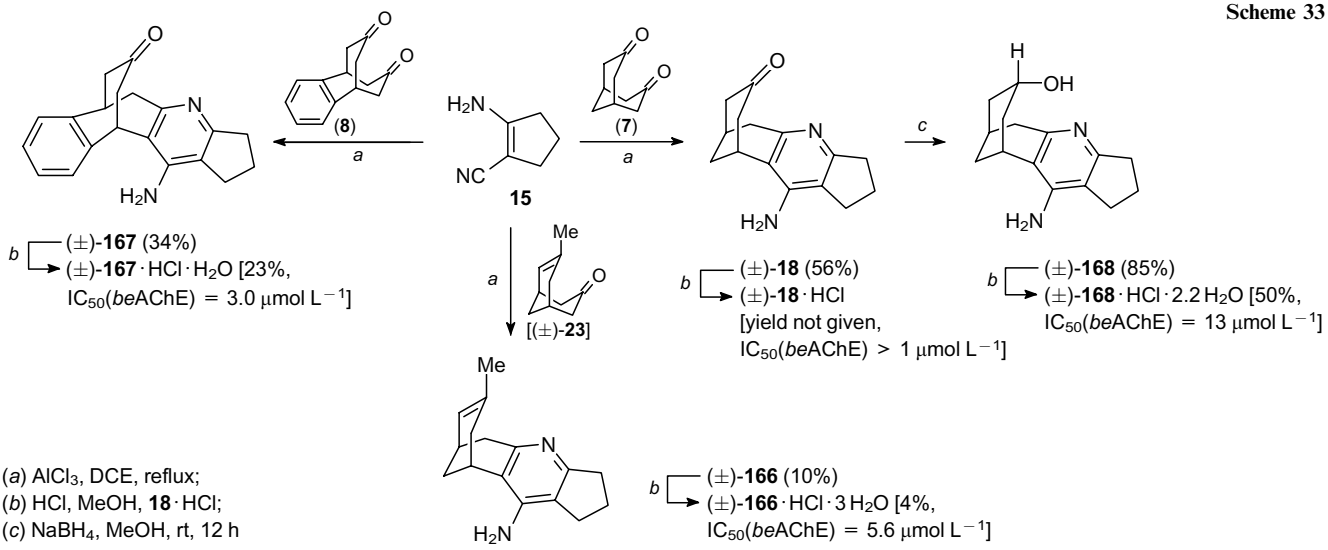
(*a*) MeOH, HCl (MeOH), then recrystallization from AcOEt – MeOH;
$R^1$ = $Pr^i$ [(±)-**85c**], All [(±)-**85f**]; $R^2$, $R^3$, $R^4$ = H, F, Cl;
(±)-**162**, $R^1$ = $Pr^i$, $R^2$ = $R^3$ = H, $R^4$ = Cl;
(±)-**163**, $R^1$ = All, $R^2$ = $R^3$ = H, $R^4$ = Cl;
(±)-**164**, $R^1$ = $Pr^i$, $R^2$ = F, $R^3$ = $R^4$ = H;
(±)-**165**, $R^1$ = All, $R^2$ = F, $R^3$ = $R^4$ = H

between 0.6 – 6 μmol $L^{-1}$). The most potent huprines, with an unsubstituted benzene ring, bear bulky moieties like a butyl (±)-**86d** or *tert*-butyl group (±)-**86e** (see Scheme 16) exhibiting $IC_{50}$ values of 0.70 and 0.88 μmol $L^{-1}$, respectively. From the series with a substituted benzene ring, the most potent were 3-chloro-substituted derivatives having a chlorine atom at position 3, out of which (±)-**1** ($IC_{50}$ = 0.8 μmol $L^{-1}$), (±)-**2** ($IC_{50}$ = 0.6 μmol $L^{-1}$) and compound (±)-**163** ($IC_{50}$ = 0.8 μmol $L^{-1}$) are highlighted. Cytotoxicity of the most pronounced huprines with trypanocidal activity was established in the L6 cell line pointing to selectivity for *T. brucei* over L6 cells (10 – 20-fold selectivity profile). Only (±)-**86g** had very poor preference with selectivity of 2.1 for *T. brucei* (see Scheme 16). From the nineteen tested huprines, only two had anti-plasmodial activity at a concentration below 10 μmol $L^{-1}$, namely (±)-**86d** ($IC_{50}$ = 6.0 μmol $L^{-1}$) and (±)-**86g** ($IC_{50}$ = 3.5 μmol $L^{-1}$) in comparison to chloroquine diphosphate ($IC_{50}$ = 0.5 μmol $L^{-1}$), which served as a positive control. Despite the interesting dual trypanocidal – anti-plasmodial profile of compounds (±)-**86d**,**g**, their therapeutic potential is limited by their low selectivity for *P. falciparum* over L6 cells SI = 1.1 [(±)-**86d**], SI = 0.5 [(±)-**86g**].

Other modifications of a tacrine-like moiety took part in the benzene region by substituting this moiety with cyclopentene or various heterocycles. Huprines (±)-**166** – **168** were prepared by the Friedländer condensation of corresponding (di)ketones **7**, **8** and (±)-**23** with 2-aminocyclopentenecarbonitrile (**15**, Scheme 33).[4, 5] The modification of derivative (±)-**18** to alcohol (±)-**168** was accomplished by reducing its carbonyl functionality with $NaBH_4$ in methanol.[5] Huprines (±)-**166** – **168** were less potent *be*AChE inhibitors than THA. Analogues (±)-**166** and (±)-**168** were also less active than their counterparts containing a benzene ring. The highest discrepancy in affinity was observed in derivative (±)-**166**; on the other hand, its benzene counterpart (±)-**3** (see Scheme 4) was almost 86 times more active.[5, 98]

The synthesis of 24 huprine derivatives was reported by Ronco *et al.*[102] in 2009. These compounds were prepared in

**Scheme 33**

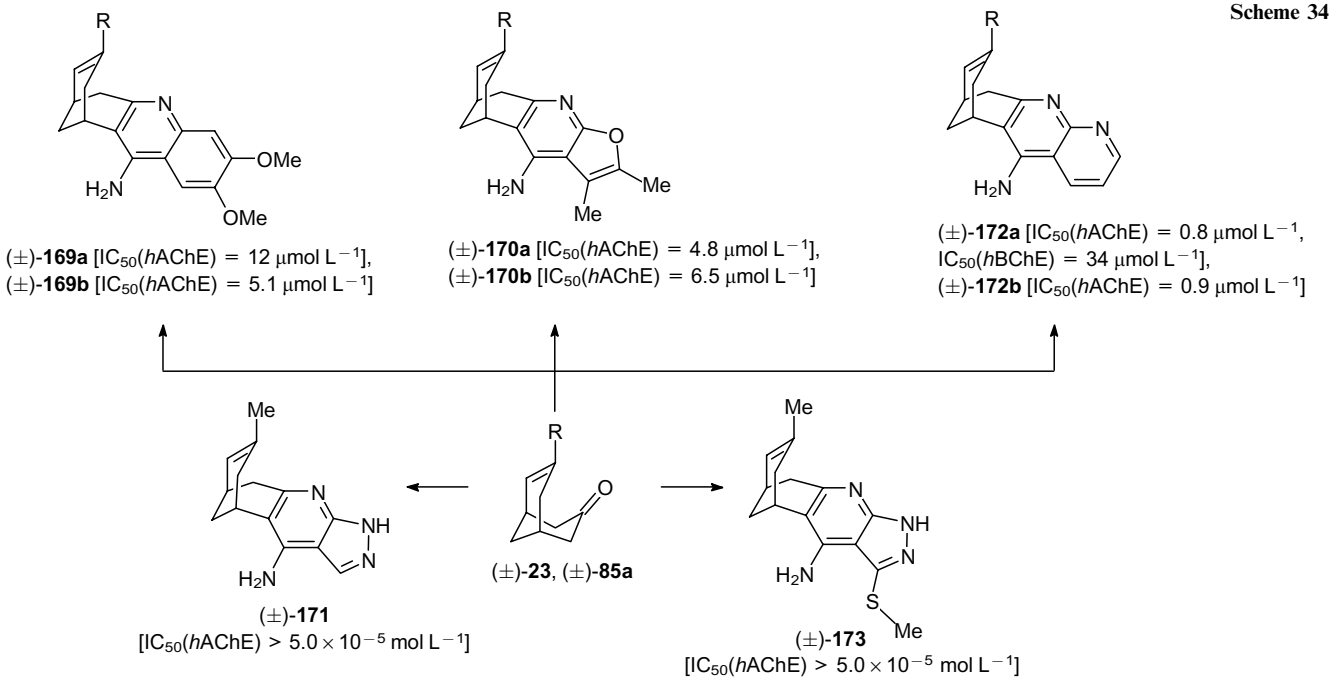



four steps according to the procedure outlined in Scheme 1. Two regions of the aminoquinoline substructure were modified. The first approach was focused on benzene ring substitution; initially two electron-donating methoxy groups [compounds (±)-**169a**,**b**] were introduced or the benzene moiety was replaced by pyridine [(±)-**172a**,**b** and (±)-**179**], furan [(±)-**170a**,**b**], oxazole [(±)-**184** – **186**], thiazole [(±)-**188** and (±)-**189**] or pyrazole ones [huprines (±)-**171** and (±)-**173**]. Similarly, the Friedländer condensation of ketone (±)-**23** or (±)-**85a** with a corresponding partner was applied.[102] The aromatic precursors for compounds (±)-**169** – **173** (Scheme 34) were commercially available. The required aromatic partners for the preparation of derivatives (±)-**179**, (±)-**184** – **186**, (±)-**188** and (±)-**189** were obtained according to procedures depicted in Schemes 35 and 36. Secondly, amino functionality at position 12 was either substituted by hydroxyl [(±)-**191**], chlorine [(±)-**192**] or elongated into a two-carbon linker with another functional group at the end of tail [(±)-**190**, (±)-**193** – **195**, see Scheme 36]. All resulting huprines were evaluated for their inhibitory capacity against *h*AChE as racemic mixtures.[102]

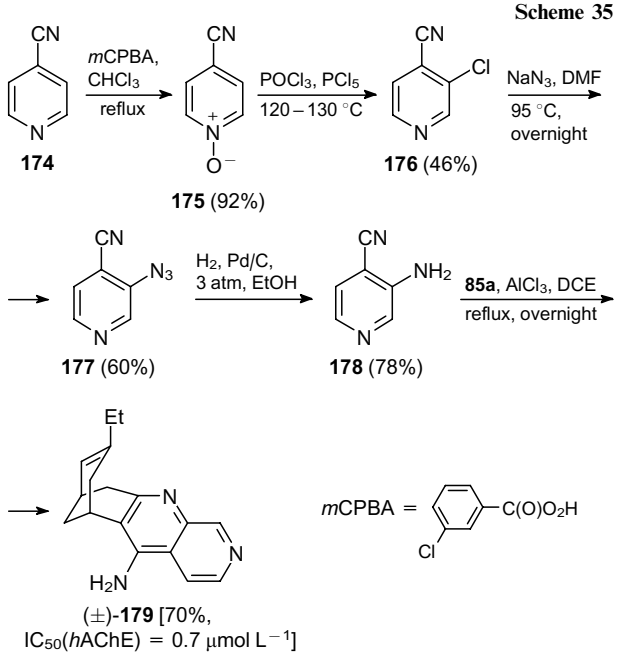
The oxidation of 4-cyanopyridine (**174**) with *m*-chloroperoxybenzoic acid (*m*CPBA) afforded *N*-oxide **175** (Scheme 35), which, upon chlorination with $PCl_5$ in refluxing $POCl_3$, produced a monochlorinated derivative **176** as a major compound. Exposure of **176** to sodium azide furnished the substitution of a chlorine atom to give **177**. In the next step, the hydrogenation in the presence of Pd/C resulted in 3-aminoisoniconitrile **178**, which was converted into huprine (±)-**179** by condensation with ketone (±)-**85a**.[102]

Cycloalkyl oxazole derivatives **182**, **183** were synthesized from aminomalononitrile tosylate (AMNT) and carboxylic acids **180**, **181** following the procedure of Freeman *et al.*[153] (Scheme 36). The Friedländer condensation of **182** and **183** with enone (±)-**23** or (±)-**85a** under standard conditions produced huprines (±)-**184** – **186**.[102] In order to obtain (±)-**188** and (±)-**189**, 2-propylthio-4-amino-5-cyano-

**Scheme 34**



**Scheme 35**

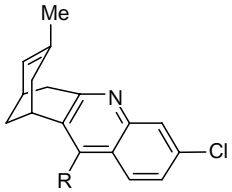



1,3-thiazole (**187**) obtained *via* the multicomponent reaction was combined with (±)-**23** and (±)-**85a**, respectively.[102]

Within the huprine family with modified benzene rings, the highest inhibitory capacity against *h*AChE was obtained for racemic mixtures of 4-amino-1,7-naphthyridine analogues (±)-**172a**,**b** (see Scheme 34) and 4-amino-1,8-naphthyridine (±)-**179** (see Scheme 35). However, these compounds were two orders of magnitude less active than the reference compounds (±)-**1**, (±)-**2**.

The structural modification of (±)-**2** and(or) (±)-**1** at position 12 was also taken into account. These analogues were designed to investigate the possible interaction with amino acid residues at the bottom of the AChE active site. Huprine analogues (±)-**190** – **195** bear heteroatoms such as Cl, O (alcohol functionality) or an azide moiety at position 12, or at the terminal position of a two-carbon chain bound to amino functionality of the aminoquinoline group.[102] Acylation of (±)-**1** was performed with chloroacetyl chloride to obtain compound (±)-**190** in 24% yield. The derivative with a fluorine at position 12 was also tested; however, only alcohol (±)-**191** could be isolated. A two-carbon linker was introduced by the nucleophilic aromatic substitution of a chlorine atom in analogues (±)-**192a**,**b** that were previously discovered through the reaction of enones (±)-**23** and (±)-**85a**, respectively, with 2-amino-4-chlorobenzoic acid in refluxing $POCl_3$ (Scheme 37). The exposure of (±)-**192a**,**b** to ethanolamine in the presence of NaI as a catalyst furnished amino alcohols (±)-**193a**,**b**. Their hydroxyl groups were substituted using $SOCl_2$, and the resulting chlorides (±)-**194a**,**b** were converted into azides (±)-**195a**,**b** upon treatment with sodium azide.[102]

**Structures 190, 191**

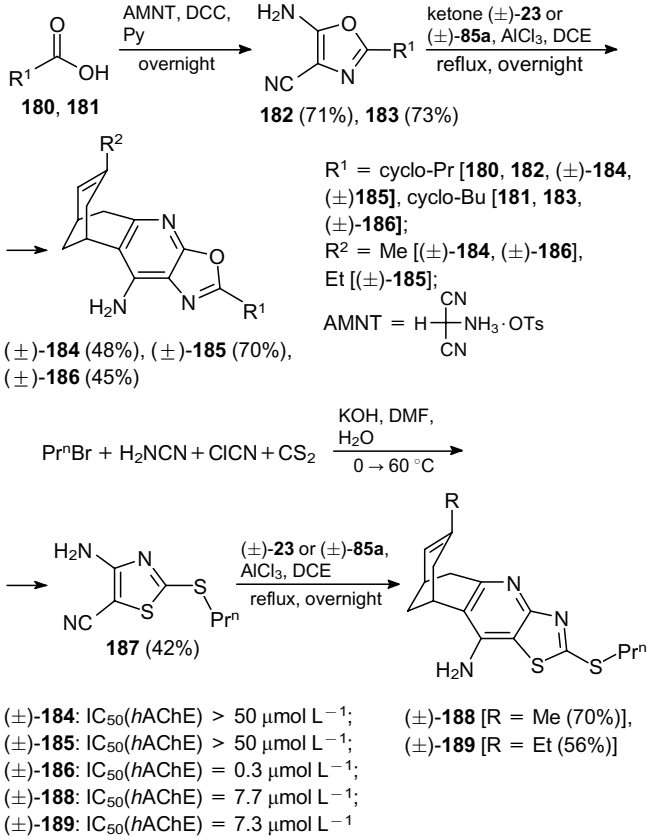



(±)-**190**, **191**

R = NHC(O)CH2Cl [(±)-**190**, IC50(*h*AChE) = 2.5 μmol L−1; OH [(±)-**191**, IC50(*h*AChE) = 15 μmol L−1]

The replacement of the amino group at position 12 decreased the inhibitoty capacity against *h*AChE by four orders of magnitude for both the Cl derivative **192** and analogue **191**. From this point of view, it can be deduced that the central 4-aminopyridine moiety of huprine is essential for its inhibitory activity and cannot be replaced by an isosteric group. On the other hand, the derivatives developed by monoalkylation of the amino group showed a *h*AChE-inhibitory activity in the nanomolar scale, with the exception of **190**. The highlighted huprine in this regard was **193b** ($IC_{50}$ = 6.8 nmol $L^{-1}$), which is only six times less potent than reference compound (±)-**2**.

**Scheme 36**

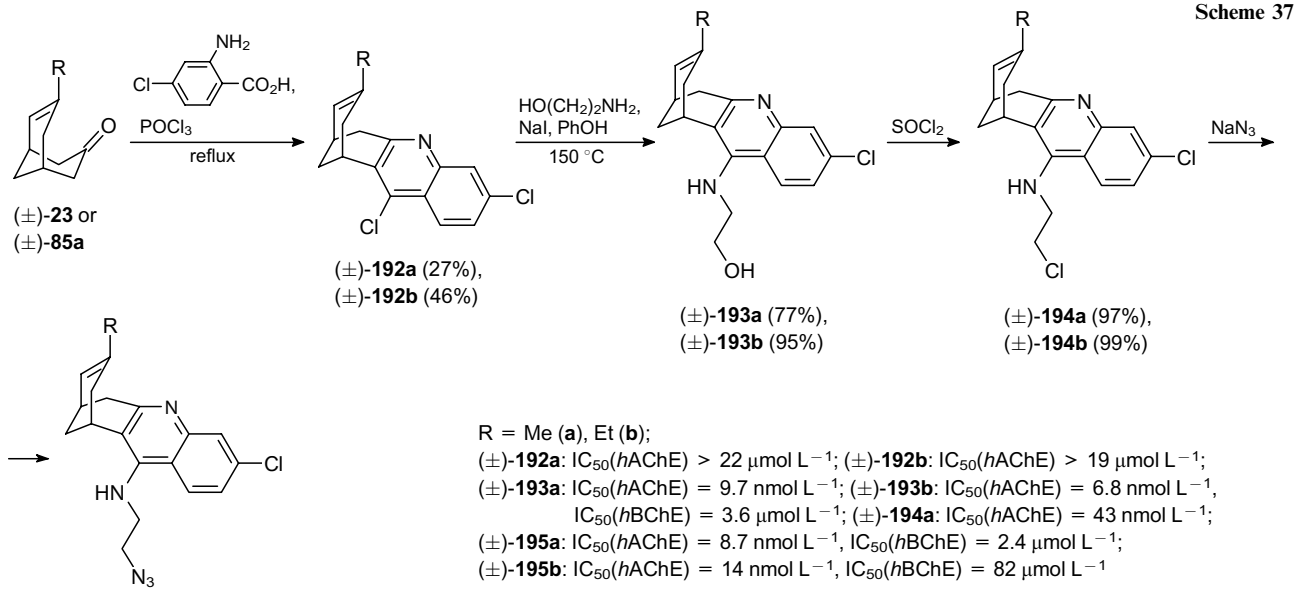



## 3.2. Enantioselective synthesis of huprines, preparation of *syn*-huprines and their biological evaluation

A series of terpenoic chiral 9-aminotetrahydroacridine analogues were synthesized from natural monoterpens. Most of this subset does not contain a bridged bicyclic moiety typical of huprines, with the exception of compounds **198**, **199**. These two were prepared by condensing ketones (+)-nopinone (**196**) and *cis*-verbanone (**197**) with 2-aminobenzonitrile in the presence of $BF_3 \cdot Et_2O$ as a catalyst to yield **198** and **199**, respectively (Scheme 38).[154] Products **198** and **199** presented inhibitory activity against rat AChE (*rat*AChE) in the micromolar range, two orders of magnitude less than the reference compound THA.

Compounds **205**, **206** were prepared as chiral bidentate P,N-ligands (Schemes 39, 40).[155] These compounds, similarly to **198** and **199** (see Scheme 38), can be conceived as

**Scheme 37**

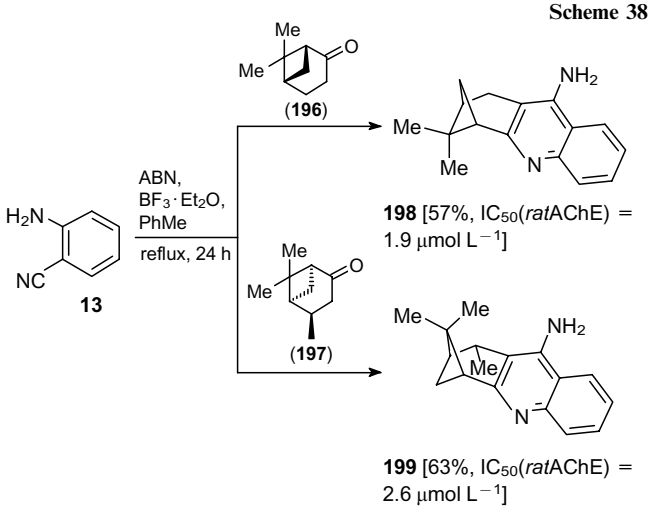



R = Me (**a**), Et (**b**);
(±)-**192a**: $IC_{50}$(*h*AChE) > 22 μmol $L^{-1}$; (±)-**192b**: $IC_{50}$(*h*AChE) > 19 μmol $L^{-1}$;
(±)-**193a**: $IC_{50}$(*h*AChE) = 9.7 nmol $L^{-1}$; (±)-**193b**: $IC_{50}$(*h*AChE) = 6.8 nmol $L^{-1}$,
$IC_{50}$(*h*BChE) = 3.6 μmol $L^{-1}$; (±)-**194a**: $IC_{50}$(*h*AChE) = 43 nmol $L^{-1}$;
(±)-**195a**: $IC_{50}$(*h*AChE) = 8.7 nmol $L^{-1}$, $IC_{50}$(*h*BChE) = 2.4 μmol $L^{-1}$;
(±)-**195b**: $IC_{50}$(*h*AChE) = 14 nmol $L^{-1}$, $IC_{50}$(*h*BChE) = 82 μmol $L^{-1}$

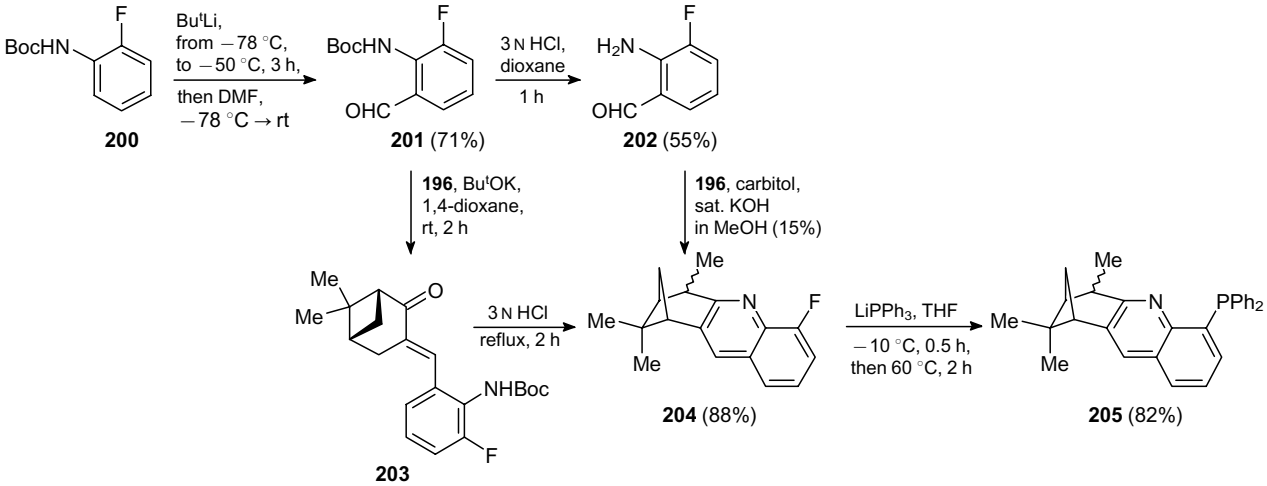
huprine analogues with a modified carbobicyclic substructure. Because of their original development as chiral ligands, these were not subjected to biological evaluation. Instead, their ability to provide asymmetric induction in metal-catalyzed processes was assessed. The treatment of **200** with Bu$^t$Li and then DMF resulted in benzaldehyde **201** that was then subjected to hydrolysis of the *N*-Boc group to produce **202** (see Scheme 39). Its Friedländer condensation with ketone **196** gave 5-fluorotetrahydroacridine **204** in low yield (9%). An alternative method of huprine **204** synthesis avoids the isolation of aldehyde **202**. The reaction of **201** with ketone **196** afforded **204** that was hydrolyzed to **204** in 88% yield. A diphenylphosphanyl group was introduced by nucleophilic substitution of an electrophilic fluorine atom with $LiPPh_2$ to afford phosphine **205**.

Using the same conditions for the synthesis of analogue **209** was unsuccessful. After benzaldehyde **202** treatment with (+)-camphor (**206**) in the presence of Bu$^t$OK, no product was isolated. Compound **207** was obtained in low yield (21%) through the reaction of the lithium enolate anion of **206** (LDA, THF, −40°C) with **202** (see Scheme 40). Cyclization of intermediate **207** with HCl in carbitol under reflux resulted in **209**, which was converted into huprine **210** in the same manner as analogue **205**.[155]

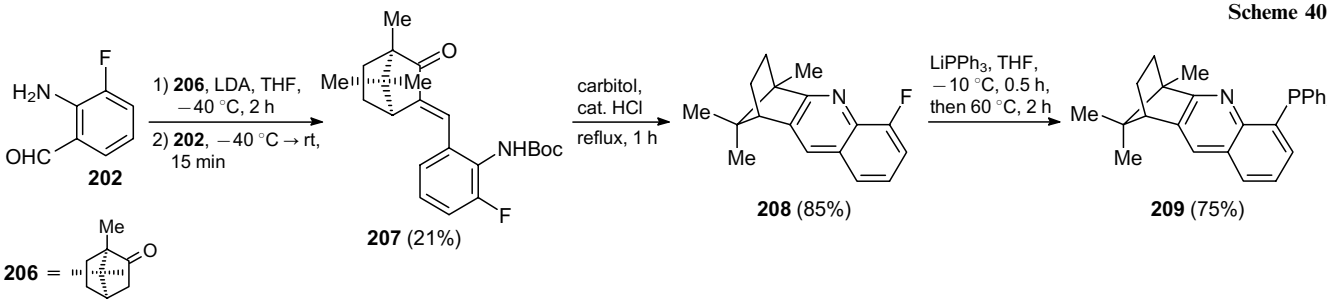
**Scheme 38**




**Scheme 39**

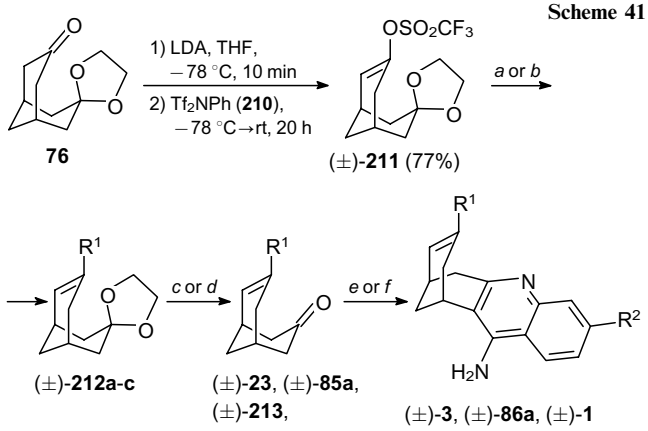


**Scheme 40**




The synthetic procedure applied for the racemic mixture of (±)-**86a**, as well as of its enantioenriched isomers (+)-**86a** and (−)-**86a**, is displayed in Schemes 41 and 42.[6] The enolization of ketone **76** was achieved with LDA to produce the corresponding racemic enolate that was submitted to reaction with *N*-phenyltriflimide (**210**) to produce triflate (±)-**211** (see Scheme 41). Its reaction with tributylvinyltin in the presence of $Pd(PPh_3)_4$ and LiCl resulted in ketal (±)-**212c**. This procedure was used to obtain (±)-**212a**,**b** but it failed probably due to the lower reactivity of tetramethyl- and tetraethyltin. Compound (±)-**212b** was prepared through the treatment of (±)-**211** with the appropriate organocuprate reagent generated *in situ* from the complex $Me_2S$.CuBr and EtMgBr (see Scheme 41). Acid hydrolysis of derivative (±)-**212b** using 2 N HCl produced ketone (±)-**85a**. Hydrolysis of (±)-**212c** was carried out on silica gel; the crude reaction mixture of vinylation products was kept for 16 h on the column before elution. The Friedländer condensation of (±)-**23** and (±)-**85a** with 2-amino-4-benzonitrile was previously described[5] and yielded (±)-**3** and (±)-**86a**, respectively. Condensation of (±)-**23** with 2-amino-4-chlorobenzonitrile furnished huprine (±)-**1**.[6]

**Scheme 41**



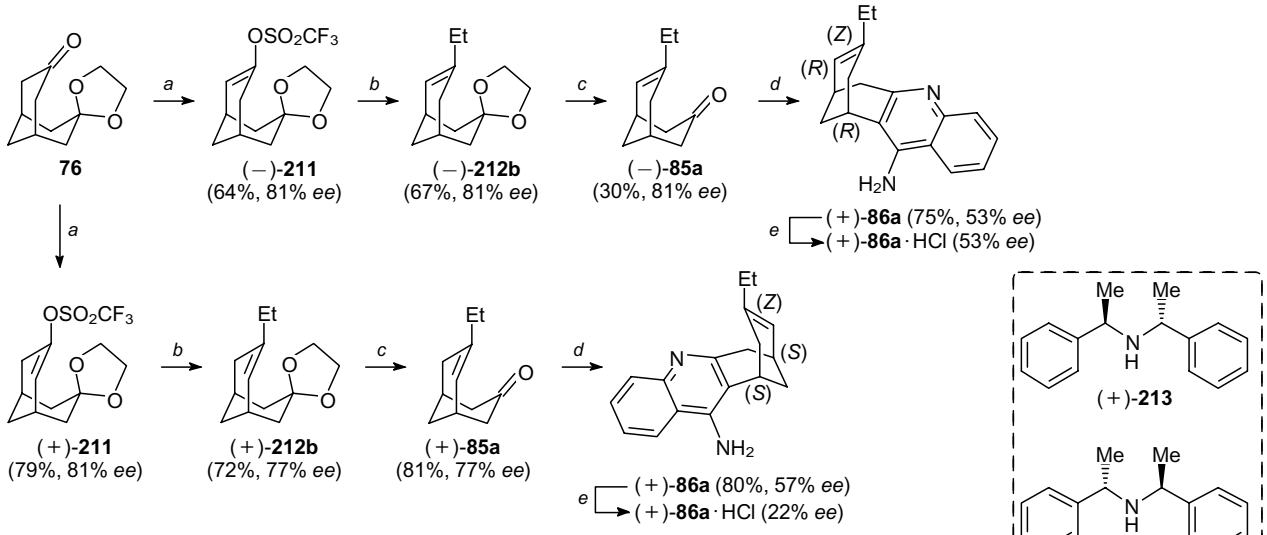

(±)-**1**, $R^1$ = Me, $R^2$ = Cl;
(±)-**3**: $R^1$ = Me, $R^2$ = H; (±)-**86a**: $R^1$ = Et, $R^2$ = H;
$R^1$ = Me [(±)-**212a**), (±)-**23**], Et [(±)-**212b**, (±)-**85a**],
CH = $CH_2$ [(±)-**212c**, (±)-**213**];
(*a*) $Me_2S$·CuBr, EtMgBr, THF, −78 °C→rt, 16 h (**212b**, 58%);
(*b*) LiCl, $Pd(PPh_3)_4$, THF, tributylvinyltin, reflux, 20 h, **212c** (51%), **213** (8%);
(*c*) 2 N HCl, THF, rt, 6 h (64%);
(*d*) this reaction was carried out under conditions described as (*b*), but for the work up the crude product was kept on the silica gel column for 16 h before elution [(±)-**213** 60% from (±)-**211**];
(*e*) previously described for (±)-**3**, (±)-**86**: 2-aminobenzonitrile, $AlCl_3$, DCE, reflux, or $ZnCl_2$, $PhNO_2$, reflux (see Schemes 4, 16);
(*f*) 2-ABN, $AlCl_3$, DCE, reflux, 7 h [(±)-**1**, 66%]

The above described procedure was used for the syntheses of enantioenriched enones (−)-**86a** and (+)-**86a**.[6] Enantioselective deprotonation of ketal **76** and its trapping under non-racemizing conditions was achieved using bis[(*S* or *R*)-1-phenylethyl]amine [(+)-**213** or (−)-**213**] (Scheme 42). The corresponding amine **213** was treated with $Bu^nLi$ and then with lithium chloride, and ketal **76** was added to generate enolate which was formed upon the reaction with *N*-phenyltriflimide. This method resulted in (−)/(+)-**211**. The treatment of each enantiomer with ethyl cuprate (prepared *in situ* from ethylmagnesium bromide and CuBr·$SMe_2$) produced (−)-**212b**. Hydrolysis of (+)-**212b** was first undertaken with 2 N HCl in THF. Under these conditions, the process was accompanied by significant amount of epimerization. However, hydrolysis of (−)/(+)-**212b** promoted by silica gel in $CH_2Cl_2$ led to enones (−)-**85a** and (+)-**85a** with high *ee* values. The Friedländer condensation of (−)/(+)-**85a** with 2-aminobenzonitrile in the presence of $AlCl_3$ furnished adequate huprines which were converted into hydrochlorides (+)-**86a**·HCl and (−)-**86a**·HCl. The observed epimerization of enones **85a** can be explained by protonation and deprotonation at the carbon–carbon double bond (thus its migration) caused by the acid conditions of this reaction. Condensation of (−)/(+)-**85a** with 2-aminobenzonitrile in the presence of $ZnCl_2$ as the Lewis catalyst in nitrobenzene resulted in a similar degree of epimerization. Both hydrochlorides (+)- and (−)-**86a**·HCl were crystallized from MeOH–EtOActo giving analytically pure samples of salts with *ee* = 99% and >99%, respectively.[6]

An alternative explanation for the reduced *ee* values observed for compounds (+)-**86a** (53% *ee*) and (−)-**86a** (57% *ee*) during the reaction of enones (−)- and (+)-**85a** under conditions *d* (see Scheme 41) is provided in Scheme 43.[156] Given the Friedländer condensation nature being non-regioselective, isomerization of generated *syn*-huprines (7*R*,11*S*)-**86a** and (7*S*,11*R*)-**86a** (migration of the endocyclic C=C double bond) takes place due to the acidic conditions of the reaction. In this manner, *syn*-derivative (7*R*,11*S*)-**86a** [or (7*S*,11*R*)-**86a**] is converted into *anti*-isomer (7*S*,11*S*)-**86a** [or (7*R*,11*R*)-**86a**] which is enantiomeric with the directly obtained (*via* condensation) *anti*-isomer (7*R*,11*R*)-**86a** [or (7*S*,11*S*)-**86a**], thus decreasing the *ee* of the desired enantioenriched product.[156]

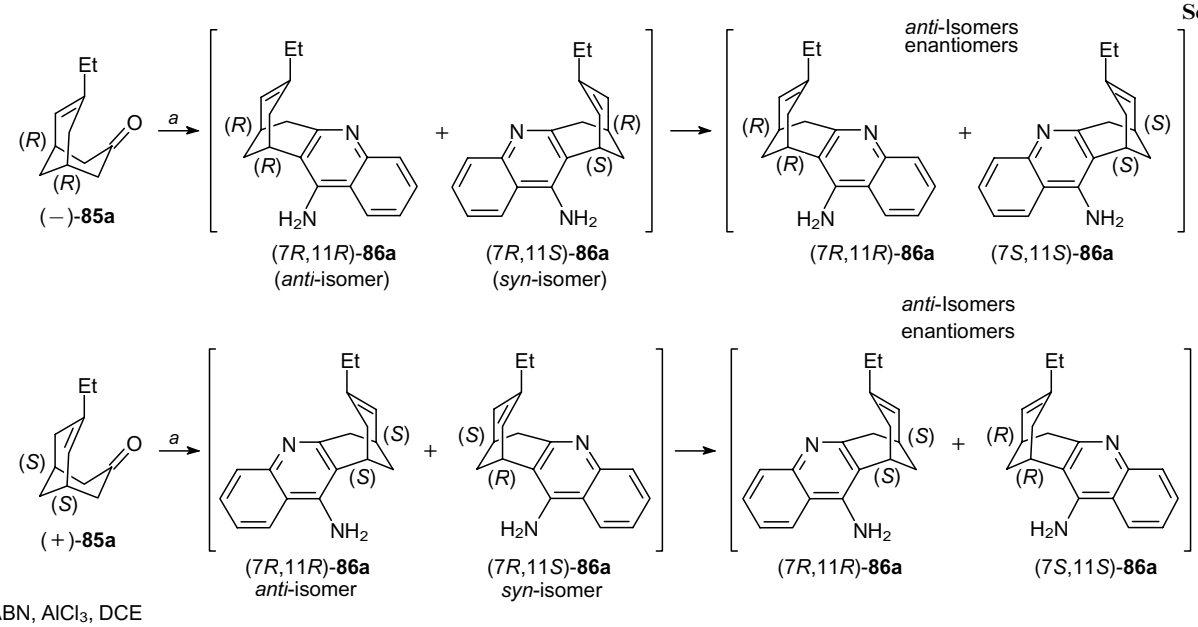
To verify this hypothesis, Camps *et al.*[156] performed an acid-promoted isomerization of *anti*- and *syn*-isomers (±)-**3**, (±)-**86a** and (±)-**215a**,**b**, racemic mixture (±)-**215b** and enantioenriched *syn*-huprines (−)-**215b** and (+)-**215b**. The synthesis of *syn*-huprines (±)-**215a** and (±)-**215b** was reported previously in two steps from enones (±)-**23** and (±)-**85a** (Scheme 44).[157] The reaction of (±)-**23** and (±)-**85a** with 2-(trifluoromethyl)aniline in refluxing toluene produced mixtures of (*E*)- and (*Z*)-stereoisomers of imines

**Scheme 42**




(*a*) 1) (+)-**213** [for the preparation of (+)-**86a**] or (−)-**213** [for the synthesis of (−)-**86a**], Bu$^n$Li, THF, −78 °C → rt, 1 h, then solution of LiCl in THF and solution of **76** in THF at −78 °C, 15 min; 2) **210**, THF, −78 °C → rt, 16 h; (*b*) EtMgBr, $Me_2S \cdot CuBr$, THF, −78 °C→ rt, 16 h; (*c*) silica gel, $CH_2Cl_2$, rt, 27 h; (*d*) ABN, $AlCl_3$, DCE, reflux, 14 h; (*e*) MeOH, sat. HCl ($Et_2O$)

**Scheme 43**



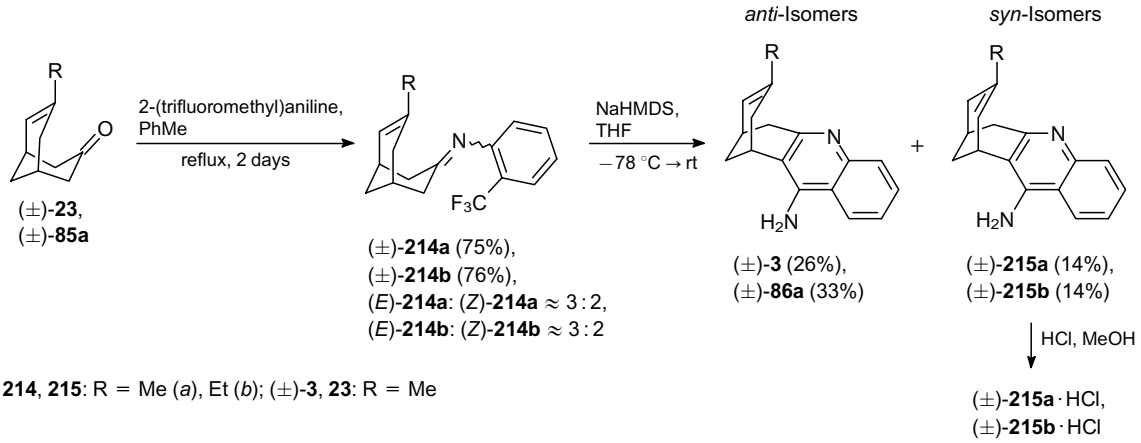

(*a*) ABN, $AlCl_3$, DCE

(±)-**214a**,**b**, which were used directly in the next step. Cyclization of (±)-**214a**,**b** upon treatment with sodium hexamethyldisilazide (NaHMDS) generated a mixture of *anti*- and *syn*-isomers (±)-**3**, (±)-**86a** and (±)-**215a**,**b**. *syn*-Regioisomers (±)-**215a** and (±)-**215b** were isolated in pure form from the corresponding mixtures by silica gel column chromatography and were then converted into their hydrochlorides (±)-**215a** · HCl · 2 $H_2O$ and (±)-**215b** · HCl.[157] Chiral medium performance liquid chromatography was used for the resolution of racemic *syn*-isomers (±)-**215b** to give enantioenriched (+)-(7*S*,11*R*)-**215b** (70% *ee*) and (−)-(7*R*,11*S*)-**215b** (84% *ee*) (Scheme 44).[156]

The treatment of (±)-**3**/(±)-**215a** (≈ 2 : 1 mixture) and pure (±)-**215b** with $AlCl_3$ in DCE resulted in the isomerization of *syn*-isomers into *anti*-derivatives and only compounds (±)-**3** and (±)-**85a** were isolated. The treatment of a mixture of (±)-**86a**/(±)-**215b** (≈ 1 : 1) with triflic acid in dioxane yielded (±)-**86a**. Under the same conditions, enantioenriched (+)-**215b** · HCl (77% *ee*) and (−)-**215b** (84% *ee*) afforded (+)-**86a** (76% *ee*) and (−)-**86a** (82% *ee*) (Scheme 45).[156] These results suggest that the observed regioselectivity of Friedlander reactions may be due to the equilibrium in the initially formed *syn*-*anti* mixtures to more stable *anti*-products.

The comparison of inhibitory activities of racemic mixtures of *syn*-isomers (±)-**3**, (±)-**86a** and *anti*-isomers (±)-**215a**, (±)-**215b** revealed that in both cases *anti*-analogues are more potent AChEIs (Table 2).

**Scheme 44**




**Scheme 45**

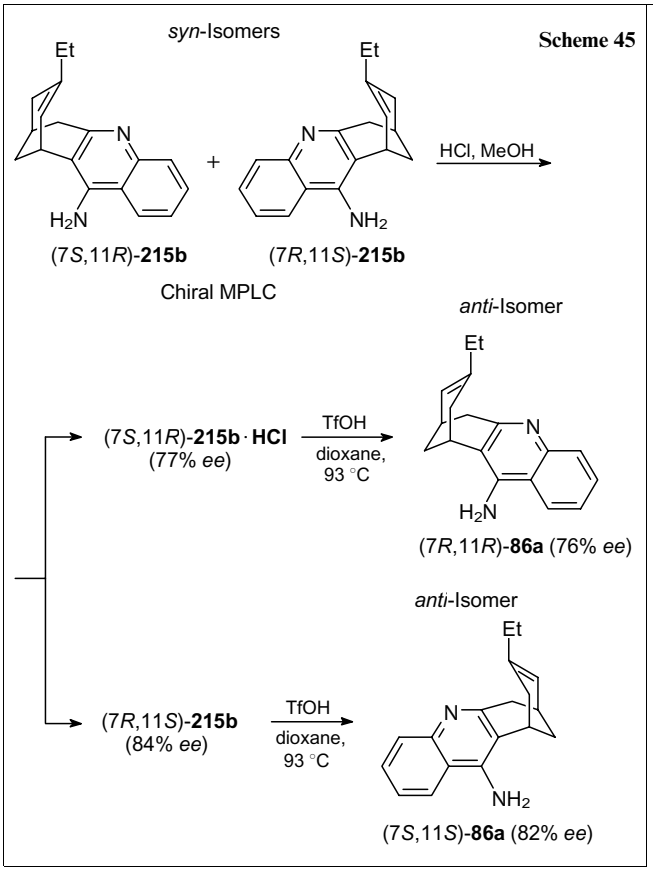
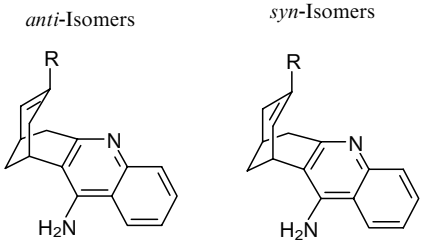



**Table 2**. Pharmacological data for racemic mixtures of *anti*- and *syn*-derivatives of **3**, **86a** and **215a – b**.

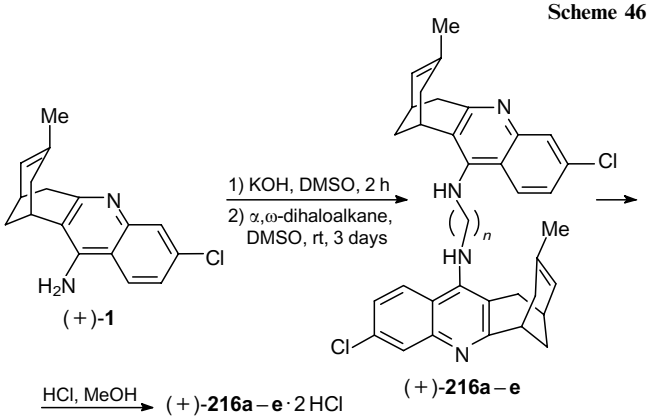



| Compound | R | $IC_{50}$ |
|---|---|---|
| (±)-**3**·HCl | Me | $IC_{50}$(*be*AChE) = 65 nmol $L^{-1}$<br>$IC_{50}$(*h*AChE) = 52 nmol $L^{-1}$<br>$IC_{50}$(*h*BChE) = 130 nmol $L^{-1}$ |
| (±)-**86a**·HCl | Et | $IC_{50}$(*be*AChE) = 39 nmol $L^{-1}$<br>$IC_{50}$(*h*AChE) = 38 nmol $L^{-1}$<br>$IC_{50}$(*h*BChE) = 79 nmol $L^{-1}$ |
| (±)-**215a**·HCl | Me | $IC_{50}$(*be*AChE) = 0.5 μmol $L^{-1}$<br>$IC_{50}$(*h*AChE) = 0.4 μmol $L^{-1}$<br>$IC_{50}$(*h*BChE) = 0.1 μmol $L^{-1}$ |
| (±)-**215b**·HCl | Et | $IC_{50}$(*be*AChE) = 0.2 μmol $L^{-1}$<br>$IC_{50}$(*h*AChE) = 0.08 μmol $L^{-1}$<br>$IC_{50}$(*h*BChE) = 0.06 μmol $L^{-1}$ |

## 4. Synthesis and biology of huprine homo- and heterodimers

The synthesis of homodimers (+)-**216a – e** linked with (+)-**1** was previously reported by Sola *et al.*[125] in 2014. Bis-huprines (+)-**216a-e** were prepared by a one-pot reaction using two equivalents of (7*R*,11*R*)-**1** and one equivalents of α,ω-dihaloalkane in the KOH – DMSO system (Scheme 46). All dimers were modified to give dihydrochlorides (+)-**216a – e**·2 HCl,[114] which were purposely developed as antiprotozoal agents. The molecular dimerization of compounds with known antiprotozoal activity was successful regarding the members of the 4-aminoquinoline family.[86,158 – 160] All these bis-huprines showed $IC_{50}$ values in the range of 0.5 – 0.9 μmol $L^{-1}$ against cultured bloodstream forms of *T. brucei*, which is comparable with that of the parent (+)-**1** [$IC_{50}$ (*T. brucei*) = 0.6 μmol $L^{-1}$]. Further, $IC_{90}$ values ranged between 0.7 – 1.1 μmol $L^{-1}$, which was lower than that for (±)-**1** [$IC_{90}$ (*T. brucei*) = 2.9 μmol $L^{-1}$]. Relative to (±)-**1**, the increased trypanocidal activity of novel huprines does not seem to be dependent upon the length of the linker or the presence of a benzene ring within the linker. Therefore, it might be ascribed to the dimerization strategy even though the mechanism of trypanosome growth inhibition remains elusive. Compounds (+)-**216a – e**·2 HCl were also evaluated against the chloroquine-resistant K1 strain of *P. falciparum*. No noticeable enhancement of anti-plasmodial activity was observed for these dimeric compounds, reaching $IC_{50}$ values > 5 μmol $L^{-1}$, which were much higher than the values for artemisin (positive control, $IC_{50}$ = 91 nmol $L^{-1}$). The tested bis-huprines were toxic against L6 cells (rat skeletal myoblasts) in a range of 1.6 – 29 μmol $L^{-1}$. Homologues (+)-**216d** with the longest alkylene tether, and (+)-**216e**, with the *p*-phenylene-bis(methylene) bridge, displayed the highest trypanocidal activity over cytotoxicity (SI = 38 and

**Scheme 46**

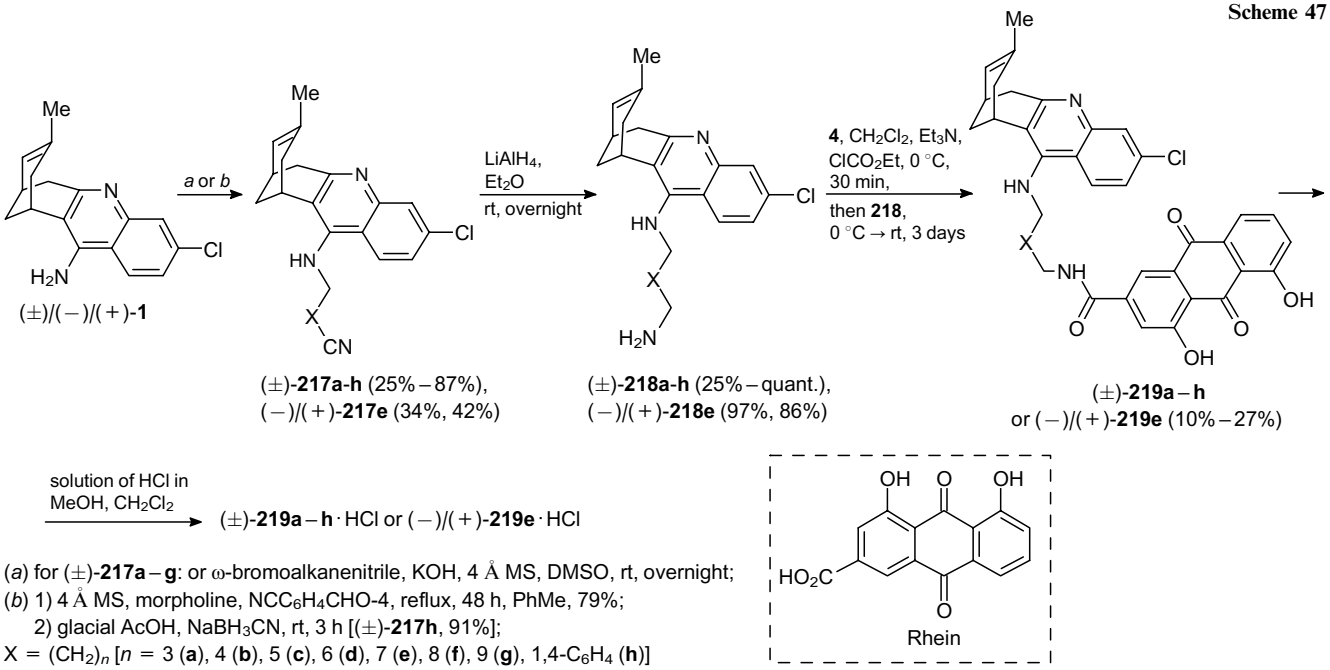



*n* = 8 [(+)-**216a**, 21%], 10 [(+)-**216b**, 25%], 12 [(+)-**216c**, 26%], 14 [(+)-**216d**, 50%], $(CH_2)_2$-(*p*-$C_6H_4$)-$(CH_2)_2$ [(+)-**216e**, 11%]

28, respectively). However, bis-huprines exhibited more pronounced anticholinesterase than trypanocidal activity showing $IC_{50}$ values for *h*AChE in the two to three-digit nanomolar range [$IC_{50}$(*h*AChE) in the range of 18 – 430 nmol $L^{-1}$)].

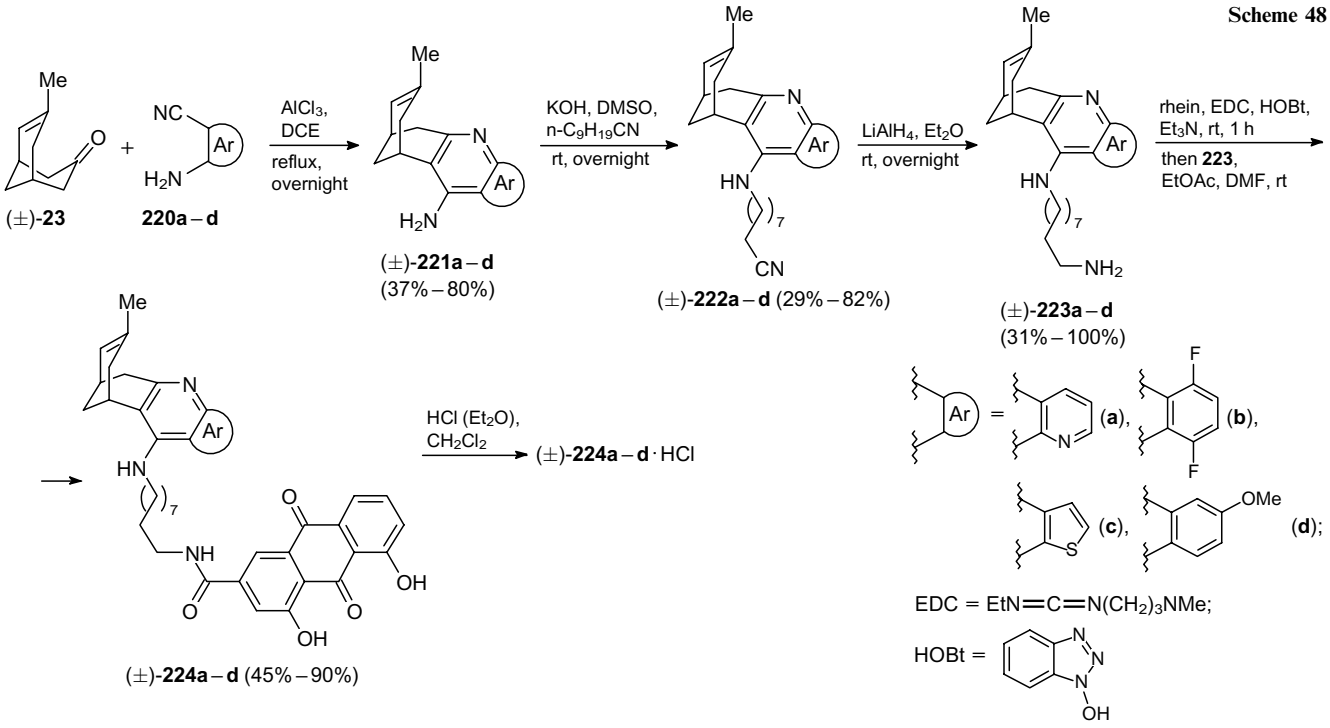
Rhein (see Fig. 9, Schemes 47 and 48) is a natural compound that can be found as a glucoside in *Rheum* species, senna leaves, and also in several species of *Cassia*.[161] Rhein possesses various pharmacological effects, including nephroprotective, hepatoprotective, anti-inflammatory, anticancer, antioxidant, and antimicrobial activities.[162] It was believed that the aromatic rings of rhein could establish π-stacking interactions with the characteristic aromatic residues at the PAS of AChE and that the hydroxyanthraquinone scaffold might confer tau anti-aggregating properties to the rhein – huprine derivatives. The synthesis of rhein – huprine hybrids (±)-**219a-h** started with the alkylation of the racemic mixture of (±)-**1** (see Scheme 47).[114] The treatment of (±)-**1** with the corresponding ω-bromoalkanenitriles gave nitriles (±)-**217a** – **h**. The subsequent reduction of nitrile with $LiAlH_4$ resulted in amines (±)-**218a** – **h**. The treatment of rhein with ethyl chloroformate furnished adequate anhydride, which was subjected to the reaction with (±)-**218a** – **h** to give huprine – rhein heterodimers (±)-**219a** – **h**. All final products were converted into corresponding HCl salts. The biological profiling of (±)-**219a** – **h** included the evaluation *in vitro* of the inhibitory activity against *h*AChE, *h*BChE, human β-secretase (*h*BACE-1) as well as against *h*AChE-induced and self-induced Aβ aggregation. All novel hybrids were also evaluated for their Aβ and tau anti-aggregating activities in *Escherichia coli* cells overexpressing these peptides. According to the obtained data, compound (±)-**219e** was the lead candidate from the series. Encouraged by these results, two enantiopure dimers (−)-**219e** and (+)-**219e** were separated and biologically evaluated. Hybrids (−)-**219e** and (+)-**219e** were synthesized from (−)-**1** or (+)-**1** following the same synthetic procedure for racemic mixtures (see Scheme 47). The levorotatory hybrid (−)-**219e** was 1200-fold more potent as an *h*AChE inhibitor than its enantiomer (+)-**219e** [$IC_{50}$(*h*AChE) = 2.4 nmol $L^{-1}$ [(−)-**219e**], $IC_{50}$(*h*AChE) = 2900 nmol $L^{-1}$ [(+)-**219e**]. Regarding *h*BChE inhibition, the hybrid (+)-**219e** was two times more potent than (−)-**219e** [$IC_{50}$(*h*BChE) = 510 nmol $L^{-1}$ [(−)-**219e**], $IC_{50}$(*h*BChE) = 270 nmol $L^{-1}$ [(+)-**219e**]]. Both of these findings were consistent with the stereoselective interaction of the parent **1**. No enantioselective differences were found in the inhibition of *h*AChE-induced aggregation of $A\beta_{40}$ (37% – 38% inhibition at 100 μmol $L^{-1}$), self-induced aggregation of $A\beta_{42}$ (38% – 43% inhibition at 10 μmol $L^{-1}$) and *h*BACE-1 activity ($IC_{50}$ = 80 nmol $L^{-1}$ for both enantiomers). The protective effect of (−)- and (+)-**219e** on the synaptic integrity against Aβ-insult was evaluated by establishing the induction of long-term potentiation. Moreover, the levels of synaptic proteins in the hippocampal sections of C57bl6 mice led to the conclusion that both enantiomers exerted a protective effect. The *in vivo* experiments with transgenic APP-PS1 mice showed that (−)-**219e** and (+)-**219e** can diminish the levels of hippocampal total

**Scheme 47**




(*a*) for (±)-**217a** – **g**: or ω-bromoalkanenitrile, KOH, 4 Å MS, DMSO, rt, overnight;
(*b*) 1) 4 Å MS, morpholine, $NCC_6H_4CHO$-4, reflux, 48 h, PhMe, 79%;
2) glacial AcOH, $NaBH_3CN$, rt, 3 h [(±)-**217h**, 91%];
X = $(CH_2)_n$ [*n* = 3 (**a**), 4 (**b**), 5 (**c**), 6 (**d**), 7 (**e**), 8 (**f**), 9 (**g**), 1,4-$C_6H_4$ (**h**)]

**Scheme 48**

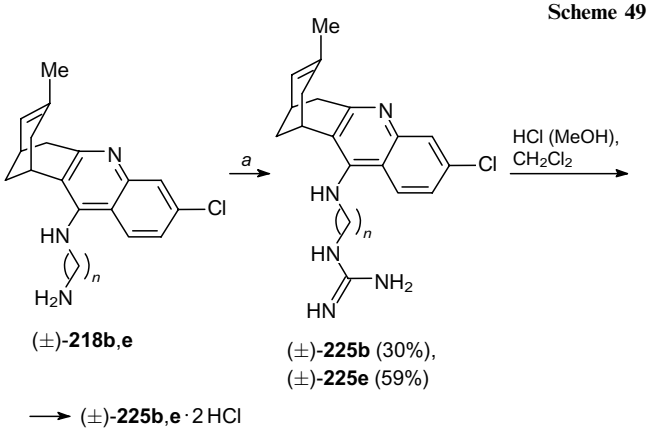



soluble Aβ and increase the levels of APP both in the initial and advanced stages of the AD model.

Seeking to improve the bioavailability of rhein – huprine heterodimers, a second generation of these hybrids was designed by the structural modification of the huprine moiety, specifically to modulate its basicity.[115] The Friedländer condensations of ketone (±)-**23** with the corresponding aromatic partners **220a** – **d** under standard conditions ($AlCl_3$, DCE, reflux) gave adequate huprine derivatives (±)-**221a** – **d** (see Scheme 48). Alkyl chains were introduced by treating (±)-**221a** – **d** with 9-bromononanenitrile in the presence of KOH in DMSO. Subsequent reduction of the nitrile moiety in (±)-**222a** – **d** gave amines (±)-**223a** – **d**. Ethyl chloroformate exposure to rhein furnished an adequate anhydride that was subjected to the reaction with (±)-**223a** – **d** to generate (±)-**224a** – **d** heterodimers. The final products were transformed into corresponding HCl salts. Novel rhein – huprine dimers were evaluated regarding their inhibition against *h*AChE, *h*BChE, *h*BACE-1, $A\beta_{42}$ and tau aggregation; further, they were also tested for antioxidant properties. All the hybrids, as well as the novel huprine analogues, were less potent *h*AChEI than **1** and **219e** (see Scheme 47) showing $IC_{50}$ values in the submicromolar to low micromolar range. Heterodimer **224a** had the best inhibitory capacity with $IC_{50}$ = 180 nmol $L^{-1}$. The kinetic studies showed that **224a** acted as a mixed-type *h*AChEI. Compounds **221a**,**c**,**d** were two – five-fold more potent against *h*BChE than *h*AChE; derivative **221b** was roughly equipotent towards both enzymes. In contrast, all hybrids were selective *h*AChEIs, with $IC_{50}$ values for *h*BChE in the micromolar range, highlighting the analogue **224a** ($IC_{50}$ = 2.55 μmol $L^{-1}$). The inhibitory activity against *h*BACE-1 was measured only for hybrids **224b** (22% at 1 μmol $L^{-1}$) and **224c** (34% at 80 nmol $L^{-1}$). The novel rhein – huprine dimers retained the $A\beta_{42}$ anti-aggregating activity of lead compound **219e** and showed slightly increased tau anti-aggregating capacity with a inhibition threshold of 10 μmol $L^{-1}$ for $A\beta_{42}$ and tau aggregation of 24% – 46% and 26% – 52%, respectively. The antioxidant activity of the novel derivatives was assessed by 2,2′-azinobis-(3-ethylbenzothiazoline-6-sulfonic acid) (ABTS), 2,2-diphenyl-1-picrylhydrazyl (DPPH) and total phenolic assays. Modified huprines **221a** – **d** exhibited 3 – 6 trolox equivalents antioxidant activities in the $ABTS^{+\bullet}$ and DPPH assays. Hybrids **224a** – **d** were 10 – 22-fold and 12 – 13-fold more potent than trolox in the $ABTS^{+\bullet}$ and DPPH assays, respectively.

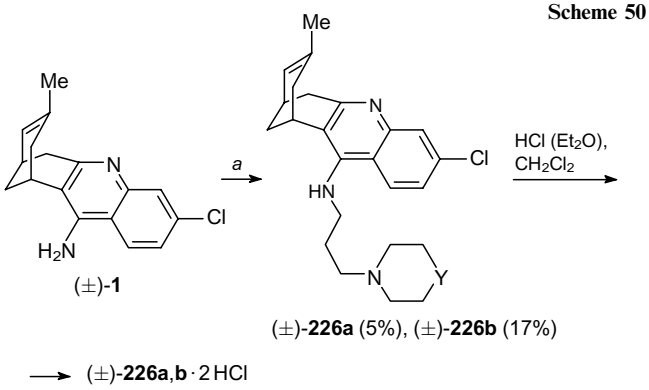
In the search for potent anti-HAT agents, ω-cyano-, ω-amino-, ω-guanidinoalkyl chains or simplified 4-aminoquinoline analogues were introduced at the primary amino group of huprines.[163] From these derivatives, cyano and aminoalkyl analogues (±)-**217a** – **h** and (±)-**218a** – **h** were previously developed (see Scheme 47). The novel compounds contain either guanidine, piperidine or morpholine at the tail of the linker. Compounds (±)-**225b** and (±)-**225e** were synthesized by the reaction of (±)-**218b** or (±)-**218e** with 1*H*-pyrazole-1-carboxamidine hydrochloride in the presence of $Et_3N$ (Scheme 49). The treatment of (±)-**1** with 1-(3-chloropropyl)piperidine hydrochloride or 3-morpholinopropyl methanesulfonate in the presence of KOH provided (±)-**226a** or (±)-**226b**, respectively (Scheme 50). The final products were converted into hydrochlorides. The racemic mixtures of compounds from the huprine and tacrine series were screened for their antitrypanosomal activity, cytotoxicity, anti-AChE activity and CNS availability. The most intriguing ones were carbonitrile (±)-**217e** (see Scheme 47) and guanidine-containing (±)-**225e** (see Scheme 49). The former compound [(±)-**217e**] displayed an $IC_{50}$ value of 320 nmol $L^{-1}$ ($IC_{90}$ = 420 nmol $L^{-1}$) against *T. brucei*, which was 14-fold more potent than the positive control nifurtimox and two-fold more potent than the parent **1** (7-fold more potent than **1** in terms of $IC_{90}$). The introduction of the guanidine moiety at the end of the side chain increased the antitrypanosomal potency relative to the corresponding primary amine intermediates. However, in the case of the carbonitrile-bearing analogue the activity

**Scheme 49**




(*a*) 1*H*-pyrazole-1-carboxamidine hydrochloride, $Et_3N$, MeCN, reflux, overnight; $n$ = 6 (**b**), 9 (**e**)

**Scheme 50**



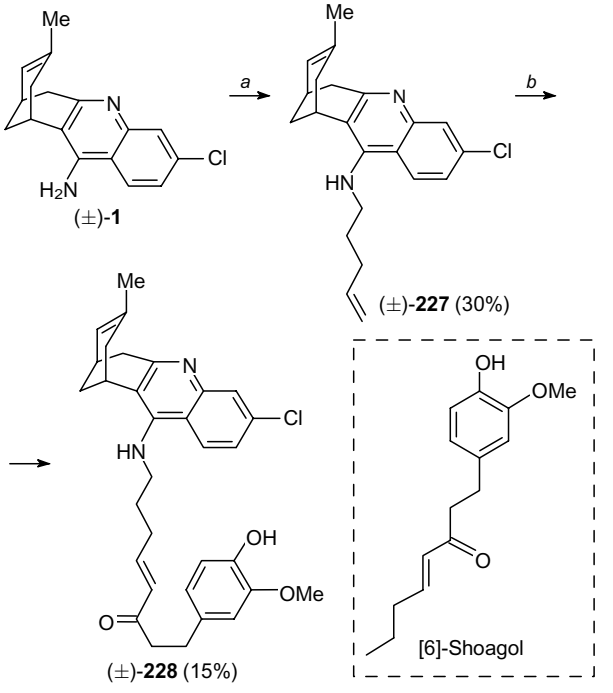

(*a*) 1) KOH, 4 Å MS, DMSO, rt, 2 h; 2) 1-(3-chloropropyl)piperidine hydrochloride or 3-morpholinopropyl methansulfonate, DMSO, rt, overnight; Y = $CH_2$ (**a**), O (**b**)

was retained with no deviation observed. Novel guanidine (±)-**225e** displayed the same antitrypanosomal potency as (±)-**217e** ($IC_{50}$ = 330 nmol $L^{-1}$). The introduction of piperidino or morpholino substituents at the side chain did not enhance antitrypanosomal potency. Carbonitriles (±)-**217a**–**h** and primary amines (±)-**218a**–**h** were less toxic to L6 cells than to *T. brucei*, with nitriles being less cytotoxic than the corresponding amines. A 25-fold selectivity profile [defined as $IC_{50}$ (*T. brucei*)/$IC_{50}$ (L6 cells)] was displayed by derivative (±)-**217e**, whereas **1** and nifurtimox were only 2- and 3.5-fold more potent, respectively. Interestingly, the introduction of ω-cyano- and ω-aminoalkyl chains at the primary amino group of **1** dropped AChE inhibitory activity (up to 500-fold), but carbonitriles (±)-**217a**–**h**, amines (±)-**218a**–**h** and novel derivatives (±)-**225b**,**e** and (±)-**226a**,**b** had more pronounced AChE inhibitory properties than it would be desirable for antitrypanosomal effect in nanomolar $IC_{50}$ values ranging between 9.7–158 nmol $L^{-1}$ against *ee*AChE.

The development of three shogaol–huprine dimers (±)-**228** and (±)-**230**–**231** was reported by Peréz-Areales *et al.*[113] These compounds combine a racemic mixture of (±)-**1** with the 4-hydroxy-3-methoxyphenylpentenone moiety of shogaols. [6]-Shogaol (see Fig. 9) is a biologically active compound found in ginger (the rhizome of *Zingiber officinale*) that exhibits potent antioxidant and anti-inflammatory activities.[164] Alkylation of (±)-**1** with 5-bromo-1-pentene resulted in intermediate (±)-**227**, which was subjected to cross metathesis with enone **228** in the presence of Hoveyda–Grubbs second generation catalyst to give dimer (±)-**228** (Scheme 51).[113] Compound (±)-**217h** was used as the starting material for the synthesis of hybrids (±)-**230** and (±)-**231** (Scheme 52).[113] Reduction of nitrile functionality of (±)-**217h** with diisobutylaluminium hydride (DIBAl-H) produced aldehyde (±)-**229**. Its transformation into dimer (±)-**230** was performed by condensation with zingerone **232** in the presence of dimethylammonium dimethyl carbamate (DIMCARB). This reaction gave the desired product (±)-**230** and side product (±)-**231** with a dimethylaminomethyl group at position 3.[113] The inhibitory capacity of the developed shogaol–huprine hybrids against recombinant *h*AChE ranged between 6.7–21 nmol $L^{-1}$, while the $IC_{50}$ values for *h*BChE were in the submicromolar range (between 180–980 nmol $L^{-1}$). Compound (±)-**228** was classified as the most AChE-selective derivative with a SI value of 147. All dimers exhibited potent antioxidant activity in the ABTS radical cation decolorization assay, DPPH assay (3–12 trolox equivalents) and also in the total phenolic assay. The $A\beta_{42}$ and tau anti-aggregating activity was in the range of 39%–71% and 35%–51%, respectively, at a concentration of 10 μmol $L^{-1}$, pointing out that the novel derivatives were more potent than **1** (about 9% inhibition at 10 μmol $L^{-1}$ for both).

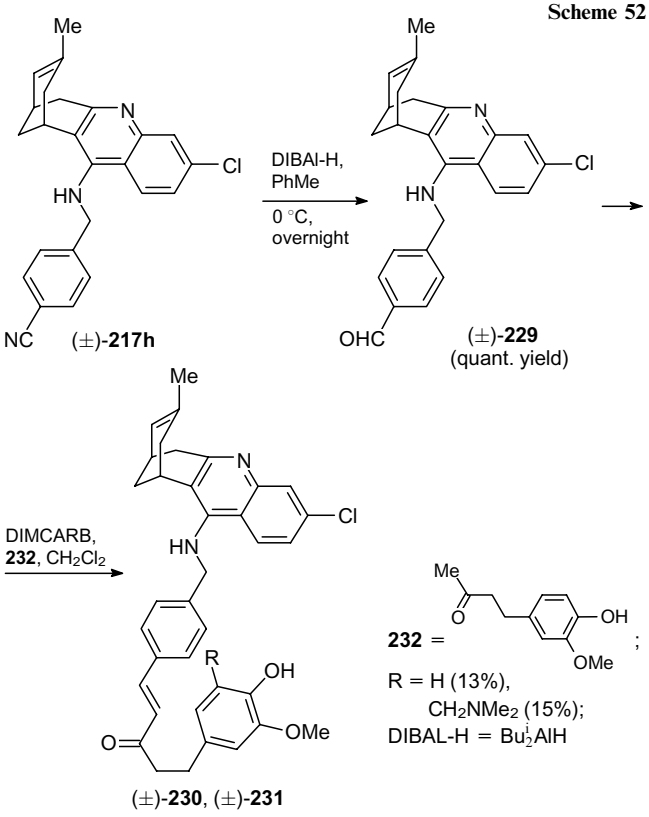
Camps *et al.*[108] developed huprine–tacrine heterodimers. The synthetic approach started from enone (±)-**85a** which was converted by condensation with anthranilic acid into a mixture of regioisomers (±)-**233** and (±)-**234** (Scheme 53). The treatment of (±)-**233** and (±)-**234** with $POCl_3$ led to the desired (±)-**236** in moderate yield and by-products (±)-**235** and (±)-**237** that were sepa-

**Scheme 51**




(a) 1) NaOH, 4 Å MS, DMSO, 1 h; 2) 5-bromo-1-pentene, rt, overnight; (*b*) **4**, p-benzoquinone, Hoveyda–Grubbs second-generation Cat., $CH_2Cl_2$

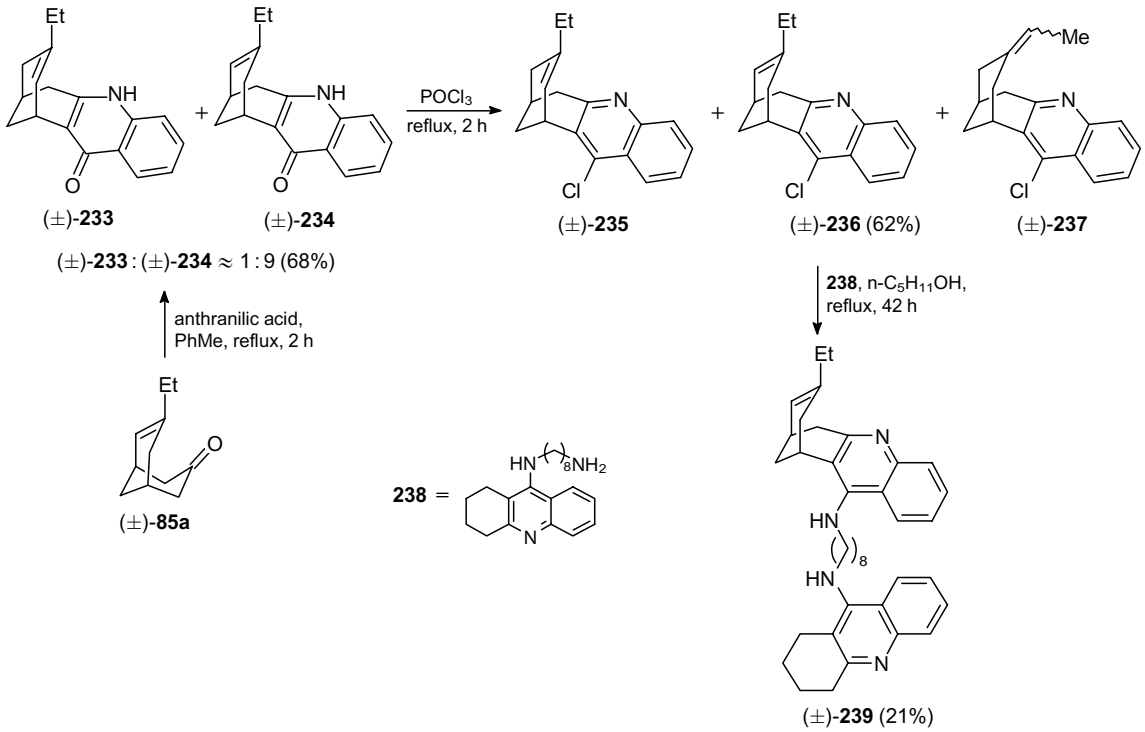
**Scheme 52**



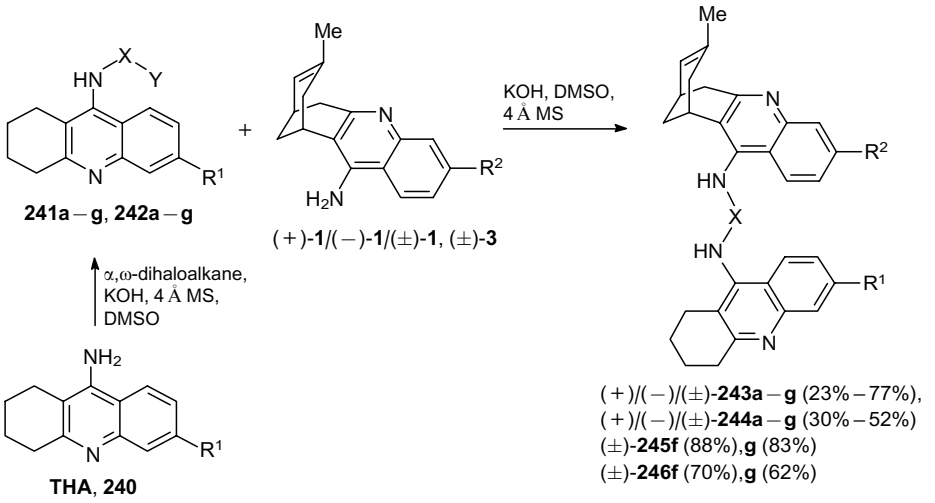

rated by column chromatography. Nucleophilic aromatic substitution of chlorine of intermediate (±)-**236** by reacting with the known amine **238** in refluxing 1-pentanol provided dimer (±)-**239**. However, the primary synthetic route was changed due to the low yield in the last step and the formation of a number of regioisomers. The linkers between the adequate subunits were introduced *via* alkylation of THA or 6-chlorotacrine (**240**) by reacting with the corresponding α,ω-dibromoalkanes (or α,ω-dichloroalkane derivative for series **d**) in the presence of KOH (Scheme 54). This resulted in the formation of compounds **241a**–**f** and **242a**–**f** which were subjected to in reaction with a racemic mixture of (±)-**1** to provide heterodimers (±)-**243a**–**d** and (±)-**244a**–**d**.[108] This synthetic route was also applied in the preparation of derivatives (±)-**243e**–**g**, (±)-**244e-g**, (±)-**245f,g** and (±)-**246f,g** (dimers with a longer chain between respective subunits), as well as enantiopure derivatives (−)-**243b**, (+)-**243b**, (−)-**244b** and (+)-**244b**.[96, 109]

All the huprine–tacrine heterodimers were very potent inhibitors of *h*AChE, exhibiting $IC_{50}$ values in the subnanomolar to low nanomolar range (between 0.3–12 nmol $L^{-1}$).[96, 109] The most potent derivatives were (±)-**243c** [$IC_{50}$(*h*AChE) = 0.4 nmol $L^{-1}$] and (±)-**244c** [$IC_{50}$(*h*AChE) = 0.3 nmol $L^{-1}$], which were approximately 1.6–2-fold more potent than the parent **1** and about 750–1000-fold more potent than tacrine. The derivatives (±)-**243a-f** and (±)-**244a-f** were tested for their ability to inhibit *h*BChE, AChE-induced Aβ aggregation, AChE-induced PrP106–126 aggregation, $Aβ_{1-42}$ self-induced aggregation and BACE-1.[96] All the huprine–tacrine heterodimers were selective inhibitors of *h*AChE, exhibiting 4–105-fold higher selective inhibitory capacity against *h*AChE than *h*BChE. Regardless, they still preserved $IC_{50}$ values against *h*BChE in the nanomolar range (between 25–140 nmol $L^{-1}$). Tested at 100 μmol $L^{-1}$, huprine–tacrine hybrids exhibited a significant inhibitory capacity against *h*AChE-induced $Aβ_{1-40}$ aggregation with a percentage of inhibition between 39%–67% for the tacrine-based heterodimers and between 23%–47% for 6-chlorotacrine-based hybrids. All of the tested heterodimers also inhibited AChE-induced PrP106–126 aggregation, showing an inhibition percentage between 79%–93% (at 100 μmol $L^{-1}$). All compounds inhibited Aβ self-induced aggregation when tested at a concentration five-fold lower than that of Aβ, showing an inhibition percentage between 28%–64%. Their ability to inhibit *in vitro* human recombinant

**Scheme 53**



**Scheme 54**




$R^1$ = H (THA, **241**), Cl (**240**, **242**);
**241a – g** (28% – 40%),
**242a – g** (19% – 44%);
$R^2$ = Cl (**1**), H (**3**);
**241**, **242**: X = $(CH_2)_n$ [*n* = 6 (**a**), 7 (**b**), 8 (**c**), 9 (**e**), 10 (**f**), 12 (**g**), $(CH_2)_3N(Me)(CH_2)_3$ (**d**)];
Y = Br (**a – c**, **e – g**), Cl (**d**);
**243**: $R^1$ = H, $R^2$ = Cl;
**244**: $R^1$ = $R^2$ = Cl;
**245**: $R^1$ = $R^2$ = H;
**246**: $R^1$ = Cl, $R^2$ = H

BACE-1 was determined at a single concentration of 5 μmol $L^{-1}$. 6-Chlorotacrine-based heterodimers exhibited BACE-1 inhibitory capacity between 18% – 47%. With the exception of the long-tethered homologues (±)-**243e** and (±)-**243f**, the heterodimers bearing an unsubstituted tacrine were inactive against BACE-1. The $IC_{50}$ values for BACE-1 inhibition were determined for the most active compounds, *i.e.* (±)-**243f**, (–)-**244b**, (+)-**244b** and (±)-**244a – d**, being between 5 to 7 μmol $L^{-1}$. Using the PAMPA-BBB assay, all the huprine-tacrine dimers were predicted to cross the BBB, with the exception of (±)-**243e** and (±)-**243c**, for which an uncertain BBB permeation was predicted.

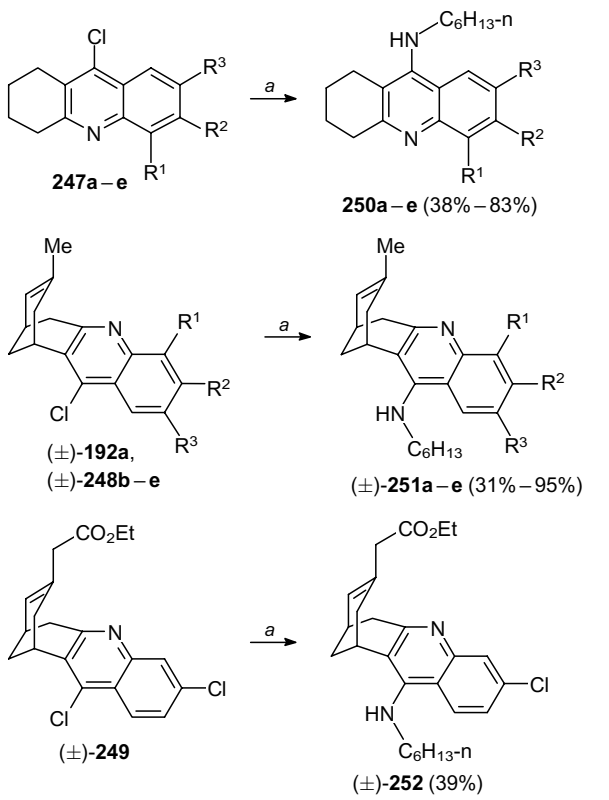
The high anti-AChE capacity of huprine – tacrine dimers represents a major drawback regarding their antiprotozoal properties. However, the presence of two 4-aminoquinoline moieties and their ability to cross the BBB still supported their use in both stages of HAT.[109] All of them exhibited $IC_{50}$ and $IC_{90}$ values in the range of 0.1 – 0.6 μmol $L^{-1}$ and 0.3 – 0.8 μmol $L^{-1}$ against *T. brucei*, respectively. This trypanocidal capacity was also observed in octa- and deca-methylene derivatives **243c**, **244c**, **243f** and **244f**. All of the tested heterodimers were more potent than monomeric **1** (up to four-fold for $IC_{50}$ and up to 10-fold for $IC_{90}$). The anti-plasmodial capacity was measured against *P. falciparum*. The heterodimers with longer linkers (deca- and dodeca-methylene analogues) were essentially inactive or only moderately potent anti-plasmodial agents. Most dimers with shorter chains displayed $IC_{50}$ values in the submicromolar range, with some of them being two – three-fold more potent than the reference chloroquine. With the exception of derivatives **243e** and **244e**, all of the tested heterodimers were more cytotoxic than **1**. Compounds **243e** and **244e** displayed similar or a five-fold lower cytotoxicity compared to **1**, therefore showing the best selectivity profile against *T. brucei* (SI = 34 and 167, respectively). Only derivative **243e** had a favourable selectivity index regarding *P. falciparum* (SI = 20). The results concerning the balanced dual trypanocidal and anti-plasmodial activity makes of **243e** the most promising hit from the series.

Another approach for the synthesis of huprine – tacrine heterodimers included the use of palladium-catalyzed amination.[165] To optimize these conditions, the reactions between **247a**,**c** and (±)-**192**, (±)-**248c** with n-hexylamine were initiated to determine the best ligand, palladium source, solvent and base, all in terms of reactivity. Chloroquinolines such as 9-chlorotacrine derivatives **247a – e** huprines (±)-**192a** and (±)-**248b – e** were then converted into *N*-alkylated compounds **250a – e**, **251a – e** and **252** using ideal conditions as BINAP (2,2′-bis(diphenylphosphino)-1,1′-binaphthyl), $Pd_2(dba)_2$ and $Cs_2CO_3$ in 1,4-dioxane (Scheme 55). The $S_NAr$ reaction of ester (±)-**249** resulted in compound decomposition,[103] while Pd-catalyzed amination furnished compound (±)-**252** in 39% yield (not optimized).[165]

The efficiency of this method was demonstrated by applying it as an initial step in the formation of (±)-**243b** and (±)-**254**, respectively. Amination of 9-chlorotacrine (**247**) with 1,7-diaminoheptane afforded the intermediate **253** (Scheme 56). Compound **253** was reacted with (±)-**248b** or (±)-**192a** to produce (±)-**243b** and (±)-**254**, respectively, following the optimized synthetic protocol.[165]

The preparation of racemic mixtures or enantiopure heterodimers **258** and **259** and their biological assessment was reported in 2010.[116] These compounds combine the huprine subunit (**2** or **1**) tethered *via* an ethylene or propylene linker to a donepezil-like moiety (piperidine ring substituted at position 4 with 5,6-dimethoxyindan-2-yl). The rational for this combinations is corroborated by the fact that huprines are well-known CAS binders, whereas the 4-[(5,6-dimethoxy-2,3-dihydro-1H-inden-2-yl)methyl]piperidine moiety is stacked at PAS in the crystal structure of AChE.[28,166] The alkylation of compound **255** with 2-bromoethanol or 3-chloro-1-propanol resulted in alcohols **256a** and **256b** which were subjected in the reaction with thionyl chloride to produce **257a** and **257b**. The final products were obtained by the alkylation of racemic mixtures or enantiopure huprines **1** and **2** with chlorides **257a**,**b** following standard conditions (Scheme 57). These huprine – donepezil heterodimers displayed $IC_{50}$ values against *h*AChE in the low nanomolar range. The levorotatory enantiomers, bearing a (7*S*,11*S*)-huprine subunit, are the automers in this family, show roughly two-fold potency over the corresponding racemic mixtures and are much more potent than the dextrorotatory isomers. The most potent *h*AChEI of the series was (–)-**259b** ($IC_{50}$ = 2.6 nmol $L^{-1}$), which was eight-fold more potent than donepezil ($IC_{50}$ = 21 nmol $L^{-1}$) but six-fold less potent than the parent (–)-**1** ($IC_{50}$ = 0.4 nmol $L^{-1}$). The most potent **2**-based dimer was derivative (–)-**258b** ($IC_{50}$ = 3.9 nmol $L^{-1}$); however, it still was 14-fold less active than (–)-**2** ($IC_{50}$ = 0.3 nmol $L^{-1}$). Given their nature, the huprine –

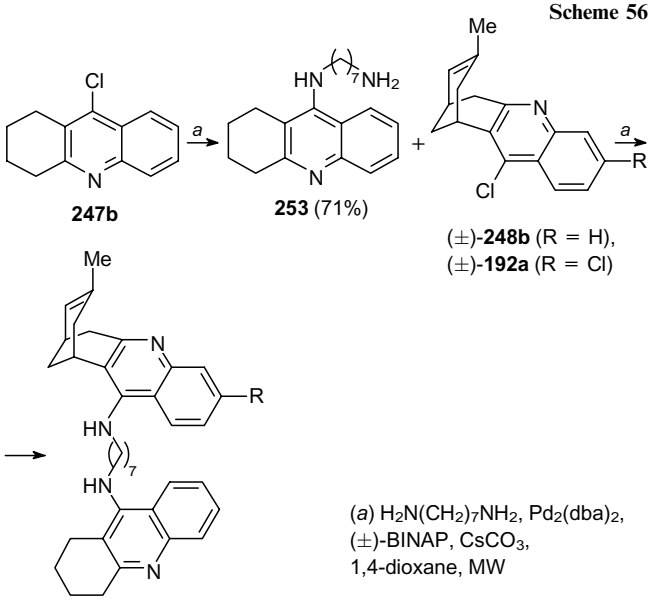
**Scheme 55**




(*a*) n-$C_6H_{13}NH_2$, (±)-BINAP, $Pd_2(dba)_2$, $CsCO_3$, 1,4-dioxane, heating; $R^1 = R^3 = H$, $R^2 = Cl$ (**a**); $R^1 = R^2$, $R^3 = H$ (**b**); $R^1 = R^2 = H$, $R^3 = NO_2$ (**c**), $R^1 = H$, $R^2 = R^3 = F$ (**d**), $R^1 = R^3 = Cl$, $R^2 = H$ (**e**)

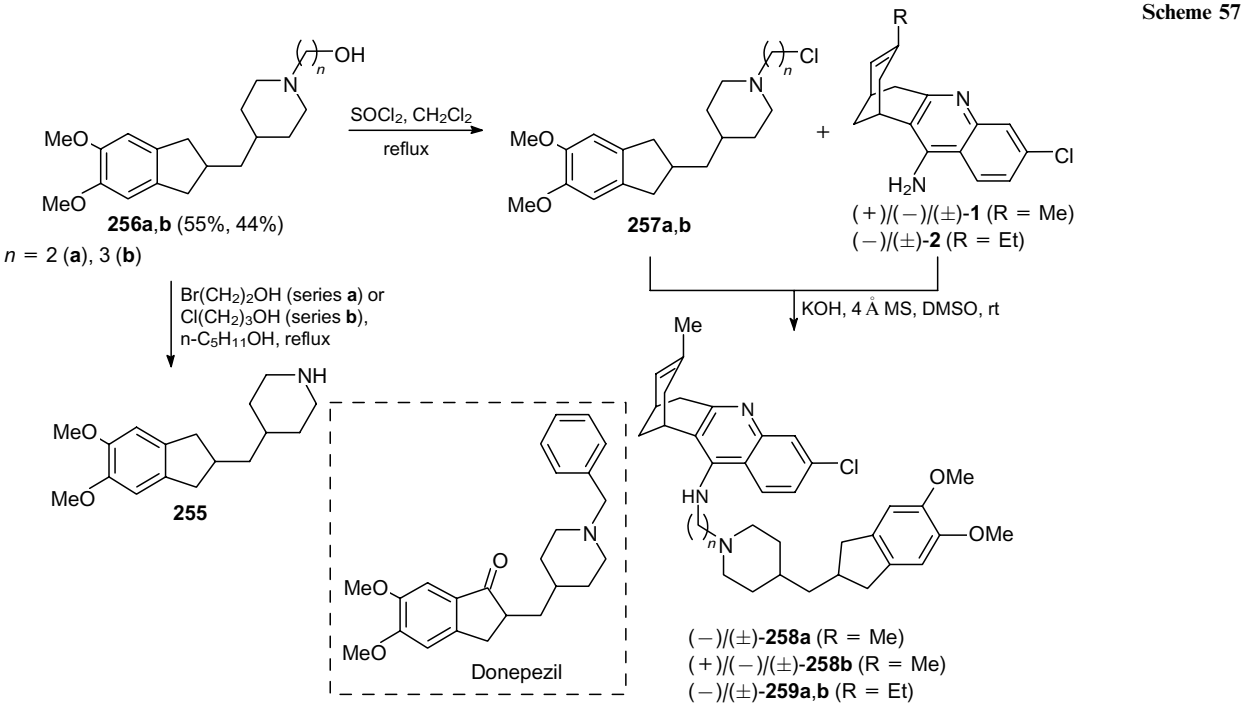
donepezil hybrids displayed a more potent *h*AChE profile over *h*BChE (2 – 143-fold) with $IC_{50}$ values for *h*BChE between 88 – 420 nmol $L^{-1}$. The *h*BChE inhibitory capacity increased in the presence of an ethyl substituent at position 9 of the huprine subunit favouring also dextrorotatory huprine moiety bearing a 7*R*,11*R*-configuration. The most

**Scheme 56**




potent *h*BChEI was racemic derivative (±)-**259b**. Novel dimers were then tested for their ability to inhibit AChE-induced $A\beta_{1-40}$ aggregation and self-induced $A\beta_{1-42}$ aggregation. The inhibition percentage against AChE-induced $A\beta_{1-40}$ aggregation at a concentration of 100 μmol $L^{-1}$ ranged between 25% – 50%. The huprine – donepezil dimers were also able to inhibit self-induced Aβ aggregation, tested at a concentration 5-fold lower than that of Aβ, and showing an inhibition percentage between 16% – 30%. The BACE-1 inhibitory capacity of these novel hybrids was screened at a single concentration (5 μmol $L^{-1}$) and all the heterodimers exhibited potent inhibitory capacity, which ranged between 12% – 31%. The most active BACE-1 inhibitors, compounds (±)-**258b** (29%), (–)-**258b** (31%, $IC_{50}$ = 11 μmol $L^{-1}$) and (–)-**258a** (25%), were more

**Scheme 57**



potent than the parent huprines and almost equipotent to donepezil. According to the PAMPA-BBB assay all these novel derivatives were able to cross the BBB.[116]

The prepared huprine – donepezil heterodimers were also tested for cytotoxicity and trypanocidal and antiplasmodial properties.[109] All of the dimers displayed potent trypanocidal activity, with $IC_{50}$ and $IC_{90}$ values ranging between 0.2 – 0.5 and 0.4 – 1.3 μmol $L^{-1}$, respectively. They were up to four-fold more potent than **1** based on the $IC_{50}$ values and up to eight-fold more potent based on $IC_{90}$ values. However, most of these novel dimers were essentially inactive against *P. falciparum* with the sole exception of (−)-**259b** ($IC_{50}$ = 0.8 μmol $L^{-1}$), which was equipotent to the reference antimalarial drug chloroquine. All the heterodimers were slightly more cytotoxic than **1**, but their superior trypanocidal capacity resulted in a similar or even better selectivity index against *T. brucei* than **1**.

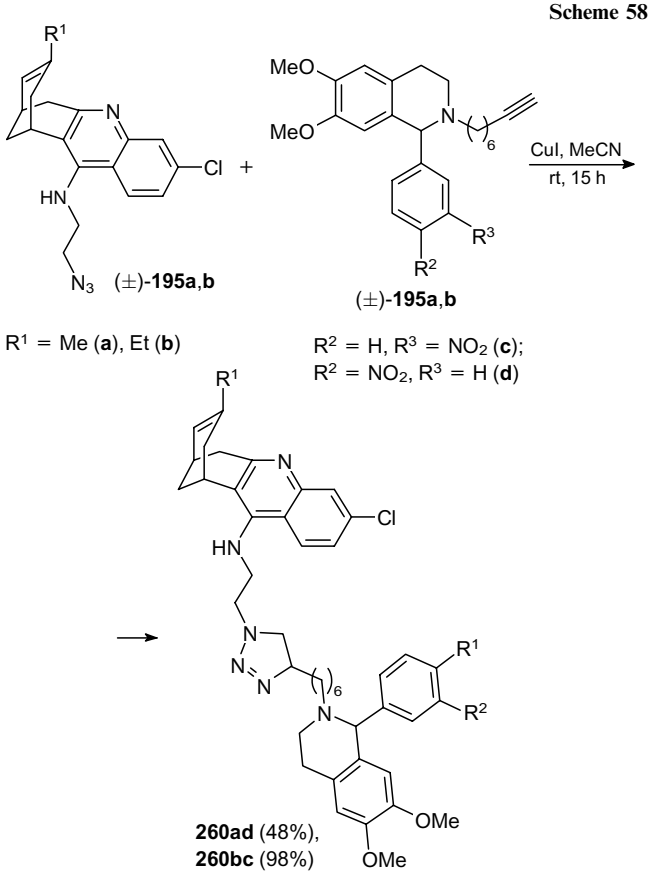
Huprines analogues (±)-**195a**,**b** with a two-carbon chain and an azide group at its tail (prepared according to the procedure depicted in Scheme 36) reacted with tetrahydroisoquinoline derivatives (±)-**5c**,**d** in the presence of CuI as a catalyst (Scheme 58).[102] This Huisgen reaction allowed the formation of heterodimers (±)-**260ad** and (±)-**260bc**, which proved to be potent *h*AChE inhibitors with $IC_{50}$ values of 4.0 and 6.0 nmol $L^{-1}$, respectively. Both compounds were highly selective *h*AChE inhibitors in comparison to *h*BChE and only 6% and 7% inhibition was observed at 10 μmol $L^{-1}$ for (±)-**260ad** and (±)-**260bc**, respectively.

Oueis *et al.*[167] followed a TGS strategy in the synthesis of new huprine heterodimers. This concept exploits biomolecule targeting (protein or DNA) to assemble its best multi-site ligands directly from a pool of fragments bearing complementary reactive functional groups. For example, if the target molecule is an enzyme, it is directly involved in the choice of its suitable ligands. Only derivatives that can fit into the active site of the enzyme should be close enough to overcome energy barrier of the reaction and thus react.[167, 168]

This approach used one of the first ever described 'click chemistry reactions' — Huisgen 1,3-dipolar cycloaddition between terminal alkynes and azides.[169] Huprine derivatives (±)-**110** and (±)-**123** bearing alkyl azide functionality and compounds **261a** – **d** bearing an alkyl acetylene group were incubated in the presence of the model enzyme — mouse AChE (*m*AChE) (Scheme 59). Control experiments without the enzyme were also performed. The reaction mixtures were analyzed by reverse phase high performance liquid chromatography (RP-HPLC) and compared to samples obtained by thermal or copper-catalyzed 1,3-dipolar cycloaddition. From ten possible dimers only (±)-**262** (*anti*-isomer) and (±)-**263** (mixture of *syn*- and *anti*-isomers, ≈ 2 : 1) were detected. The same series of reagents were incubated in the presence of recombinant *h*AChE and similar results were obtained.[167]

Heterodimer **264** is composed of a levetiracetam-like unit and (+)-**1** or (−)-**1** linked with a heptamethylene chain.[112] Levetiracetam [2-(2-oxopyrrolidin-1-yl)butyramide] is used as anti-epileptic drug.[170] The chronic treatment with this drug can effectively inhibits the aberrant network activity and help improve memory function in patients with amnestic mild cognitive impairment as well as in APP/PS1 and hAPPJ20 AD mouse models.[171 – 173] The first step in the synthesis of compounds **264** was the alkylation of enantiopure huprines (−)-(7*S*,11*S*)-**1** or (+)-(7*R*,11*R*)-**1** with 7-bromoheptanenitrile (Scheme 60). These reactions led to nitriles (7*S*,11*S*)-**217c** and (7*R*,11*R*)-**217c** that were subsequently reduced using $LiAlH_4$ to give

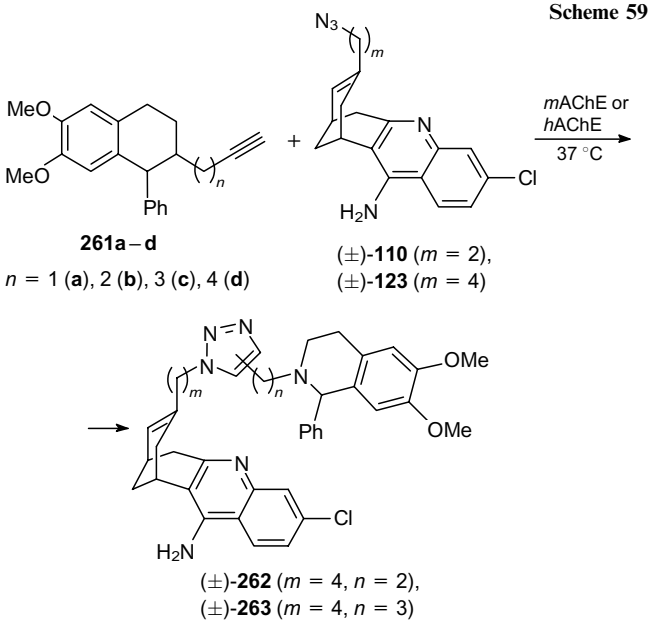
**Scheme 58**



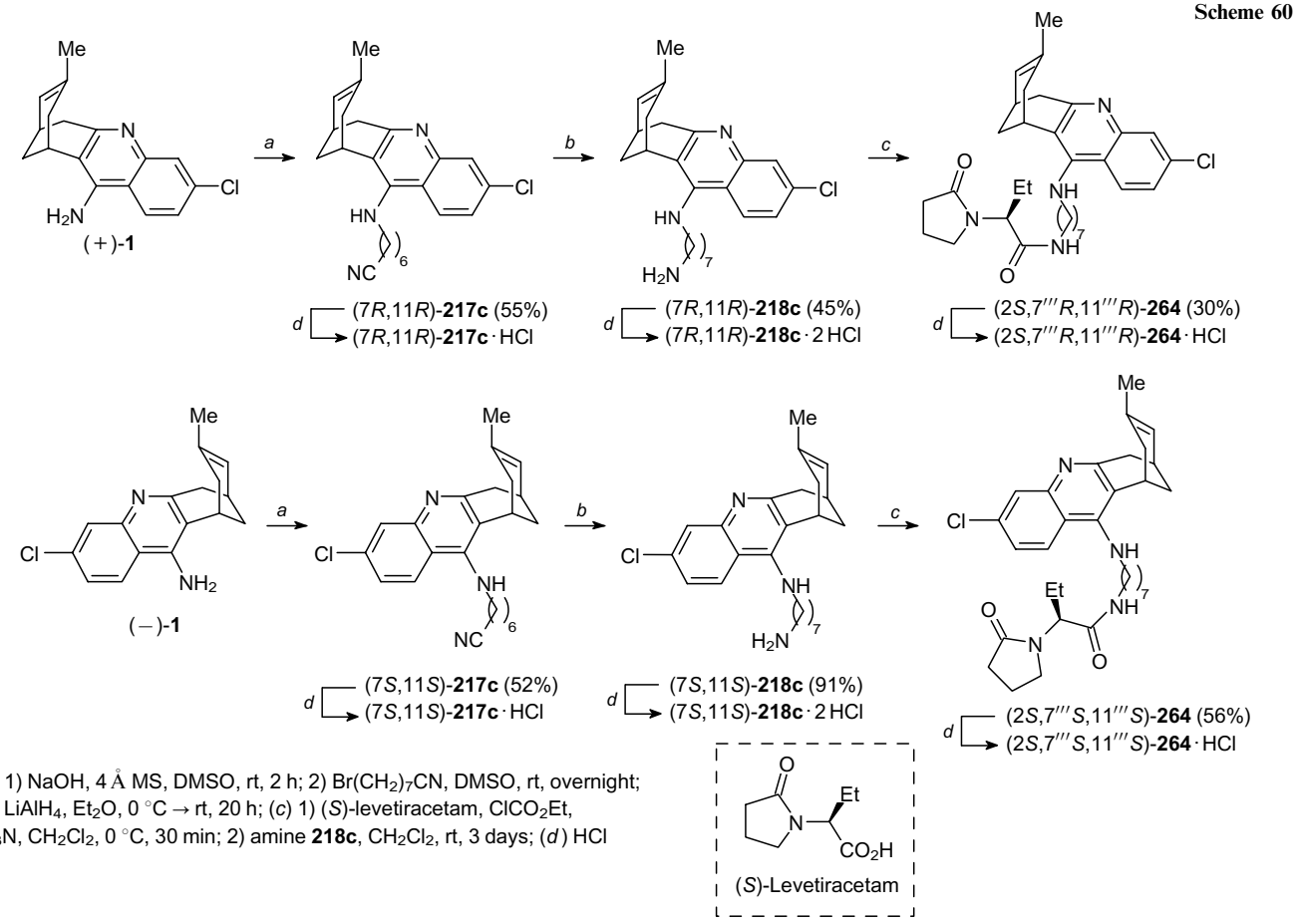

amines (7*S*,11*S*)-**218c** and (7*R*,11*R*)-**218c**. The treatment of the carboxylic acid (*S*)-levetiracetam with ethyl chloroformate afforded an anhydride which was submitted to the reaction with **218c** to give enantiopure amides (2*S*,7‴*R*,11‴*R*)-**264** and (2*S*,7‴*S*,11‴*S*)-**264**.[112] The final products were then converted into corresponding hydrochloride salts.

The combination of **1** and a levetiracetam-subunit was used to hit several biological targets of interest potentially involved in AD: a) *h*AChE [for (2*S*,7‴*S*,11‴*S*)-**264**: $IC_{50}$ = 4.2 nmol $L^{-1}$; for (2*S*,7‴*R*,11‴*R*)-**264**: $IC_{50}$ = 56 nmol $L^{-1}$]

**Scheme 59**



**Scheme 60**




(*a*) 1) NaOH, 4 Å MS, DMSO, rt, 2 h; 2) $Br(CH_2)_7CN$, DMSO, rt, overnight; (*b*) $LiAlH_4$, $Et_2O$, 0 °C → rt, 20 h; (*c*) 1) (*S*)-levetiracetam, $ClCO_2Et$, $Et_3N$, $CH_2Cl_2$, 0 °C, 30 min; 2) amine **218c**, $CH_2Cl_2$, rt, 3 days; (*d*) HCl

and *h*BChE [for (2*S*,7‴*S*,11‴*S*)-**264**: $IC_{50}$ = 230 nmol $L^{-1}$; for (2*S*,7‴*R*,11‴*R*)-**264**: $IC_{50}$ = 58 nmol $L^{-1}$], b) tau aggregation (54% inhibition for (2*S*,7‴*S*,11‴*S*)-**264**; 50% inhibition for (2*S*,7‴*R*,11‴*R*)-**264** at 20 μmol $L^{-1}$ drug concentration) and c) $A\beta_{42}$ aggregation (36% inhibition for (2*S*,7‴*S*,11‴*S*)-**264**; 26% inhibition for (2*S*,7‴*R*,11‴*R*)-**264** at 20 μmol $L^{-1}$ drug concentration). The brain AChE inhibitory capacity of these derivatives and their ability to penetrate the BBB was demonstrated after intraperitoneal injection into C57BL6J mice. In addition, hybrid (2*S*,7‴*S*,11‴*S*)-**264** reduced the incidence of epileptic seizures, cortical amyloid burden and neuroinflammation in APP/PS1 mice after a 4-week treatment with a 5 mg $kg^{-1}$ dose. Derivative (2*S*,7‴*S*,11‴*S*)-**264** also rescued transgenic mice from cognitive deficits.

## 5. Conclusion

The huprine family represents a successful example of the merging approach. The structures of THA and (−)-HupA are overlapped resulting in a novel group of inhibitors of ChEs. The most potent first generation analogue was **2** with a sub-nanomolar $IC_{50}$ against *h*AChE. This derivative in its racemic form was >270-times more potent *h*AChE inhibitor than THA and over 340 times more potent than (−)-HupA. In its enantiopure form, (−)-**2** reached over 800- and 640-fold higher inhibitory capacity than the parent compounds. The development of second generation huprines was driven by molecular modeling studies using the crystallographic structures of *Tc*AChE complexes with different inhibitors. The introduction of triazole attached *via* a carbon chain at position 9 led to analogues **124** and **125**, which had even higher inhibitory capacity against AChE than **2**. Further, an interesting class of huprines is formed by homo- and heterodimers. These derivatives were mostly developed in accordance with the concept of MTDLs and the so-called linking approach was used in their design. Two molecular pharmacophores were conjugated by a distinct linker that was not a part of the original templates. The resulting ligands displayed a broader spectrum of activities associated to AD besides the inhibitory capacity against ChEs. The primary objective was, in most cases, to target Aβ and tau aggregation. Other significant characteristics of AD that were also inspected were OS and neuroinflammation.

The chemistry of huprines is simple and straightforward and most of the derivatives with structural changes in all parts of the scaffold were prepared in elegant few-step syntheses. The relatively easy generation of different structural analogues led to the exploration of SAR and the development of one of the most potent ChEIs. However, a major limitation can be seen in the inability to obtain enantioenriched products with satisfactory *ee* values. This phenomenon was explained by the equilibrium shift of the initial *syn*/*anti*-mixtures during the Friedländer reaction towards more stable *anti*-products. Thus, some other techniques like chiral HPLC or MPLC should be used to obtain enantioenriched samples. The huprine-based homo- and heterodimers were also prepared in one to several step syntheses.

The potential application of huprines is reflected by their inhibitory capacity against ChEs. Likewise, inhibitors of these enzymes, specifically, donepezil, galantamine and

rivastigmine, provide symptomatic relief in patients with AD. The current trend in the search for new AD therapeutic drugs has been focused into the complex nature of the disease. One potential strategy suggests the proper design of so-called MTDLs with multiple biological targets.[174] The huprine scaffold is used in the design of several such ligands. ChEs inhibitors (*e.g.*, pyridostigmine bromide, neostigmine bromide) are also used in the treatment of MG, providing once again symptomatic relief for all forms of this disorder. Similarly, huprines containing a permanent charge in their structure have also been proposed in the treatment of MG, though with limited success. The huprine scaffold contains an aminoquinoline substructure, which is a core framework in the construction of HAT and malaria agents. The treatment of these protozoan parasite diseases is difficult because of drug resistance, the limited range of available drugs, as well as their high cost and significant toxicity. Several huprine derivatives exhibit potent trypanocidal and anti-plasmodial capacity and represent interesting lead structures in the development of novel HAT and malaria therapeutic drugs. Thanks to the similar features of AD and PrD, therapeutic approaches involving antioxidant, chelators and protein aggregation inhibitors could be beneficial for both disorder types. Moreover, these findings shed light into huprines as a versatile scaffold with broad therapeutic implications.

The authors declare no conflict of interest.

The work was supported by the Ministry of Education, Youth and Sports of Czech Republic (Project ERDF IT4N no. CZ.02.1.01/0.0/0.0/18_069/0010054), by a grant of Ministry of Defence 'Long Term Development Plan' Medical Aspects of Weapons of Mass Destruction of the Faculty of Military Health Sciences (University of Defence), by Grant Agency of Czech Republic (Project No. 20-29633J), and by MH CZ-DRO (University Hospital Hradec Kralove, No. 00179906).

## References

1. P.Camps, D.Muñoz-Torrero. *Mini Rev. Med. Chem.*, **1**, 163 (2001)
2. J.Z.Long, B.F.Cravatt. *Chem. Rev.*, **111**, 6022 (2011)
3. D.Muñoz-Torrero, P.Camps. *Expert Opin. Drug. Discov.*, **3**, 65 (2008)
4. F.Aguado, A.Badía, J.Baños, F.Bosch, C.Bozzo, P.Camps, J.Contreras, M.Dierssen, C.Escolano, D.Görbig, D.Muñoz-Torrero, M.Pujol, M.Simón, M.Vázquez, N.Vivas. *Eur. J. Med. Chem.*, **29**, 205 (1994)
5. A.Badia, J.E.Baños, P.Camps, J.Contreras, D.M.Görbig, D.Muñoz-Torrero, M.Simón, N.M.Vivas. *Bioorg. Med. Chem.*, **6**, 427 (1998)
6. P.Camps, J.Contreras, M.Font-Bardia, J.Morral, D.Muñoz-Torrero, X.Solans. *Tetrahedron: Asymmetry*, **9**, 835 (1998)
7. M.L.Crismon. *Ann. Pharmacother.*, **28**, 744 (1994)
8. M.Bartolini, C.Bertucci, V.Cavrini, V.Andrisano. *Biochem. Pharmacol.*, **65**, 407 (2003)
9. P.B.Watkins, H.J.Zimmerman, M.J.Knapp, S.I.Gracon, K.W.Lewis. *JAMA*, **271**, 992 (1994)
10. E.Zeiger, G.Erexson, K.Mortelmans, A.Thilagar. *Mutat. Res.*, **393**, 189 (1997)
11. M.Farlow, S.I.Gracon, L.A.Hershey, K.W.Lewis, C.H.Sadowsky, J.Dolan-Ureno. *JAMA*, **268**, 2523 (1992)
12. W.-Y.Wu, Y.-C.Dai, N.-G.Li, Z.-X.Dong, T.Gu, Z.-H.Shi, X.Xue, Y.-P.Tang, J.-A.Duan. *J. Enzyme Inhib. Med. Chem.*, **32**, 572 (2017)
13. K.Spilovska, J.Korabecny, E.Nepovimova, R.Dolezal, E.Mezeiova, O.Soukup, K.Kuca. *Curr. Top. Med. Chem.*, **17**, 1006 (2017)
14. Z.M.Qian, Y.Ke. *Front. Aging Neurosci.*, **6**, Article 216 (2014)
15. P.Williams, A.Sorribas, M.-J.R.Howes. *Nat. Prod. Rep.*, **28**, 48 (2011)
16. M.-J.R.Howes, R.Fang, P.J.Houghton. *Int. Rev. Neurobiol.*, **135**, 29 (2017)
17. X.Q.Xiao, H.Y.Zhang, X.C.Tang. *J. Neurosci. Res.*, **67**, 30 (2002)
18. X.Q.Xiao, J.W.Yang, X.C.Tang. *Neurosci. Lett.*, **275**, 73 (1999)
19. H.S.Ved, M.LKoenig, J.R:Dave, B.P.Doctor. *NeuroReport*, **8**, 963 (1997)
20. P.Camps, B.Cusack, W.D.Mallender, R.E.El Achab, J.Morral, D.Muñoz-Torrero, T.L.Rosenberry. *Mol. Pharmacol.*, **57**, 409 (2000)
21. Y.Miao, N.He, J.-J.Zhu. *Chem. Rev.*, **110**, 5216 (2010)
22. I.Silman, J.L.Sussman. *Chem. Biol. Interact.*, **175**, 3 (2008)
23. M.Bajda, A.Więckowska, M.Hebda, N.Guzior, C.A.Sotriffer, B.Malawska. *Int. J. Mol. Sci.*, **14**, 5608 (2013)
24. J.L.Sussman, M.Harel, F.Frolow, C.Oefner, A.Goldman, L.Toker, I.Silman. *Science*, **253**, 872 (1991)
25. Y.Nicolet, O.Lockridge, P.Masson, J.C.Fontecilla-Camps, F.Nachon. *J. Biol. Chem.*, **278**, 41141 (2003)
26. M.Harel, I.Schalk, L.Ehret-Sabatier, F.Bouet, M.Goeldner, C.Hirth, P.H.Axelsen, I.Silman, J.L.Sussman. *Proc. Natl. Acad. Sci. USA*, **90**, 9031 (1993)
27. M.L.Raves, M.Harel, Y.P.Pang, I.Silman, A.P.Kozikowski, J.L.Sussman. *Nat. Struct. Biol.*, **4**, 57 (1997)
28. H.Dvir, D.M.Wong, M.Harel, X.Barril, M.Orozco, F.J.Luque, D.Muñoz-Torrero, P.Camps, T.L.Rosenberry, I.Silman, J.L.Sussman. *Biochemistry*, **41**, 2970 (2002)
29. R.M.Lane, S.G.Potkin, A.Enz. *Int. J. Neuropsychopharmacol.*, **9**, 101 (2006)
30. I.Silman, J.L.Sussman. *Curr. Opin. Pharmacol.*, **5**, 293 (2005)
31. H.Soreq, S.Seidman. *Nat. Rev. Neurosci.*, **2**, 294 (2001)
32. N.H.Greig, T.Utsuki, Q.Yu, X.Zhu, H.W.Holloway, T.Perry, B.Lee, D.K.Ingram, D.K.Lahiri. *Curr. Med. Res. Opin.*, **17**, 159 (2001)
33. S.Darvesh, D.A.Hopkins, C.Geula. *Nat. Rev. Neurosci.*, **4**, 131 (2003)
34. M.Noetzli, C.B.Eap. *Clin. Pharmacokinet.*, **52**, 225 (2013)
35. Y.Yang, H.Aloysius, D.Inoyama, Y.Chen, L.Hu. *Acta Pharmaceutica Sinica B*, **1**, 143 (2011)
36. O.Lockridge. *Pharmacol. Ther.*, **148**, 34 (2015)
37. J.L.Cummings. *N. Engl. J. Med.*, **351**, 56 (2004)
38. A.Contestabile. *Behav. Brain Res.*, **221**, 334 (2011)
39. G.K.Wilcock, M.M.Esiri, D.M.Bowen, C.C.T.Smith. *J. Neurol. Sci.*, **57**, 407 (1982)
40. N.R.Sims, D.M.Bowen, S.J.Allen, C.C.T.Smith, D.Neary, D.J.Thomas, A.N.Davison. *J. Neurochem.*, **40**, 503 (1983)
41. R.J.Rylett, M.J.Ball, E.H.Colhoun. *Brain Res.*, **289**, 169 (1983)
42. L.Nilsson, A.Nordberg, J.Hardy, P.Wester, B.Winblad. *J. Neural Transmission*, **67**, 275 (1986)
43. R.T.Bartus, R.L.Dean, B.Beer, A.S.Lippa. *Science*, **217**, 408 (1982)
44. R.C.Mohs, R.S.Doody, J.C.Morris, J.R.Ieni, S.L.Rogers, C.A.Perdomo, R.D.Pratt, *Neurology*, **57**, 481 (2001)
45. J.Cummings, N.Fox. *J. Prev. Alzheimers Dis.*, **4**, 109 (2017)
46. H.W.Querfurth, F.M.LaFerla. *N. Engl. J. Med.*, **362**, 329 (2010)
47. A.Agis-Torres, M.Sölhuber, M.Fernandez, J.M.Sanchez-Montero. *Curr. Neuropharmacol.*, **12**, 2 (2014)
48. P.Tiraboschi, L.A.Hansen, L.J.Thal, J.Corey-Bloom. *Neurology*, **62**, 1984 (2004)
49. K.A.Jellinger. *J. Neural. Transm. (Vienna)*, **116**, 1111 (2009)
50. S.H.Barage, K.D.Sonawane. *Neuropeptides*, **52** (Supplement C), 1 (2015)
51. M.Medina, J.Avila. *Biochem. Pharmacol.*, **88**, 540 (2014)
52. M.Valko, D.Leibfritz, J.Moncol, M.T.D.Cronin, M.Mazur, J.Telser. *Int. J. Biochem. Cell Biol.*, **39**, 44 (2007)
53. J.K.Andersen. *Nat. Med.*, 10 Suppl, S18 (2004)
54. X.Huang, R.D.Moir, R.E.Tanzi, A.I.Bush, J.T.Rogers. *Ann. NY Acad. Sci.*, **1012**, 153 (2004)

55. M.T.Heneka, M.J.Carson, J.El Khoury, G.E.Landreth, F.Brosseron, D.L.Feinstein, A.H.Jacobs, T.Wyss-Coray, J.Vitorica, R.M.Ransohoff, K.Herrup, S.A.Frautschy, B.Finsen, G.C.Brown, A.Verkhratsky, K.Yamanaka, J.Koistinaho, E.Latz, A.Halle, G.C.Petzold, T.Town, D.Morgan, M.L.Shinohara, V.H.Perry, C.Holmes, N.G.Bazan, D.J.Brooks, S.Hunot, B.Joseph, N.Deigendesch, O.Garaschuk, E.Boddeke, C.A.Dinarello, J.C.Breitner, G.M.Cole, D.T.Golenbock, M.P.Kummer. *Lancet Neurol.*, **14**, 388 (2015)
56. R.H.Swerdlow, J.M.Burns, S.M.Khan. *Biochim. Biophys. Acta*, **1842**, 1219 (2014)
57. A.Cavalli, M.L.Bolognesi, A.Minarini, M.Rosini, V.Tumiatti, M.Recanatini, C.Melchiorre. *J. Med. Chem.*, **51**, 347 (2008)
58. E.Mezeiova, K.Spilovska, E.Nepovimova, L.Gorecki, O.Soukup, R.Dolezal, D.Malinak, J.Janockova, D.Jun, K.Kuca, J.Korabecny. *J. Enzyme Inhib. Med. Chem.*, **33**, 583 (2018)
59. M.C.Carreiras, E.Mendes, M.J.Perry, A.P.Francisco, J.Marco-Contelles. *Curr. Top. Med. Chem.*, **13**, 1745 (2013)
60. J.Korábečný, E.Nepovimová, T.Cikánková, K.Špilovská, L.Vašková, E.Mezeiová, K.Kuča, J.Hroudová. *Neuroscience*, **370**, 191 (2018)
61. U.Rashid, F.L.Ansari In *Drug Design and Discovery in Disease*. (Eds A.-ur-Rafman, M.I.Choudhary). (Bentham, Elsevier, 2014). P. 40
62. L.H.Phillips. *Ann. NY Acad. Sci.*, **998**, 407 (2003)
63. M.Hill. *J. Neurol., Neurosurg. Psychiatry*, **74** (suppl 2) (2003)
64. M.Komloova, K.Musilek, M.Dolezal, F.Gunn-Moore, K.Kuca. *Curr. Med. Chem.*, **17**, 1810 (2010)
65. V.C.Juel, J.M.Massey. *Curr. Treat. Options Neurol.*, **7**, 3 (2005)
66. R.Cappai, K.J.Barnham. *Neurochem. Res.*, **33**, 526 (2008)
67. E.E.Congdon, E.M.Sigurdsson. *Nat. Rev. Neurol.*, **14**, 399 (2018)
68. G.Šimić, M.Babić Leko, S.Wray, C.R:Harrington, I.Delalle, N.Jovanov-Milošević, D.Bažadona, L.Buée, R.de Silva, G.Di Giovanni, C.M.Wischik, P.R.Hof. *Prog. Neurobiol.*, **151**, 101 (2017)
69. H.Hampel, M.-M.Mesulam, A.C.Cuello, M.R.Farlow, E.Giacobini, G.T.Grossberg, A.S.Khachaturian, A.Vergallo, E.Cavedo, P.J.Snyder, Z.S.Khachaturian. *Brain*, **141**, 1917 (2018)
70. D.R.Lynch, R.P.Guttmann. *J. Pharmacol. Exp. Ther.*, **300**, 717 (2002)
71. R.Wang, P.H.Reddy. *J. Alzheimers Dis.*, **57**, 1041 (2017)
72. C.Beinat, S.Banister, I.Moussa, A.J.Reynolds, C.S.P.McErlean, M.Kassiou. *Curr. Med. Chem.*, **17**, 4166 (2010)
73. L.Ismaili, A.Romero, M.do C.Carreiras, J.Marco-Contelles. In *Design of Hybrid Molecules for Drug Development*. (Ed. M.Decker). (Elsevier, 2017). P. 5
74. P.I.Moreira, C.Carvalho, X.Zhu, M.A.Smith, G.Perry. *Biochim. Biophys. Acta, Molecular Basis of Disease*, **1802**, 2 (2010)
75. L.Pagani, A.Eckert. *Int. J. Alzheimers Dis.*, **2011**, 925050 (2011)
76. Z.S.Khachaturian. *Neurobiol. Aging*, **8**, 345 (1987)
77. D.H.Small. *Neurochem. Res.*, **34**, 1824 (2009)
78. T.Wyss-Coray, J.Rogers. *Cold Spring Harb. Perspect. Med.*, **2** (2012)
79. M.Njoroge, N.M.Njuguna, P.Mutai, D.S.B.Ongarora, P.W.Smith, K.Chibale. *Chem. Rev.*, **114**, 11138 (2014)
80. P.P.Simarro, G.Cecchi, J.R.Franco, M.Paone, A.Diarra, J.A.Ruiz-Postigo, E.M.Fèvre, R.C.Mattioli, J.G.Jannin. *PLoS Negl. Trop. Dis.*, **6**, e1859 (2012)
81. *Organisation mondiale de la santé. World Malaria Report 2018*. (2018)
82. P.P.Simarro, A.Diarra, J.A.R.Postigo, J.R.Franco, J.G.Jannin. *PLOS Negl. Trop. Dis.*, **5**, e1007 (2011)
83. C.C.Musonda, J.Gut, P.J.Rosenthal, V.Yardley, R.C.Carvalho de Souza, K.Chibale. *Bioorg. Med. Chem.*, **14**, 5605 (2006)
84. C.C.Musonda, V.Yardley, R.C.C.de Souza, K.Ncokazi, T.J.Egan, K. Chibale. *Org. Biomol. Chem.*, **6**, 4446 (2008)
85. W.Obexer, C.Schmid, J.Barbe, J.P.Galy, R.Brun. *Trop. Med. Parasitol.*, **46**, 49 (1995)
86. S.Girault, P.Grellier, A.Berecibar, L.Maes, E.Mouray, P.Lemière, M.-A.Debreu, E.Davioud-Charvet, C.Sergheraert. *J. Med. Chem.*, **43**, 2646 (2000)
87. A.Saravanamuthu, T.J.Vickers, C.S.Bond, M.R.Peterson, W.N.Hunter, A.H.Fairlamb. *J. Biol. Chem.*, **279**, 29493 (2004)
88. K.Chibale. *Pure Appl. Chem.*, **77**, 1957 (2005)
89. R.L.Krauth-Siegel, O.Inhoff. *Parasitol. Res.*, **90** (Suppl 2), 77 (2003)
90. S.B.Prusiner. *Science*, **252**, 1515 (1991)
91. N.J.Cobb, W.K.Surewicz. *Biochemistry*, **48**, 2574 (2009)
92. D.R.Brown, H.Kozlowski. *Dalton Trans.*, (13), 1907 (2004)
93. K.J.Barnham, R.Cappai, K.Beyreuther, C.L.Masters, A.F.Hill. *Trends Biochem. Sci.*, **31**, 465 (2006)
94. H.-Y-Zhang. *Biochem. Biophys. Res. Commu.*, **351**, 578 (2006)
95. A.J.Thompson, C.J.Barrow. *Curr. Med. Chem.*, **9**, 1751 (2002)
96. C.Galdeano, E.Viayna, I.Sola, X.Formosa, P.Camps, A.Badia, M.V.Clos, J.Relat, M.Ratia, M.Bartolini, F.Mancini, V.Andrisano, M.Salmona, C.Minguillón, F.C.González-Muñoz, M.I.Rodríguez-Franco, A.Bidon-Chanal, F.J.Luque, D.Muñoz-Torrero. *J. Med. Chem.*, **55**, 661 (2012)
97. Z.Rankovic. *J. Med. Chem.*, **58**, 2584 (2015)
98. P.Camps, R.El Achab, J.Morral, D.Muñoz-Torrero, A.Badia, J.E:Baños, N.M.Vivas, X.Barril, M.Orozco, F.J.Luque. *J. Med. Chem.*, **43**, 4657 (2000)
99. P.Camps, E.Gómez, D.Muñoz-Torrero, M.Font-Bardia, X.Solans. *Tetrahedron*, **59**, 4143 (2003)
100. P.Camps, E.Gómez, D.Muñoz-Torrero. *Tetrahedron*, **60**, 5423 (2004)
101. P.Camps, E.Gómez, D.Muñoz-Torrero, A.Badia, M.V.Clos, C.Curutchet, J.Muñoz-Muriedas, F.J.Luque. *J. Med. Chem.*, **49**, 6833 (2006)
102. C.Ronco, G.Sorin, F.Nachon, R.Foucault, L.Jean, A.Romieu, P.-Y.Renard. *Bioorg. Med. Chem.*, **17**, 4523 (2009)
103. C.Ronco, L.Jean, P.-Y.Renard. *Tetrahedron*, **66**, 7399 (2010)
104. C.Ronco, R.Foucault, E.Gillon, P.Bohn, F.Nachon, L.Jean, P.-Y.Renard. *ChemMedChem*, **6**, 876 (2011)
105. C.Ronco, E.Carletti, J.-P.Colletier, M.Weik, F.Nachon, L.Jean, P.-Y.Renard. *ChemMedChem*, **7**, 400 (2012)
106. F.Prati, A.Cavalli, M.L.Bolognesi. *Molecules*, **21**, 466 (2016)
107. R.Morphy, Z.Rankovic. *J. Med. Chem.*, **48**, 6523 (2005)
108. P.Camps, X.Formosa, D.Muñoz-Torrero, J.Petrignet, A.Badia, M.V.Clos. *J. Med. Chem.*, **48**, 1701 (2005)
109. I.Sola, S.Castellà, E.Viayna, C.Galdeano, M.C.Taylor, S.Y.Gbedema, B.Pérez, M.V.Clos, D.C.Jones, A.H.Fairlamb, C.W.Wright, J.M.Kelly, D.Muñoz-Torrero. *Bioorg. Med. Chem.*, **23**, 5156 (2015)
110. A.S.Lawrenson, D.L.Cooper, P.M.O'Neill, N.G.Berry. *J. Mol. Model.*, **24**, Article 237 (2018)
111. P.M.O'Neill, S.A.Ward, N.G.Berry, J.P.Jeyadevan, G.A.Biagini, E.Asadollaly, B.K.Park, P.G.Bray. *Curr. Top. Med. Chem.*, **6**, 479 (2006)
112. I.Sola, E.Aso, D.Frattini, I.López-González, A.Espargaró, R.Sabaté, O.Di Pietro, F.J.Luque, M.V.Clos, I.Ferrer, D.Muñoz-Torrero. *J. Med. Chem.*, **58**, 6018 (2015)
113. F.J.Pérez-Areales, O.Di Pietro, A.Espargaró, A.Vallverdú-Queralt, C.Galdeano, I.M.Ragusa, E.Viayna, C.Guillou, M.V.Clos, B.Pérez, R.Sabaté, R.M.Lamuela-Raventós, F.J.Luque, D.Muñoz-Torrero. *Bioorg. Med. Chem.*, **22**, 5298 (2014)
114. E.Viayna, I.Sola, M.Bartolini, A.De Simone, C.Tapia-Rojas, F.G.Serrano, R.Sabaté, J.Juárez-Jiménez, B.Pérez, F.J.Luque, V.Andrisano, M.V.Clos, N.C.Inestrosa, D.Muñoz-Torrero. *J. Med. Chem.*, **57**, 2549 (2014)

115. F.J.Pérez-Areales, N.Betari, A.Viayna, C.Pont, A.Espargaró, M.Bartolini, A.De Simone, J.F.Rinaldi Alvarenga, B.Pérez, R.Sabate, R.M.Lamuela-Raventós, V.Andrisano, F.J.Luque, D.Muñoz-Torrero. *Future Med. Chem.*, **9**, 965 (2017)
116. E.Viayna, T.Gómez, C.Galdeano, L.Ramírez, M.Ratia, A.Badia, M.V.Clos, E.Verdaguer, F.Junyent, A.Camins, M.Pallàs, M.Bartolini, F.Mancini, V.Andrisano, M.P.Arce, M.I.Rodríguez-Franco, A.Bidon-Chanal, F.J.Luque, P.Camps, D.Muñoz-Torrero. *ChemMedChem*, **5**, 1855 (2010)
117. N.C.Inestrosa, A.Alvarez, C.A.Pérez, R.D.Moreno, M.Vicente, C.Linker, O.I.Casanueva, C.Soto, J.Garrido. *Neuron*, **16**, 881 (1996)
118. N.C.Inestrosa, J.P.Sagal, M.Colombres. *Subcell. Biochem.*, **38**, 299 (2005)
119. A.P.Pawar, K.F.Dubay, J.Zurdo, F.Chiti, M.Vendruscolo, C.M.Dobson. *J. Mol. Biol.*, **350**, 379 (2005)
120. R.Scherzer-Attali, R.Pellarin, M.Convertino, A.Frydman-Marom, N.Egoz-Matia, S.Peled, M.Levy-Sakin, D.E.Shalev, A.Caflisch, E.Gazit, D.Segal. *PLoS ONE*, **5**, e11101 (2010)
121. R.Scherzer-Attali, M.Convertino, R.Pellarin, E.Gazit, D.Segal, A.Caflisch. *J. Phys. Chem. B*, **117**, 1780 (2013)
122. R.J.Castellani, X.Zhu, H.Lee, P.I.Moreira, G.Perry, M.A.Smith. *Expert Rev. Neurother.*, **7**, 473 (2007)
123. G.T.Sutherland, B.Chami, P.Youssef, P.K.Witting. *Redox Rep.*, **18**, 134 (2013)
124. E.Oueis, G.Santoni, C.Ronco, O.Syzgantseva, V.Tognetti, L.Joubert, A.Romieu, M.Weik, L.Jean, C.Sabot, F.Nachon, P.Y.Renard. *Org. Biomol. Chem.*, **12**, 156 (2014)
125. I.Sola, A.Artigas, M.C.Taylor, S.Y.Gbedema, B.Pérez, M.V.Clos, C.W.Wright, J.M.Kelly, D.Muñoz-Torrero. *Bioorg. Med. Chem. Lett.*, **24**, 5435 (2014)
126. W.Carruthers. In *Comprehensive Organometallic Chemistry*. (Eds G.Wilkinson, F.G.A.Stone, E.W.Abel). (Oxford: Pergamon, 1982). P. 661
127. J.Marco-Contelles, E.Pérez-Mayoral, A.Samadi, M.do C.Carreiras, E.Soriano. *Chem. Rev.*, **109**, 2652 (2009)
128. P.Camps, R.El Achab, M.Font-Bardia, D.Görbig, J.Morral, D.Muñoz-Torrero, X.Solans, M.Simon. *Tetrahedron*, **52**, 5867 (1996)
129. P.Camps, D.Görbig, V.Muñoz-Torrero, F.Pérez. *Collect. Czech. Chem. Commun.*, **62**, 1585 (1997)
130. P.Camps, J.Contreras, M.Font-Bardia, X.Solans. *Synth. Commun.*, **26**, 9 (1996)
131. D.H.R.Barton, D.Crich, W.B.Motherwell. *J. Chem. Soc., Chem. Commun.*, (17), 939 (1983)
132. S.Vanlaer, A.Voet, C.Gielens, M.De Maeyer, F.Compernolle. *Eur. J. Org. Chem.*, **2009**, 643 (2009)
133. P.Camps, R.El Achab, D.M.Görbig, J.Morral, D.Muñoz-Torrero, A.Badia, J.E.Baños, N.M.Vivas, X.Barril, M.Orozco, F.J.Luque. *J. Med. Chem.*, **42**, 3227 (1999)
134. Y.G.Gololobov, I.N.Zhmurova, L.F.Kasukhin. *Tetrahedron*, **37**, 437 (1981)
135. A.P.Krapcho, J.F.Weimaster, J.M.Eldridge, E.G.E.Jahngen, A.J.Lovey, W.P.Stephens. *J. Org. Chem.*, **43**, 138 (1978)
136. A.Kadir, A.Nordberg. *J. Nucl. Med.*, **51**, 1418 (2010)
137. N.I.Bohnen, K.A.Frey. *Mol. Imaging. Biol.*, **9**, 243 (2007)
138. X.Shao, R.A.Koeppe, E.R.Butch, M.R.Kilbourn, S.E.Snyder. *Bioorg. Med. Chem.*, **13**, 869 (2005)
139. E.Da Costa Branquinho, G.Becker, C.Bouteiller, L.Jean, P.-Y.Renard, L.Zimmer. *Nucl. Med. Biol.*, **40**, 554 (2013)
140. K.Oukoloff, S.Chao, M.Cieslikiewicz-Bouet, R.Mougeot, L.Jean, P.-Y.Renard. *Eur. J. Org. Chem.*, **2016**, 1337 (2016)
141. S.Chao, E.Krejci, V.Bernard, J.Leroy, L.Jean, P.-Y.Renard. *Chem. Commun.*, **52**, 11599 (2016)
142. G.R.Proctor, A.L.Harvey. *Curr. Med. Chem.*, **7**, 295 (2000).
143. V.E.Gregor, M.R.Emmerling, C.Lee, C.J.Moore. *Bioorg. Med. Chem. Lett.*, **2**, 861 (1992)
144. S.Roman, N.M.Vivas, A.Badia, M.V.Clos. *Neurosci. Lett.*, **325**, 103 (2002)
145. S.Roman, A.Badia, P.Camps, M.V.Clos. *Neuropharmacology*, **46**, 95 (2004)
146. M.Pera, P.Camps, D.Muñoz-Torrero, B.Perez, A.Badia, M.V.Clos Guillen. *PLoS ONE*, **8**, e74344 (2013)
147. J.Relat, B.Pérez, P.Camps, D.Muñoz-Torrero, A.Badia, M.Victòria Clos. *Basic Clin. Pharmacol. Toxicol.*, **122**, 94 (2018)
148. M.M.Hedberg, M.V.Clos, M.Ratia, D.Gonzalez, C.U.Lithner, P.Camps, D.Muñoz-Torrero, A.Badia, L.Giménez-Llort, A.Nordberg. *NDD*, **7**, 379 (2010)
149. M.Ratia, L.Giménez-Llort, P.Camps, D.Muñoz-Torrero, B.Pérez, M.V.Clos, A.Badia. *NDD*, **11**, 129 (2013)
150. M.Ratia, L.Giménez-Llort, P.Camps, D.Muñoz-Torrero, M.V.Clos, A.Badia. *Pharmacol. Biochem. Behav.*, **95**, 485 (2010)
151. C.Galdeano, N.Coquelle, M.Cieslikiewicz-Bouet, M.Bartolini, B.Pérez, M.V.Clos, I.Silman, L.Jean, J.-P.Colletier, P.-Y.Renard, D.Muñoz-Torrero. *Molecules*, **23**, 634 (2018)
152. J.Defaux, M.Sala, X.Formosa, C.Galdeano, M.C.Taylor, W.A.A.Alobaid, J.M.Kelly, C.W.Wright, P.Camps, D.Muñoz-Torrero. *Bioorg. Med. Chem.*, **19**, 1702 (2011)
153. F.Freeman, T.Chen, J.B.van der Linden. *Synthesis*, **1997**, 861 (1997)
154. D.dos Santos Pisoni, J.S.da Costa, D.Gamba, C.L.Petzhold, A.C.de Amorim Borges, M.A.Ceschi, P.Lunardi, C.A.S.Gonçalves. *Eur. J. Med. Chem.*, **45**, 526 (2010)
155. G.Chelucci, G.Orrù. *Tetrahedron Lett.*, **46**, 3493 (2005)
156. P.Camps, E.Gómez, D.Muñoz-Torrero, M.Arnó. *Tetrahedron: Asymmetry*, **12**, 2909 (2001)
157. P.Camps, E.Gómez, D.Muñoz-Torrero, A.Badia, N.M.Vivas, X.Barril, M.Orozco, F.J.Luque. *J. Med. Chem.*, **44**, 4733 (2001)
158. A.F.Cowman, L.W.Deady, E.Deharo, J.Desneves, L.Tilley. *Aust. J. Chem.*, **50**, 1091 (1997)
159. F.Ayad, L.Tilley, L.W.Deady. *Bioorg. Med. Chem. Lett.*, **11**, 2075 (2001)
160. S.Girault, P.Grellier, A.Berecibar, L.Maes, P.Lemière, E.Mouray, E.Davioud-Charvet, C.Sergheraert. *J. Med. Chem.*, **44**, 1658 (2001)
161. N.Mehta, K.S.Laddha. *Indian J. Pharm. Sci.*, **71**, 128 (2009)
162. Y.-X.Zhou, W.Xia, W.Yue, C.Peng, K.Rahman, H.Zhang. *Evid.-Based Complementary Alter. Med.*, **2015**, 1 (2015)
163. I.Sola, A.Artigas, M.C.Taylor, F.J.Pérez-Areales, E.Viayna, M.V.Clos, B.Pérez, C.W.Wright, J.M.Kelly, D.Muñoz-Torrero. *Bioorg. Med. Chem.*, **24**, 5162 (2016)
164. D.Dugasani, M.R.Pichika, V.D.Nadarajah, M.K.Balijepalli, S.Tandra, J.N.Korlakunta. *J. Ethnopharmacol.*, **127**, 515 (2017)
165. C.Ronco, L.Jean, H.Outaabout, R.-Y.Renard. *Eur. J. Org. Chem.*, **2011**, 302 (2011)
166. J.Cheung, M.J.Rudolph, F.Burshteyn, M.S.Cassidy, E.N.Gary, J.Love, M.C.Franklin. *J. Med. Chem.*, **55**, 10282 (2012)
167. E.Oueis, G.Santoni, C.Ronco, O.Syzgantseva, V.Tognetti, L.Joubert, A.Romieu, M.Weik, L.Jean, C.Sabot, F.Nachon, P.-Y.Renard. *Org. Biomol. Chem.*, **12**, 156 (2013)
168. P.Thirumurugan, D.Matosiuk, K.Jozwiak. *Chem. Rev.*, **113**, 4905 (2013)
169. H.C.Kolb, M.G.Finn, K.B.Sharpless. *Angew. Chem., Int. Ed.*, **40**, 2004 (2001)
170. T.Wu, S.-N.Lim, J.-J.Tsai, Y.-C.Chuang, C.-W.Huang, C.-C.Lin, C.-H.Hsu, H.-C.Fung, C.-H.Lee. *Seizure*, **62**, 84 (2018)
171. A.Bakker, G.L.Krauss, M.S.Albert, C.L.Speck, L.R.Jones, C.E.Stark, M.A.Yassa, S.S.Bassett, A.L.Shelton, M.Gallagher. *Neuron*, **74**, 467 (2012)
172. P.E.Sanchez, L.Zhu, L.Verret, K.A.Vossel, A.G.Orr, J.R.Cirrito, N.Devidze, K.Ho, G.-Q.Yu, J.J.Palop, L.Mucke. *Proc. Natl. Acad. Sci. USA*, **109**, E2895 (2012)
173. J.-Q.Shi, B.-R.Wang, Y.-Y.Tian, J.Xu, L.Gao, S.-L.Zhao, T.Jiang, H.-G.Xie, Y.-D.Zhang. *CNS Neurosci. Ther.*, **19**, 871 (2013)
174. O.Benek, J.Korabecny, O.Soukup. *Trends Pharm Sci.*, **41**, 434 (2020)